

WIRELESS POWER TRANSFER VIA MAGNETIC RESONANT COUPLING

by

Farid Jolani

Submitted in partial fulfillment of the requirements
for the degree of Doctor of Philosophy

at

Dalhousie University
Halifax, Nova Scotia
August 2015

© Copyright by Farid Jolani, 2015

Dedication

I dedicate this thesis to my beloved parents, Shams and Ali, and to my brothers, Farjad and Farbod. May their lives be full of love, health, and happiness.

TABLE OF CONTENTS

LIST OF TABLES	v
LIST OF FIGURES.....	vi
ABSTRACT	x
LIST OF ABBREVIATIONS USED	xi
ACKNOWLEDGMENTS	xii
CHAPTER 1 INTRODUCTION.....	1
1.1 Background and Motivation	1
1.2 Research Objectives	2
1.3 Contributions.....	3
1.4 Thesis Organization	4
CHAPTER 2 BACKGROUND AND LITERATURE REVIEW	6
2.1 Wireless Power Transfer.....	6
2.1.1 Microwave Beamforming	6
2.1.2 Inductive Coupling.....	7
2.1.3 Magnetically-Coupled Resonance (MCR).....	7
2.2 WPT Using Magnetically-Coupled Resonant (MCR) for Small Electronic Devices	11
2.3 Discussion	12
CHAPTER 3 NON-PLANAR MAGNETICALLY-COUPLED RESONANT WIRELESS POWER TRANSFER (MCR-WPT) FOR SMALL DEVICES	13
3.1 Theory	13
3.2 Design	17
3.3 Results.....	18
3.4 Discussion.....	25

CHAPTER 4	FULLY-PLANAR MCR-WPT FOR SMALL ELECTRONIC DEVICES	26
4.1	Theory	26
4.2	Self-Resonant and Capacitive-Loaded Planar MCR-WPT	33
4.2.1	Effect of Ferrite Material	37
4.2.2	Effects of Conductive Objects	38
4.3	Optimization of Planar MCR-WPT System	39
4.3.1	Efficiency Improvement by Auxiliary Strips.....	41
4.3.2	Multilayer Planar MCR-WPT system.....	45
4.3.3	Asymmetrical MCR-WPT System	49
4.4	Discussion	53
CHAPTER 5	ARRAY COIL FOR PLANAR MCR-WPT SYSTEMS.....	55
5.1	Background.....	55
5.2	Conventional MCR-WPT Array System	56
5.3	Position-Free MCR-WPT Array System	59
5.4	Optimization Scheme.....	62
5.4.1	Simulation and Measurement Results.....	65
5.5	MCR-WPT Array with Small Receiver.....	71
5.5.1	Array of 2×2.....	71
5.5.2	Array of 3×3.....	77
5.6	Discussion.....	85
CHAPTER 6	CONCLUSION AND FUTURE WORK	86
6.1	Conclusion	86
6.2	Future Work	87
REFERENCES	89

LIST OF TABLES

Table 3-1: Parameters of coils for the three designs.....	18
Table 3-2: Physical parameters and electrical properties of the stratified medium at 18.5 MHz [50].....	21
Table 4-1: Design parameters	35
Table 4-2: The maximum power transmission efficiency of the proposed planar structures	38
Table 4-3: Design parameters, RLC values	40
Table 4-4: The maximum transmission efficiency of the proposed WPT system with auxiliary strips.....	45
Table 4-5: Maximum transmission efficiency of the proposed multilayer MCR-WPT systems	49
Table 4-6: Design parameters, RLC values of asymmetrical WPT system.....	51
Table 5-1: Transmission Efficiency of the array of 1×2 in axial-misalignment condition	69
Table 5-2: Transmission Efficiency of the array of 2×2 in axial-misalignment condition	69
Table 5-3: Design parameters, RLC values of MCR-WPT array.....	73
Table 5-4: Parameters of MCR-WPT array system with nine transmitting resonators	78
Table 5-5: Value of capacitors for MCR-WPT array system with nine resonators	80

LIST OF FIGURES

Figure 2-1: WPT using inductive coupling.....	7
Figure 2-2: Schematic of the MCR-WPT system	8
Figure 2-3: Transmission efficiency $ S_{21} $ as a function of frequency and transmitter-to-receiver coupling. The highlighted red volume is the over-coupled region where frequency splitting occurs [35].	10
Figure 3-1: Equivalent circuit of a conventional MCR-WPT system.....	14
Figure 3-2: The proposed MCR-WPT system using magnetic resonance coupling.	17
Figure 3-3: Simulated and measured transmission efficiencies of design #1 at different distances of d	19
Figure 3-4: Simulated and measured transmission efficiency of design #2 at different distances.	19
Figure 3-5: S_{21} of design #3 at a transmission distance of 10 cm.	20
Figure 3-6: Simulation setup for design #3 with the receiver placed inside a stratified medium consisting of skin, fat and muscle layers.	21
Figure 3-7: Simulation setup for design #3 with the receiver placed inside a stratified medium consisting of skin, fat and muscle layers.	22
Figure 3-8: (a) The fabricated design #3, (b) the receiver coils are inserted into a 4-cm thick pork meat and at a transmission distance of 10 cm.....	23
Figure 3-9: Measured power efficiency of design #3 at different distances of d	24
Figure 3-10: Measured power efficiency of design #3 with different orientation angles of receiver coils at a transmission distance of 8 cm.	24
Figure 4-1: Equivalent circuit model of the planarized MCR-WPT system.....	28
Figure 4-2: The structure of planar MCR-WPT design	30
Figure 4-3: (a) Overview of the proposed planar WPT system, (b) the front-view of the transmitter design in the planar WPT system with self-resonant PSC, (c) the back-view of the transmitter design in the planar WPT system with capacitor-loaded PSC.....	34
Figure 4-4: Simulated power transmission efficiency of the planar WPT with self-resonant and capacitor-loaded PSC resonators over various transmission distances.	35
Figure 4-5: (a) The fabricated planar capacitor-loaded WPT system, (b) measurement setup.	36
Figure 4-6: Measured and simulated power transmission efficiency of the capacitor-loaded WPT system at 13.56 MHz.	36
Figure 4-7: Measured power transmission efficiency of the capacitor-loaded WPT system as a function of distance and operating frequency.....	37

Figure 4-8: Simulated power transmission efficiency of the capacitor-loaded WPT system at a distance of 200 mm with and without ferrite plates.	38
Figure 4-9: PSCs design flowchart.	41
Figure 4-10: (a) Geometry of the proposed PSC, (c) geometry of the auxiliary strips on the bottom side of the substrate	42
Figure 4-11: Geometry of the proposed PSC with auxiliary strips on the backside of the substrates.	43
Figure 4-12: Analytical, simulated, and measured transmission efficiency of the proposed planar MCR-WPT system at a distance of 10 cm.	44
Figure 4-13: Measured transmission efficiency at different transmission distances.	44
Figure 4-14: Geometry of the proposed planar MCR-WPT systems with 2-layer PSC resonator using a conductive shorting wall.....	46
Figure 4-15: Geometry of the proposed planar MCR-WPT systems with 3-layer PSC resonator using a conductive shorting wall.....	46
Figure 4-16: Fabricated 3-layer PSC resonator with conductive shorting walls; a) top view, b) side view.	47
Figure 4-17: Transmission efficiency of conventional planar MCR-WPT and proposed planar MCR-WPT at a nominal distance of 10 cm.	48
Figure 4-18: Measured transmission efficiency against distance at 13.56 MHz.	49
Figure 4-19: Equivalent circuit model of the MCR-WPT system with matching circuit..	50
Figure 4-20: Transmission efficiency of asymmetrical MCR-WPT system against distance at 13.56 MHz.	51
Figure 4-21: Transmission efficiency of asymmetrical planar MCR-WPT system.....	52
Figure 4-22: Geometry of asymmetrical MCR-WPT system with different orientation angles of the receiver at a transmission distance of 7 cm.	52
Figure 4-23: Transmission efficiency of asymmetrical MCR-WPT system with different orientation angles of the receiver at a transmission distance of 7 cm.	53
Figure 5-1: Conventional MCR-WPT array transmitter with one resonator and three repeaters.	57
Figure 5-2: Simulated transmission efficiency of conventional planar MCR-WPT array system at a distance of 10 cm aligned with resonator.....	57
Figure 5-3: Simulated transmission efficiency of conventional planar MCR-WPT array system at a distance of 10 cm aligned with repeater.....	58
Figure 5-4: Measured transmission efficiency of conventional planar MCR-WPT system with one Tx resonator and three repeaters.	58

Figure 5-5: (a) Transmitter design of conventional MCR-WPT; (b) transmitter design of the proposed MCR-WPT with an array of 1×2 resonator.....	60
Figure 5-6: Transmitter design of conventional MCR-WPT.....	60
Figure 5-7: Proposed position-free MCR-WPT array system with an array of 2×2 resonator.....	61
Figure 5-8: Normalized coupling factor between the receiver and transmitter resonators with regard to normalized transmission distance.....	61
Figure 5-9: Equivalent circuit model of the proposed planar MCR-WPT array.	63
Figure 5-10: Block diagram of simulation and optimization processes.	64
Figure 5-11: Flowchart of optimization algorithm for optimization of proposed MCR-WPT	65
Figure 5-12: Configuration of proposed the array of 2×2	66
Figure 5-13: Measured and simulated transmission efficiency at a distance of 10 cm in between the transmitter and receiver.	67
Figure 5-14: Measured and simulated transmission efficiency of proposed MCR-WPT system with transmitting resonator array.	67
Figure 5-15: Measured S_{21} of the array of 2×2	68
Figure 5-16: Measured transmission efficiency of proposed planar MCR-WPT system with an array of 2×2	69
Figure 5-17: Magnetic field distribution of (a)-(c) conventional MCR-WPT array (repeater), (d)-(f) conventional MCR-WPT system, and (g)-(i) proposed MCR-WPT array system.	70
Figure 5-18: Geometry of MCR-WPT array transmitter: (a) top, (b) bottom.	72
Figure 5-19: Geometry of MCR-WPT array (2×2) with different orientation angles of the receiver at a transmission distance of 10 cm.....	74
Figure 5-20: Transmission efficiency of MCR-WPT array against distance at 13.56 MHz.	74
Figure 5-21: Transmission efficiency of MCR-WPT array at a transmission distance of 10 cm.....	75
Figure 5-22: Transmission efficiency of MCR-WPT array with different orientation angles of the receiver at a transmission distance of 10 cm.	75
Figure 5-23: Picture of the developed MCR-WPT array system for multiple charging electronic devices.....	76
Figure 5-24: Geometry of transmitting array of 3×3	78
Figure 5-25: Transmission efficiency of MCR-WPT array system with 9 transmitting resonators at a distance of 90 mm.....	79

Figure 5-26: Transmission efficiency of MCR-WPT array system with 9 transmitting resonators using different lumped capacitors at a distance of 90 mm.	80
Figure 5-27: MCR-WPT array system with an array of 3×3 transmitting resonators.	81
Figure 5-28: Picture of MCR-WPT array system with an array of 3×3 transmitting resonators: (a) top layer, (b) bottom layer.....	81
Figure 5-29: Transmission efficiency of MCR-WPT array system with an array of 3×3 transmitting resonators versus transmission distance.	82
Figure 5-30: Transmission efficiency of MCR-WPT array system with an array of 3×3 transmitting resonators at a distance of 90 mm	83
Figure 5-31: : Transmission efficiency of MCR-WPT array system with an array of 3×3 transmitting resonators with different orientation angles of the receiver at the transmission distance of 9 cm.	84
Figure 5-32: Geometry of the MCR-WPT array system with an array of 3×3 transmitting resonators using auxiliary strips.....	84
Figure 5-33: Transmission efficiency of MCR-WPT array system with an array of 3×3.	85

ABSTRACT

Small electronic devices such as smartphones and tablets are increasingly rooted in everyday life. To eliminate cable mess and make it easy to stay connected with always-charged electronic devices, magnetically coupled resonant wireless power transfer (MCR-WPT), which can power electronic devices wirelessly at midrange distances, is the most practical solution. A long-standing goal has been to transfer power wirelessly over a large area with a compact and easy-to-implement receiver that can be used for electronic and medical devices.

However, existing technology falls short of this goal. MCR-WPT systems are bulky and highly sensitive to axial and lateral misalignment, and MCR-WPT systems are limited to the size of the transmitter. Furthermore, simply exciting an MCR-WPT array system cannot address the issue due to transfer efficiency fluctuations over the covered area. The transfer efficiency of the system drops dramatically when the receiver is not perfectly aligned with the transmitter resonator and is limited to the size of the transmitter.

This thesis explores several novel topologies and models of non-planar and planar transmitter, receivers for an MCR-WPT system. The proposed MCR-WPT can achieve higher transfer efficiency compared to previous works of comparable size and transmission distance. Two novel techniques are proposed to increase the quality factor of resonators, and various planar WPT systems are studied regarding size constraints.

The second contribution of this thesis is to overcome the problem of misalignment between the transmitter and receiver resonators. To address this issue, a planar MCR-WPT array system consisting of two to nine transmitting array resonators using a novel feeding structure is proposed. The aim is to have a simple and easy-to-implement structure with a transfer efficiency that is less sensitive to axial- and lateral-misalignment.

The proposed MCR-WPT system consists of five subsystems (an amplifier, MCR-WPT, a rectifier, a DC-to-DC converter, and a load) which are applied to verify the performance of the proposed WPT systems. It is shown that the proposed systems are more desirable and feasible to implement inside walls and under desks to charge small electronic devices anywhere inside its confines.

LIST OF ABBREVIATIONS USED

WPT	Wireless Power Transfer
MCR	Magnetically-Coupled Resonant
PSC	Printed Spiral Coil

ACKNOWLEDGMENTS

First, I sincerely wish to thank my supervisor Prof. Zhizhang (David) Chen, who gave me the opportunity to join his group, and let me work on various projects. It was a real pleasure for me to work under such an exceptional scholar, and it was my honor to be his Ph.D student.

I also want to thank my co-supervisor Dr. Yiqiang Yu, for his valuable discussions and suggestions during our projects. I am immensely grateful to him. He inspired me with his brilliant ideas and novel concepts.

Furthermore, I would like to thank my committee members, Dr. Sergey Ponomarenko and Dr. William J. Phillips for their review of my dissertation and their constructive comments and feedback.

I would also like to say thank you to Kate Hide and Nicole Smith in the department office for their friendly help in day-to-day correspondence matters.

Special gratitude goes to my dearest friends, Parvaneh and Fariborz for always being supportive.

Finally, I want to thank my parents, Shamsi and Ali, for their love and support, and my brothers, Farjad and Farbod, who make my life happier.

1.1 Background and Motivation

As a means of transferring electric power without any physical connections, wireless power transfer (WPT) provides a safe, mobile and more convenient solution to recharging the batteries of small electronic and medical devices. Most of the WPT systems developed thus far over the past few decades devices utilize inductive coupling, which consists of a source (transmitter) coil and a load (receiver) coil separated by an air gap to transfer power. Inductive coupling WPT systems are easy to implement but can provide high transfer efficiency only at very short distances. The transfer efficiency decreases dramatically with increasing distance and axial-misalignment between the source coil and the load coil.

To overcome the aforementioned drawbacks, the magnetically coupled resonant WPT (MCR-WPT) was introduced in 2007 [1]. MCR-WPT technology is a mid-range non-radiative coupling method wherein energy exchange of an MCR-WPT system occurs in a strong-coupling regime with high transfer efficiency. It is based on the principle that both the transmitting and receiving coils are tuned at the same resonant frequency. Since their introduction, MCR-WPT systems have been extensively investigated and developed for charging electric vehicles [2-4], medical implantable devices [5, 6], and small electronic devices [7].

Recently, much research has been focused on extending the transmission distance of MCR-WPT systems using different techniques, such as the application of intermediate resonant coils [8, 9], the application of metamaterials [10, 11], frequency tracking [12], simultaneous matching [13], and multi-loop feed [14, 15]. However, the two major drawbacks of an MCR-WPT system, namely, low transfer efficiency at the under-coupled region, and decrease of transfer efficiency due to an axial-misalignment have yet to be tackled.

In order to address those two issues, a few techniques have been proposed. They include antiparallel resonant loop technique [16], adaptive matching network [17], and arrayed transmitting coils [18-20]. Furthermore, most reported MCR-WPT systems utilize three-dimensional wire loops, spiral loops or helical antennas for the design of transmitting and

receiving coils, and the coils are often bulky in geometry and require precise fabrication to maintain a high quality factor. This, in turn, poses technical difficulties for the WPT systems to be applied to small electronic devices and implanted medical devices.

Compared to three-dimensional coils, printed spiral coils (PSCs) are more effective than three-dimensional structures as a candidate for a low profile, small-footprint and easy-to-fabricate WPT system. However, only a small number of studies have investigated the use of PSCs in MCR-WPT systems [21-23]. In addition, an effective scheme to optimize the structural parameters of driving/load loops and resonator coils has not been reported; but it could prove helpful in increasing the transmission efficiency of MCR-WPT systems. Also, in terms of practical applications, a simple and easy-to-implement WPT system with a transmission efficiency that is less sensitive to axial-misalignment and transmission distance is always more desirable and more feasible, especially when it needs to be installed inside walls or below desks to charge small electronic devices anywhere within its confines.

1.2 Research Objectives

The primary goal of the thesis is to develop a novel WPT system for recharging small electronic devices. It is based on magnetically coupled resonant (MCR) and the main aspects of this work are:

1. Studying non-planar, four-coil MCR-WPT systems and the feasibility of implementing the proposed system for small electronic and medical devices.
2. Developing an easy-to-implement and low-profile, fully planar MCR-WPT system and derivation of the precise equivalent circuit model of the proposed planar WPT system.
3. Developing an optimization scheme for the structural parameters of the MCR-WPT system to maximize the transmission efficiency.
4. Researching a position-free and distance-insensitive MCR-WPT system using arrayed transmitting resonators.
5. Evaluating the performance of the proposed MCR-WPT systems for small electronic devices through the fabrication and testing of prototypes.

1.3 Contributions

This thesis contributes to the state of art in the following ways:

1. An efficient non-planar MCR-WPT system is developed with different sizes of transmitting and receiving coils. It is embedded into biological objects to validate the effectiveness of the proposed system on charging implantable medical devices, such as pacemakers.
2. A novel WPT system is presented for wireless power transfer via coupled magnetic resonances. In the proposed design, both the transmitting and receiving coil sets are planarized. The planar structure and the high power transmission efficiency render the proposed design a practical candidate as WPT systems for small portable electronic devices and implantable medical devices. In addition, the effects of ferrite sheets are also investigated. They are applied to the proposed system as magnetic reflectors, leading to efficiency improvement. The sensitivity of the proposed WPT system in the presence of conductive objects is investigated as well.
3. Various planar MCR-WPT systems with PSCs of different numbers of turns are studied and compared in terms of both efficiency and input impedance. An optimization scheme is developed to improve the transmission efficiency of the planar MCR-WPT system.
4. Two new techniques are proposed to improve the transmission efficiency of the planar MCR-WPT. Firstly, parasitic strips are applied to the backside of the substrates to decrease parasitic resistance and increase the quality factor of the PSC resonators. Secondly, multiplayer PSC resonators with or without shorting walls are proposed to further increase the transmission efficiency of the planar WPT system.
5. A novel and easy-to-fabricate array-coil technique is developed to improve the transmission efficiency of an MCR-WPT system when the receiver is axially misaligned with the transmitter. In the proposed design, the conventional transmitter coil set is replaced by an array of smaller resonators and a single driving loop. The results show that with the proposed design, the transmission efficiency of the MCR-WPT system under axial-misalignment can be significantly improved

without any adaptive matching techniques. Furthermore, the transmission efficiencies in both over- and under-coupled regions are also improved, contributing to the distance-insensitivity of the proposed design.

6. All MCR-WPT designs have been fabricated and tested. The results show that the proposed MCR-WPT systems are good candidates for practical applications such as charging small electronic devices and IMDs.

1.4 Thesis Organization

The dissertation is divided into six chapters, together with the abstract, the list of publications, and the references. The contents of the dissertation chapters are as follows:

- Chapter 1 presents the background, research motivations and objectives of this work, where specific goals, new contributions, and methodology of the research work are described.
- Chapter 2 provides a literature review of the traditional wireless power transfer (WPT) systems and the concept of an WPT system using magnetically coupled resonant (MCR) technology. The equivalent circuit modeling of the conventional MCR-WPT system and analytical equations of planar MCR-WPT systems is also provided in this chapter.
- Chapter 3 introduces efficient and compact non-planar MCR-WPT systems designed for recharging small electronic and implantable medical devices. A receiving resonator coil and a load loop are studied and developed under size restrictions of portable devices. Three design configurations of the MCR-WPT system, each consisting of two coils at the transmitter and two coils at the receiver, are developed. Furthermore, the receiver coils are implanted inside a biological object to show that the power can be transferred effectively.
- Chapter 4 proposes a novel MCR-WPT with fully planar transmitting coil and receiving coil sets. More specifically, it comprises two printed spiral resonator coils, a co-planar source loop and a load loop. Comparisons of both quality factors and power transmission efficiency of the design with self-resonant printed spirals and with capacitor-loaded printed spirals are made. In addition, the effects of ferrite material and conductive objects on the proposed system are also investigated. An

equivalent circuit model of the proposed planar WPT system is derived to facilitate the design, and a flowchart is provided for the optimization of the system with given size constraints. Finally, a novel technique is developed to decrease parasitic resistance and to increase the quality factor of the PSC resonators, which in turn improves the transmission efficiency of the proposed planar MCR-WPT system. The proposed designs are fabricated and measured to validate the performances.

- Chapter 5 introduces a new MCR-WPT system using an array of printed spiral resonators, after which the effect of a misalignment of a receiver coil on a conventional transmitting array is studied. The effect of replacing the single transmitting resonator of a conventional MCR-WPT with an array of smaller resonators on the transmission efficiency of the planar WPT system in both over-coupled region and under-coupled region is also investigated. It is shown that the proposed MCR-WPT array system is able to provide consistent transmission efficiency, even when the receiver is axially misaligned with the transmitter. Finally, a comparison between the simulation and the measurement results is provided.
- Chapter 6 concludes the thesis. Future work in the proposed research area is also presented in this chapter.

Chapter 2 **BACKGROUND AND LITERATURE REVIEW**

This chapter provides the background and literature review of wireless power transfer (WPT) systems. The various types of WPT systems are first presented and then followed by a discussion of planar and non-planar wireless power transfer via magnetically coupled resonant (MCR-WPT) for small electronic and implantable devices. Finally, a review of different methods to improve transmission efficiency is then provided.

2.1 Wireless Power Transfer

Most electrical appliances and electronic devices require transmission lines, wires or power cords for electrical power supply or battery charging. To get rid of lines, wires and power cords, power transmission without the use of wires has become an interesting alternative that provides more convenient use of electronic devices. The idea of wireless power transfer (WPT) was studied already in the 19th century, when some experiments were conducted to transmit energy wirelessly between a transmitter and a receiver [24]. Since then, many studies have been performed to develop the concept of transferring large amounts of energy wirelessly over large distances, and different methods such as microwave beamforming, inductive coupling and magnetically coupled resonant (MCR) have been proposed and developed. They are described below.

2.1.1 Microwave Beamforming

Wireless power transfer (WPT) using microwave beam power transmission was presented in 1963 using a rectifying antenna. It achieved an efficiency of 50% at an output of 4W [25]. This microwave technique, which uses the far-field components of electromagnetic waves to transfer energy between a transmitter, a receiver and transmission distance is much larger than the wavelength of the transferred power signal. The power of electromagnetic waves decays as the inverse square of separation distance d . A high-gain antenna or an antenna array is used at a transmitter and a rectenna array is used at a receiver to transfer radiative energy ranging from watts to kilowatts over a distance of several kilometers [26, 27]. However, the transmission efficiency is very low due to the

spreading and attenuation nature of the radiative power in space; it also requires line-of-sight.

2.1.2 Inductive Coupling

Wireless power transfer using inductive coupling to transfer energy from a transmitting coil to a receiving induction coil through a magnetic near field. The transmitting coil is driven by a time-varying current, which in turn generates a magnetic field that induces a time-varying current in the receiving coil, as shown in Figure 2-1. The receiving coil can be attached to a portable device and the induced electrical current is used for charging a battery [28-32]. An inductive coupling WPT system can provide very high efficiency. It can exhibit a transmission efficiency exceeding 90% for charging electric vehicles and 70% for charging small electronic devices [33]. However, it has a very short range of transmission distance and the transmission efficiency decreases rapidly when the receiver coil moves away from the transmitter (in the order of $1/d^3$).

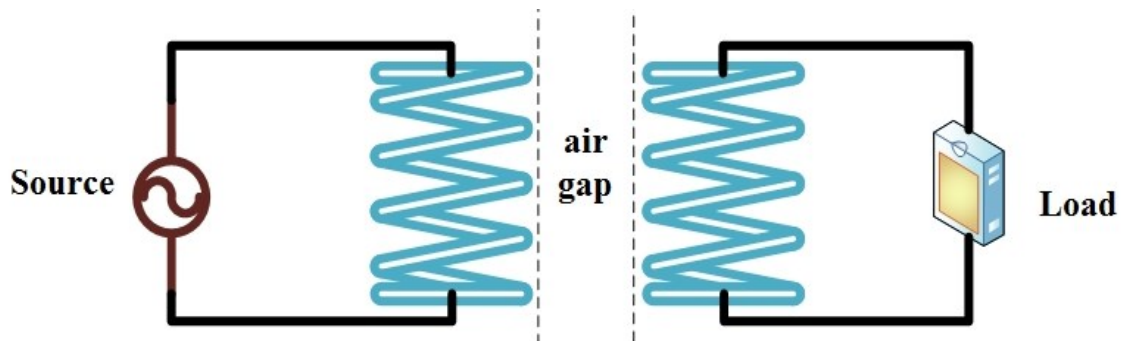


Figure 2-1: WPT using inductive coupling

2.1.3 Magnetically-Coupled Resonance (MCR)

A new wireless power transfer technique was introduced by a Massachusetts Institute of Technology (MIT) research group in 2007. It extends the transmission distance based on strongly coupled magnetic resonance [34]. It is a novel non-radiative mid-range wireless power transfer system that consists of four components: a source coil, a transmitting/receiving coil that serves as a high quality factor LC resonator, and a load coil. The transmission distance between the transmitting resonator coil and the receiving

resonator coil can be as large as several times the size of the resonator coils. When the MCR-WT system is properly designed, energy is inductively coupled from a driver loop to the transmitting resonator coil and then coupled to the receiving resonator coil via magnetic resonance. Both the transmitting and receiving resonators resonate at the same operating frequency. Under this coupling process, the energy or power is delivered from the transmitter to the load at the receiver load loop, as shown in Figure 2-2.

The MCR-WPT systems transmit longer transmission distances in comparison to inductive coupling WPT systems, providing an omnidirectional energy transfer and only the slight electromagnetic interference due to the use of magnetic resonance coupling. However, the maximum transmission efficiency of the MCR-WPT system occurs only at the optimum transmission distance between the transmitting and receiving coils. When the receiving coil is moved away from its optimal transmission distance, transmission efficiency decreases rapidly.

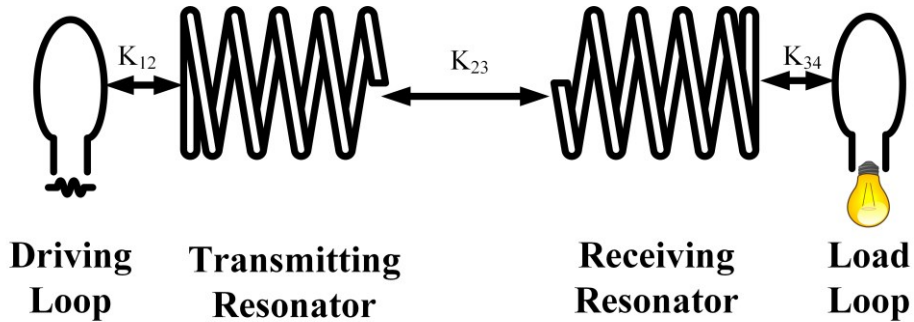


Figure 2-2: Schematic of the MCR-WPT system

In a four-coil MCR-WPT system (as shown in Figure 2-2), three different coupling regions can be defined based on the separation of transmitting coils and receiving coils:

1. **Over-Coupled:** When the transmission distance is below a certain threshold, a frequency-splitting phenomenon takes place due to large coupling of transmitting and receiving coils. This results in a decrease of transmission efficiency at the operating frequency. In [35], the frequency-splitting phenomenon is shown to be caused by two different modes resonating at different frequencies. In [36], the same

phenomenon is explained by the circuit theory. Possible solutions for reducing this phenomenon are proposed.

2. **Critically-Coupled:** As the transmission distance is increased to the optimum distance, the resonant frequencies of the two modes converge to the same operating frequency and transmission efficiency reaches its maximum which is called the critically-coupled region.
3. **Under-Coupled:** Conversely, when the transmission distance is larger than the optimum value, coupling between the transmitting resonator coil and the receiving resonator coil decreases. The transmission efficiency begins to decrease, and the system; then operates in the so-called under-coupled region.

Figure 2-3 shows all three different regions in terms of transmission efficiency. To alleviate negative impacts of the frequency splitting-phenomenon and improve the transmission efficiency of a WPT system in the under-coupled region, an adaptive matching method based on frequency tracking is proposed in [5, 12]. The transmission efficiency of the WPT system not only increases in the under-coupled region, but also improves at the over-coupled region. However, in practice, the wireless power transfer should stay inside an allowable industrial, scientific, and medical band (e.g., 13.56 MHz) which is narrow. Therefore, tuning frequency is not a feasible method for an MCR-WPT system [37]. Antiparallel resonant loops are then introduced in the transmitting and receiving coils [16], but the drawback of this technique is that transmission efficiency decreases in the under-coupled region.

To improve the transmission efficiency in the under-coupled region, many techniques have been proposed, one of which is a variable coupling method that improves transmission efficiency from 29.3% to 46.2% [13]. However, the distance between the source/load loop and the transmitting/receiving resonator coil needs to be adjusted. This makes it impractical for portable devices, since the distance between the receiving resonator coil and the load loop is fixed. In [14, 15], adaptive impedance matching using a loop switching technique is proposed to increase transmission efficiency in both under- and over-coupled regions, with an improvement of up to 24%. However, the switching capacitor at both the source

and load loops for the impedance matching needs be satisfied simultaneously, sometimes making the proposed system too complicated to implement.

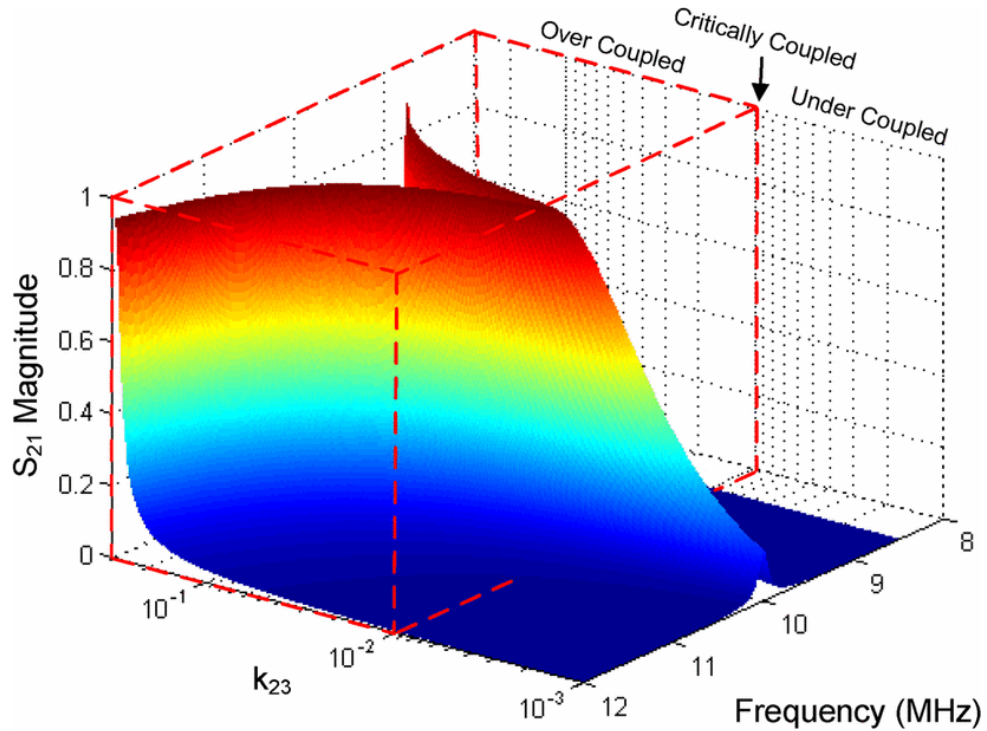


Figure 2-3: Transmission efficiency $|S_{21}|$ as a function of frequency and transmitter-to-receiver coupling. The highlighted red volume is the over-coupled region where frequency splitting occurs [35].

In order to improve the distance of power transfer, the use of repeaters or relay resonators has been investigated in many recent papers. In [38], by installing a repeater between the transmitting and receiving resonators, the transmission distance increased from 30 cm to 61 cm. In [8], the perpendicularly arranged intermediate resonator is introduced. It is shown that despite the power transfer of the coaxially arranged intermediate resonator system begin higher than the perpendicularly arranged intermediate resonator system, the latter one is more practical, since it can be implemented adaptively in the space.

Using a nonadjacent relay resonator to further improve power transfer at the optimal frequency is investigated in [39]. It is shown that transmission efficiency is higher by 3% in the nonadjacent 5-resonator system in comparison with an equally spaced system. A relay resonator utilizing adjacent and nonadjacent resonators in both coaxial and

noncoaxial domino resonators is presented in [40], while in [41], a new method for analyzing the maximum transmission efficiency of the WPT system with multiple resonators and asymmetrical relay resonators is introduced. The circuit model for multiple repeaters is quite difficult to solve and use for a design. To overcome this issue, a new design method with an arbitrary number of repeaters is presented in [9]. To further improve the transmission efficiency of the WPT system an intermediate resonant coil is presented in [42].

In [43], it is shown that a negative-index material can amplify evanescent waves which is of interest due to the nature of evanescent wave's resonant coupling. Because of the decoupling of the magnetic and electric field, a negative-index material requires either effective permittivity or permeability to be negative in a deep subwavelength limit. It will enhance the evanescent wave coupling and the transmission efficiency improves from 17% to 47% in [44].

A metamaterial-enhanced WPT system is investigated in [10]. With a metamaterial slab, transmission efficiency reduces more gradually with transmission distance, thus presenting an improved overall efficiency. However, in the over-coupled region, the overall improvement of transmission efficiency is not significant, due to impedance mismatching caused by mutual coupling. In addition, although a metamaterial slab in a WPT system can improve transmission efficiency, the structure does occupy some space between the transmission and receiving resonators. To overcome this issue, coupled resonance enhancement using strong paramagnetic responses of transmitter resonators is introduced in [45]. It does not need any additional resonator or metamaterial slab in between a transmitting and receiving resonator. The traditional driving coil is equipped with an additional resonator with a resonance frequency that is higher than the resonance frequency of the WPT system which increases the effective permeability. This boosts the transmission efficiency from 57.8% to 64.2%.

2.2 WPT Using Magnetically-Coupled Resonant (MCR) for Small Electronic Devices

Nowadays, small portable electronic devices such as smart phones, laptops and tablets are becoming essential gadgets in our daily lives. They are usually powered by batteries

and the batteries often need to be charged almost daily. Most charging is done through wire or cable connections. To remove the cables and provide a more convenient solution to wireless charging, there has been a rapid growth of interest in recent years in developing an MCR-WPT system for small electronic devices.

In order to apply an MCR-WPT system for small portable devices, the size of the receiving coils needs to be comparable. For compact portable devices, the receiving coils need to be small, and consequently the transmitting coils need to be designed to be large enough to retain a desirable transmission distance to the MCR-WPT systems. The coupling between the coils depends on the amount of magnetic flux linked between the transmitting and receiving coils.

In [5], the design and optimization steps of MCR-WPT systems for small devices are discussed. A WPT system with a diameter of 64 mm and 22 mm for transmitting and receiving coils, respectively, is developed, and a transmission efficiency of 82% at a transmission distance of 20 mm is achieved. A WPT system with transmitting and receiving coils with diameters of 114 mm and 20 mm and heights of 10mm and 5 mm, respectively, is designed in [46], and a transmission efficiency of 88% at a distance of 40 mm is achieved.

2.3 Discussion

The recent progress in WPT systems, including mid-range MCR-WPT, is reviewed in this chapter. Although different techniques have been studied to improve transmission efficiency and enable the transmission distance to be maximized, they share a common drawback in that high transmission efficiency and compactness of design are achieved at the cost of reducing transmission distance. The need for developing low-profile, highly efficient, less sensitive and less complicated WPT systems for small electronic and medical devices makes this research worth exploring.

Chapter 3 **NON-PLANAR MAGNETICALLY-COUPLED RESONANT WIRELESS POWER TRANSFER (MCR-WPT) FOR SMALL DEVICES**

In this chapter, efficient and compact non-planar MCR-WPT systems are investigated for charging small devices. A receiver resonator coil and a load loop are studied in correspondence to size restrictions, of small devices. Three different configurations, each consisting of two coils at the transmitter and two coils at the receiver, are studied. The transmission efficiency is measured over different transmission distances and with different orientation angles of the receiver coils. Furthermore, the receiver coils are implanted inside a biological object to show that power can be transferred effectively.

3.1 Theory

Most commercial small devices currently available on the market carry large bulky batteries due to high-energy capacity requirements. These requirements have been proven a persistent obstacle in the design of compact small devices. One of the methods proposed to overcome the problem is wirelessly charging using MCR-WPT systems. An MCR-WPT system consists of four coils, two on the transmitter side and two on the receiver side. When the system is properly designed, electromagnetic energy is inductively coupled from a driver loop to a transmitting resonant coil, creating a magnetic resonance coupled to the receiving resonant coil. The energy or power is then delivered from the transmitter to the load at the load loop.

It has been shown that using two identical resonators to operate in a strongly coupled regime can be highly efficient. However, due to the small size of the receiver devices, both the receiver coils and the transmitter coils have to be small. Hence, if such a design is applied, the power transmission distance will be very limited. In order to improve the power transfer range, the transmitter coils must be large enough to increase the inductance of the coils on the transmitter side and improve the Q-factor of the entire system. As shown in Figure 3-1, the MCR-WPT system utilizes magnetic resonant coupling. The key elements of designing such a system are the compensation capacitors that are used to

achieve resonant coupling between the large transmitter resonator coils and the small receiver resonator coils.

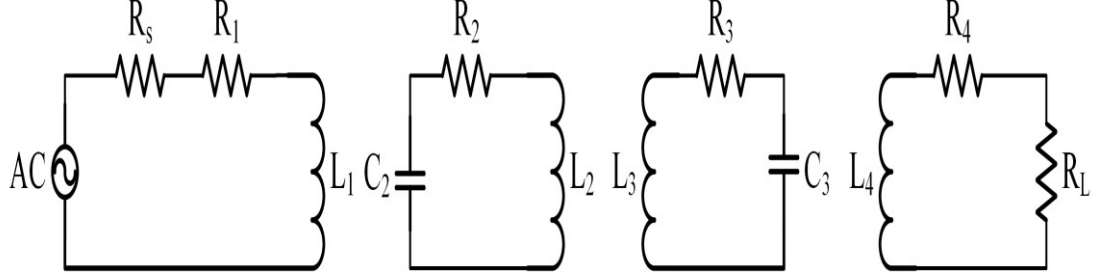


Figure 3-1: Equivalent circuit of a conventional MCR-WPT system.

An MCR-WPT system consists of four coils that can be modeled as a lumped RLC network using equivalent circuit theory. Theoretically, all four coils are coupled with each other, but the cross couplings are very weak and thus can be neglected. In an equivalent RLC circuit, the self-inductance of a loop is calculated as in [47]

$$L = \mu_0 a \left(\ln\left(\frac{8a}{r}\right) - 2 \right) \quad (3-1)$$

where μ_0 is the space permeability, a is the radius of the loop, and r_1 and r_2 are the radii of the two wires. For perfectly aligned coils, the mutual inductance of two parallel single-turn coils can be calculated as

$$M(r_1, r_2, \rho = 0, d) = \mu_0 \sqrt{r_1 r_2} \left[\left(\frac{2}{k} - k \right) K(k) - \frac{2}{k} E(k) \right] \quad (3-2)$$

where

$$k = \left(\frac{4r_1 r_2}{(r_1 + r_2)^2 + d^2} \right)^{\frac{1}{2}} \quad (3-3)$$

and $K(k)$ and $E(k)$ are the complete elliptical integrals of the first and second kind, respectively [47]. For two coaxial circular coils, if the dimension of the wire is relatively small compared to the dimension of the coils, the mutual inductance between two coils can be calculated by:

$$M = \sum_{i=1}^{n_1} \sum_{j=1}^{n_2} M_{ij} \quad (3-4)$$

where n_1 and n_2 are the number of turns of the two coils and M_{ij} is the mutual inductance between the i turn of the first coil and the j turn of the second coil. Considering the skin effect, the loss resistance of a loop is

$$R_L = \frac{\pi a}{r} \left(\frac{f \mu_0}{\pi \sigma} \right) \quad (3-5)$$

where σ is the conductivity of the wire and f is the operating frequency. To achieve identical resonant frequencies for the transmitting and receiving coils, the lumped capacitors are calculated as follows:

$$C_i = \frac{1}{(2\pi f)^2 L_i} \quad (3-6)$$

For a general four-coil MCR-WPT system with two coupled resonators, the circuit equation can be expressed in a matrix form:

$$\begin{bmatrix} Z_{11} & (j\omega M_{12}) & (j\omega M_{13}) & (j\omega M_{14}) \\ (j\omega M_{12}) & Z_{22} & (j\omega M_{23}) & (j\omega M_{24}) \\ (j\omega M_{13}) & (j\omega M_{23}) & Z_{33} & (j\omega M_{34}) \\ (j\omega M_{14}) & (j\omega M_{24}) & (j\omega M_{34}) & Z_{44} \end{bmatrix} \begin{bmatrix} I_1 \\ I_2 \\ I_3 \\ I_4 \end{bmatrix} = \begin{bmatrix} V_1 \\ V_2 \\ V_2 \\ V_4 \end{bmatrix}$$

$$Z_{11} = (R_s + R_1 + j\omega L_1)$$

$$Z_{22} = \left(R_2 + j\omega L_2 + \frac{1}{j\omega C_2} \right) \quad (3-7)$$

$$Z_{33} = \left(R_3 + j\omega L_3 + \frac{1}{j\omega C_3} \right)$$

$$Z_{44} = (R_4 + R_L + j\omega L_4)$$

The imaginary part of the equivalent impedance of the WPT system using magnetic resonance coupling can be assumed to be zero while it operates in resonance. Therefore, the transmission efficiency can be calculated as

$$\eta = \frac{\text{Output Power}}{\text{Input Power}} = |S_{21}|^2 \quad (3-8)$$

The transmission efficiency decreases with the transmission distance and increases with the quality factor, which can be written as:

$$Q = \frac{2\pi fL}{R_L} \quad (3-9)$$

To maximize the transmission distance for a four-coil MCR-WPT system, the mutual coupling between the transmitting resonator and the receiving resonator should be minimized.

3.2 Design

Most small electronic devices have size limitations. For instance, a typical pacemaker has a size of $44 \times 59 \times 7.9 \text{ mm}^3$; hence, in order to realize a practical wireless charging system for small devices, both the receiver resonator coil and the load loop should be small, and the wireless power should be transferred efficiently from the transmitting coils to the small receiving coils with reasonable transmission distances. To improve the transmission efficiency, [48] suggests the application of multi-turn coils for the receiver, whereas [49] uses the rectangular shaped receiver coil with a size of $10 \text{ cm} \times 5 \text{ cm}$. However, those designs are still too large to be applied.

To derive a highly efficient MCR-WPT system with a size suitable for small electronic devices, three symmetrical and asymmetrical designs are proposed and studied. As shown in Figure 3-2, each of the proposed designs consists of four single-turn loops and no matching circuits are required.

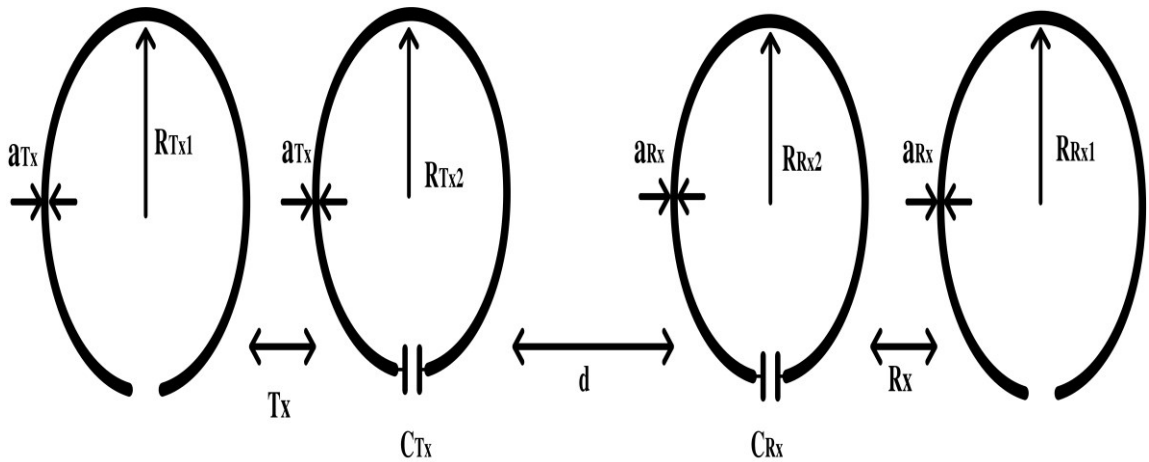


Figure 3-2: The proposed MCR-WPT system using magnetic resonance coupling.

The geometric sizes and design parameters for each set of WPT systems are listed in Table 3-1. Three sets of structures are studied, with various sizes of transmitting and

receiving resonators. The radii of transmitting resonators are chosen to be 200 mm, 50 mm and 50 mm, while the radii of the receiving resonators are chosen to be 50 mm, 50 mm, and 25 mm respectively. Proposed structures were designed to operate at around 18.5 MHz. The key parameters of the systems were first calculated, and then simulated and analyzed with the High Frequency Structural Simulator (HFSS). Due to the intrinsic tolerance of the lumped capacitors, fine-tuning of the capacitors was performed to achieve optimum transmission efficiency.

Table 3-1: Parameters of coils for the three designs

	Design #1	Design #2	Design #3
R_{Tx1} (mm)	150	50	50
R_{Tx2} (mm)	200	50	50
R_{Rx1} (mm)	50	50	25
R_{Rx2} (mm)	50	50	25
a_{Tx} (mm)	12.7	2.8	2.8
a_{Rx} (mm)	2.8	2.8	0.785
T_x (mm)	180	36	36
R_x (mm)	3.25	3.25	3.25
d (mm)	100	100	100
C_{Tx} (pF)	100	360	360
C_{Rx} (pF)	330	360	652

3.3 Results

Figure 3-3 shows the simulated and measured transmission efficiency of design #1 with different distances d between the transmitting and receiving coils. It is shown that the measured transmission efficiency is about 88%, 82%, 63%, 39% and 25% at the distance of 5 cm, 10 cm, 15 cm, 20 cm and 25 cm, respectively. It is shown in [49] that the magnetic coupling between coils can be enhanced by making the transmitter and receiver coil sets identical. Such a strategy was applied to the second design, where the dimensions of the transmitting coils are the same as the receiving coils in the second design, all four coils have a radius of 5 cm. As depicted in Figure 3-4, the measured efficiency at distances of 10 cm, 15 cm, and 20 cm are about 73%, 24%, and 6%, respectively. The capacitances of C_{Tx} and C_{Rx} are 360 pF and 360 pF, respectively.

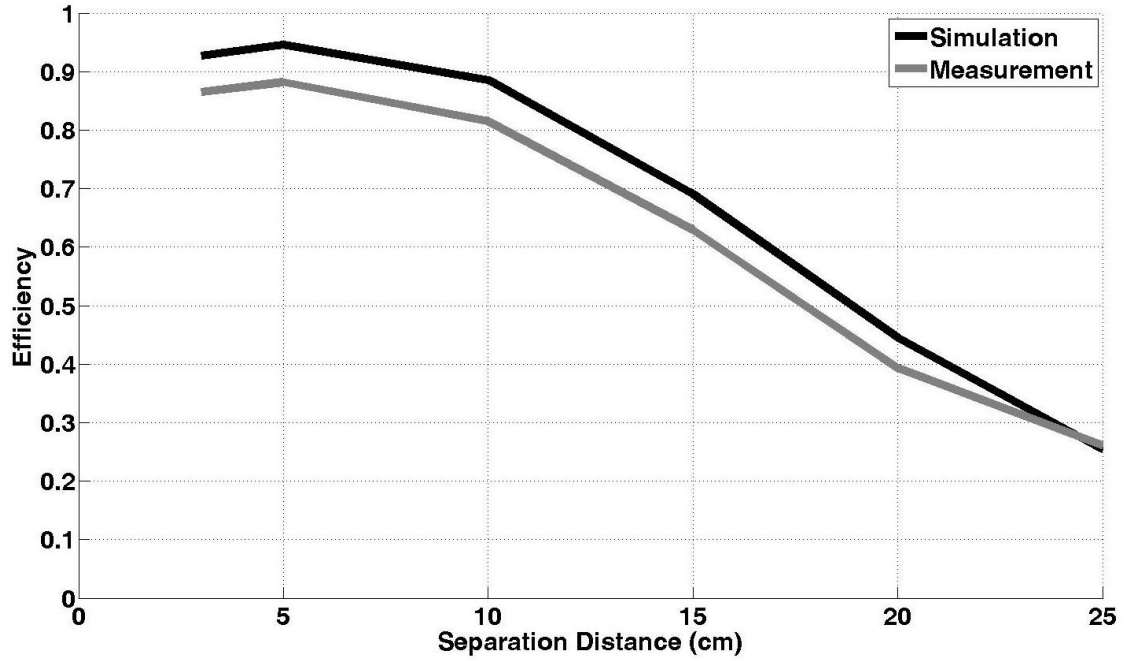


Figure 3-3: Simulated and measured transmission efficiencies of design #1 at different distances of d .

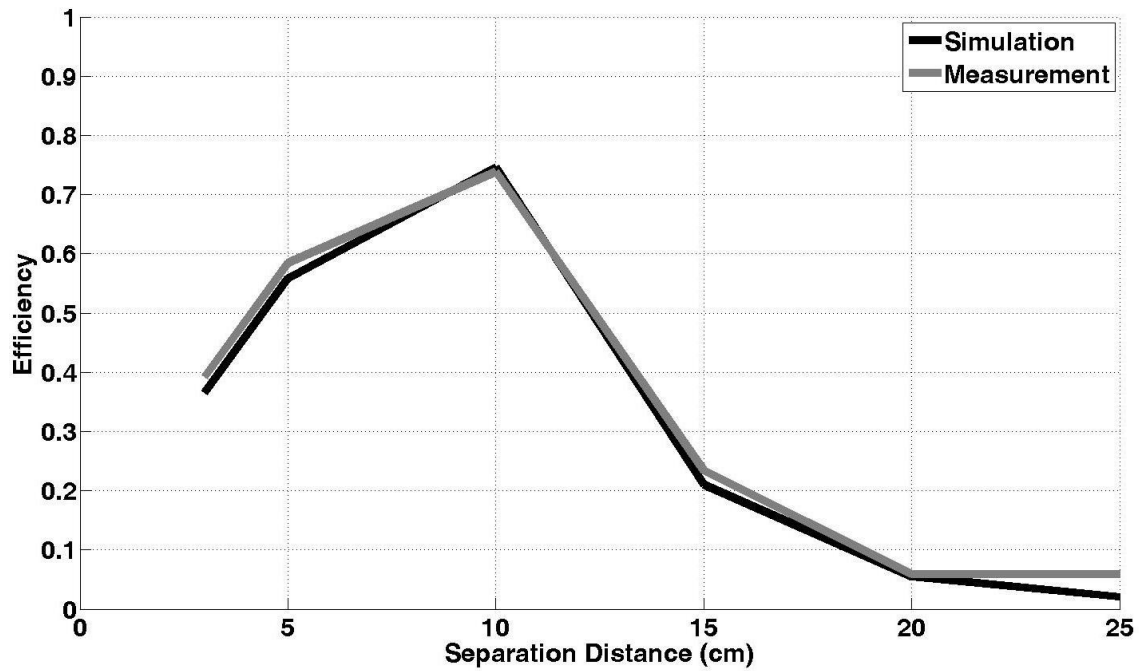


Figure 3-4: Simulated and measured transmission efficiency of design #2 at different distances.

To develop the WPT system for small electronic devices, the third design was carried out with further reduction of the dimensions of the receiver coils. In it, the radius of the resonator coil and the load coil at the receiver side is reduced to 2.5 cm, which is comparable to the cross-sectional dimension of a commercial pacemaker. The compensation capacitors C_{Tx} and C_{Rx} are selected to be 360 pF and 652 pF, respectively. Figure 3-5 plots the S_{21} parameters of design #3 at a transmission distance of 10 cm, where the results computed from the equivalent circuit model are included for comparison. The RLC values of the design are calculated with (3-1)-(3-6) and deployed in the equivalent circuit model to analyze of scattering parameters and transmission efficiency.

The overall performance of design #3 when it is implanted into tissues is also investigated. Figure 3-6 shows the configuration of the simulation setup, where the receiving coil set is embedded inside a stratified medium consisting of skin, fat and muscle layers of different thickness, and placed 10 cm away from a transmitting coil set. Table 3-2 shows the thickness, mass density and electrical properties of different human tissues layers that are used in the full-wave simulation to evaluate the power transmission efficiency of design #3.

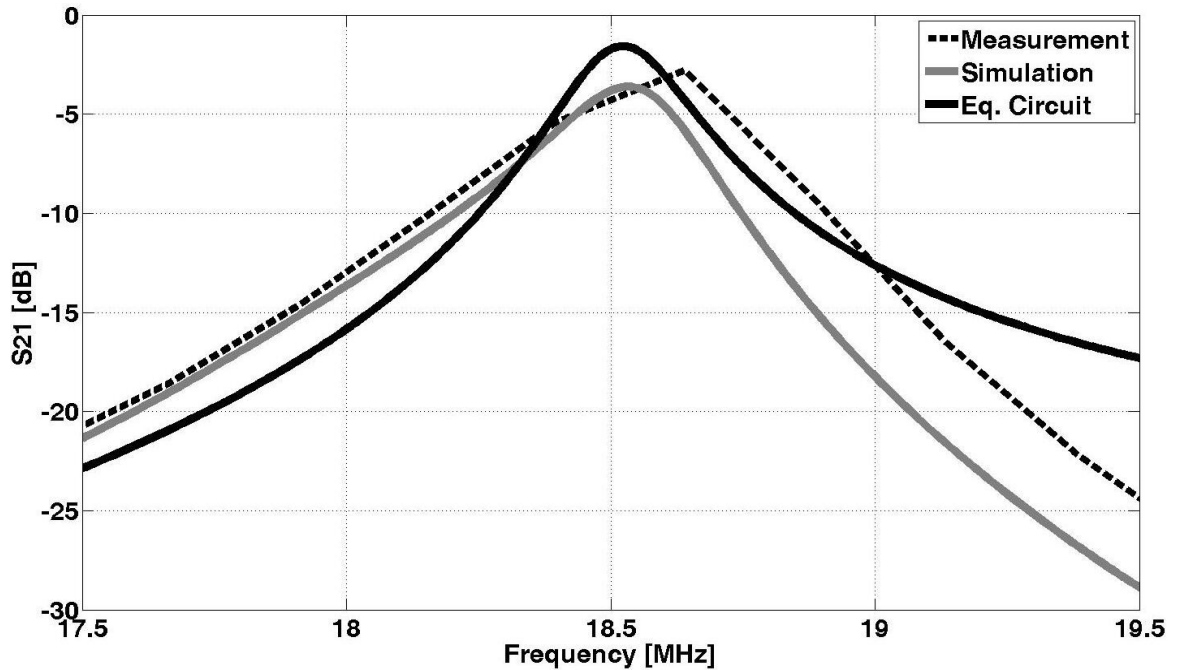


Figure 3-5: S_{21} of design #3 at a transmission distance of 10 cm.

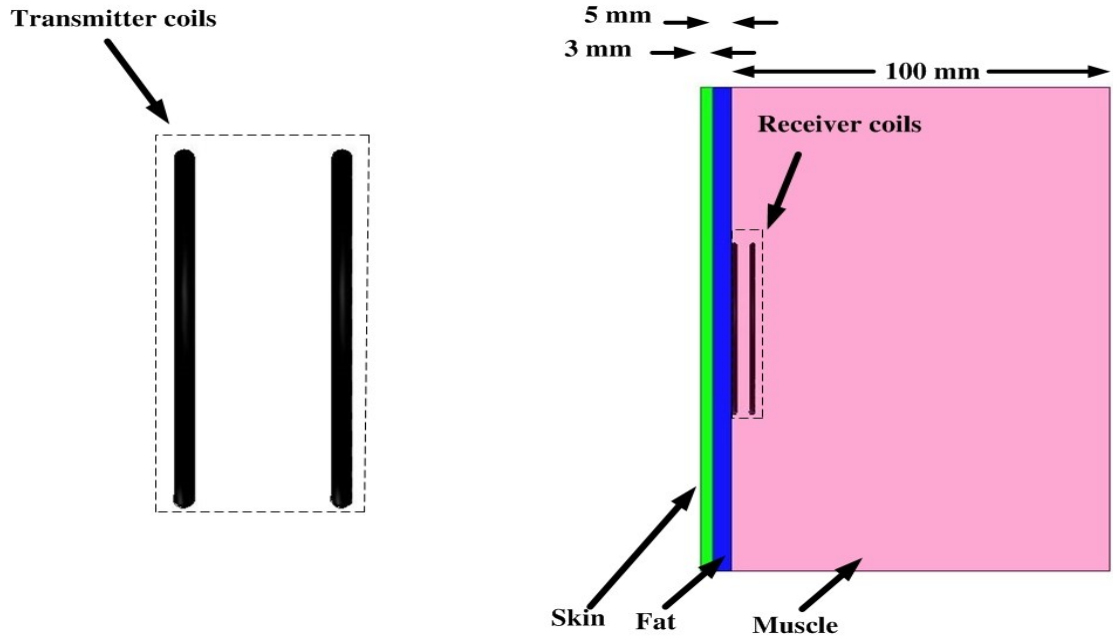


Figure 3-6: Simulation setup for design #3 with the receiver placed inside a stratified medium consisting of skin, fat and muscle layers.

Table 3-2: Physical parameters and electrical properties of the stratified medium at 18.5 MHz [50].

Tissue	Relative electric permittivity (ϵ_r)	Conductivity (S/m)	Thickness (mm)	Mass Density (10^3 kg/m ³)
Skin	222.61	0.279	3	1.1
Fat	10.275	0.031	5	0.92
Muscle	115.28	0.639	100	1.04

Figure 3-7 shows the power transmission efficiency of design #3 at a transmission distance of 10 cm, before and after the receiver was placed into human tissues. As can clearly be seen, the transmission efficiency of the design is 53% when operated in the air and higher than 43% after implantation.

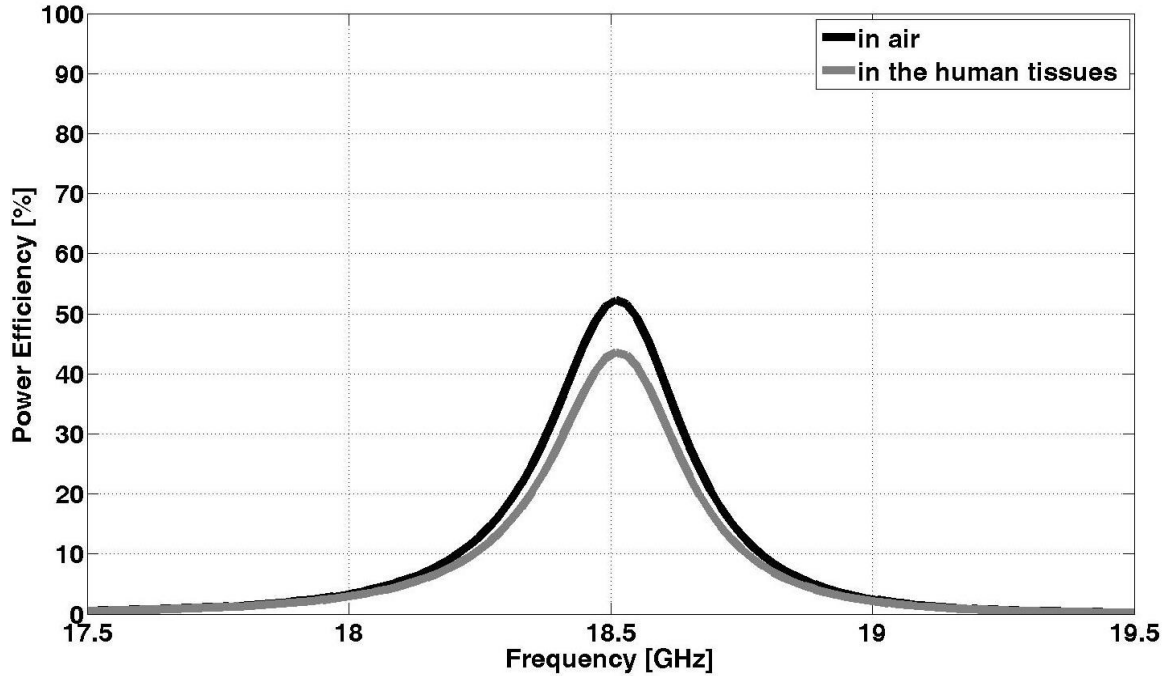
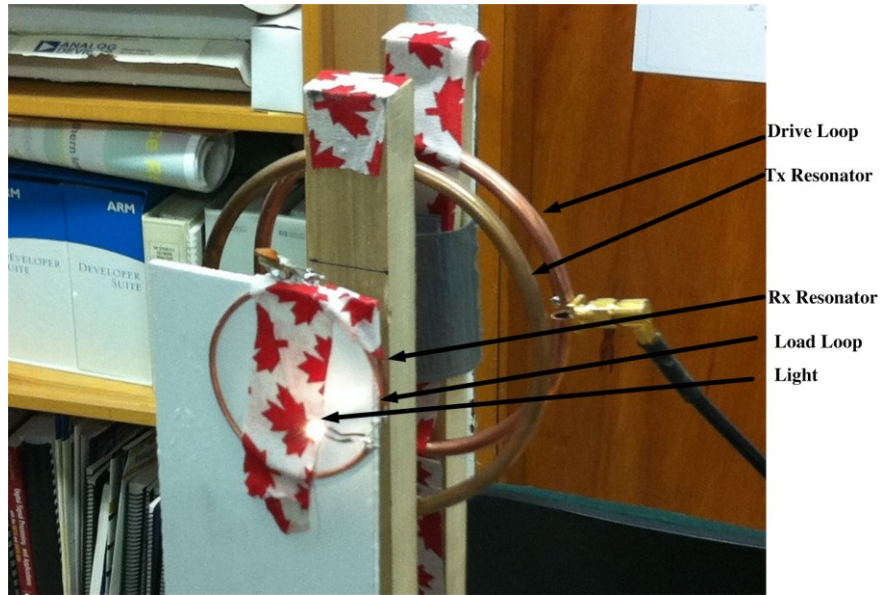


Figure 3-7: Simulation setup for design #3 with the receiver placed inside a stratified medium consisting of skin, fat and muscle layers.

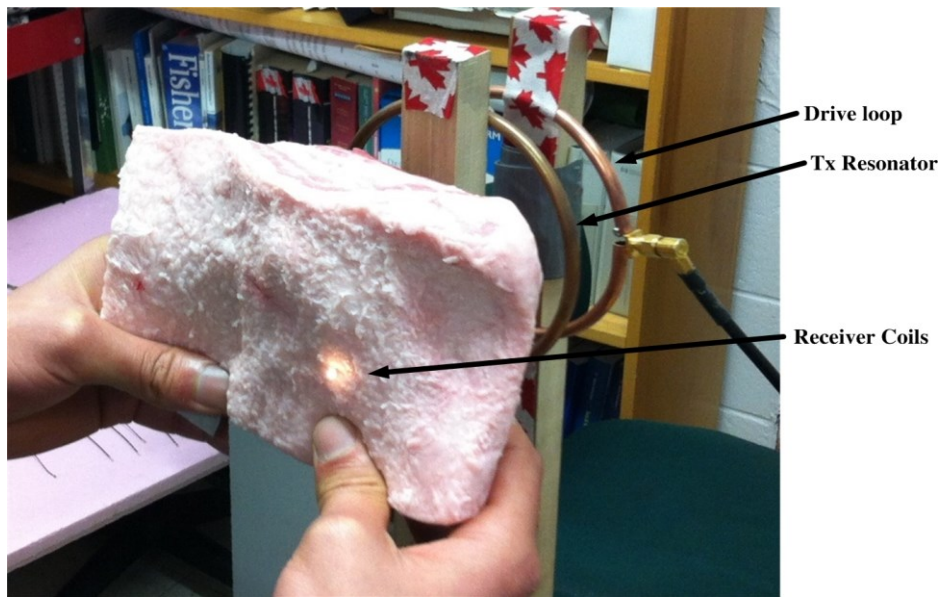
Figure 3-8(a) shows the fabricated third design. To imitate a practical situation, the receiver coils were placed inside a piece of pork meat and tested (see Figure 3-8(b)). A LED light was used as the receiver load and was placed outside skin to be visible.

As shown in Figure 3-9, the measured transmission efficiency at distances of 8 cm, 10 cm, and 15 cm is about 61%, 53%, and 8%, respectively. Furthermore, there was only a small decrease in transmission efficiency when the receiver coils were implanted inside the pork meat.

The performance of the third design with the receiver coils moving around the transmitter coils was also measured. Figure 3-10 shows the transmission efficiency at a distance of 8 cm with varying orientation offset angles between the receiver coils and transmitter coils. As can clearly be seen, power efficiency remains higher than 56% even when the receiver coil is moved up to 60 degrees off the axis of the coils on the transmitter sides. This indicates the nearly omnidirectional performance of the proposed WPT system.



(a)



(b)

Figure 3-8: (a) The fabricated design #3, (b) the receiver coils are inserted into a 4-cm thick pork meat and at a transmission distance of 10 cm.

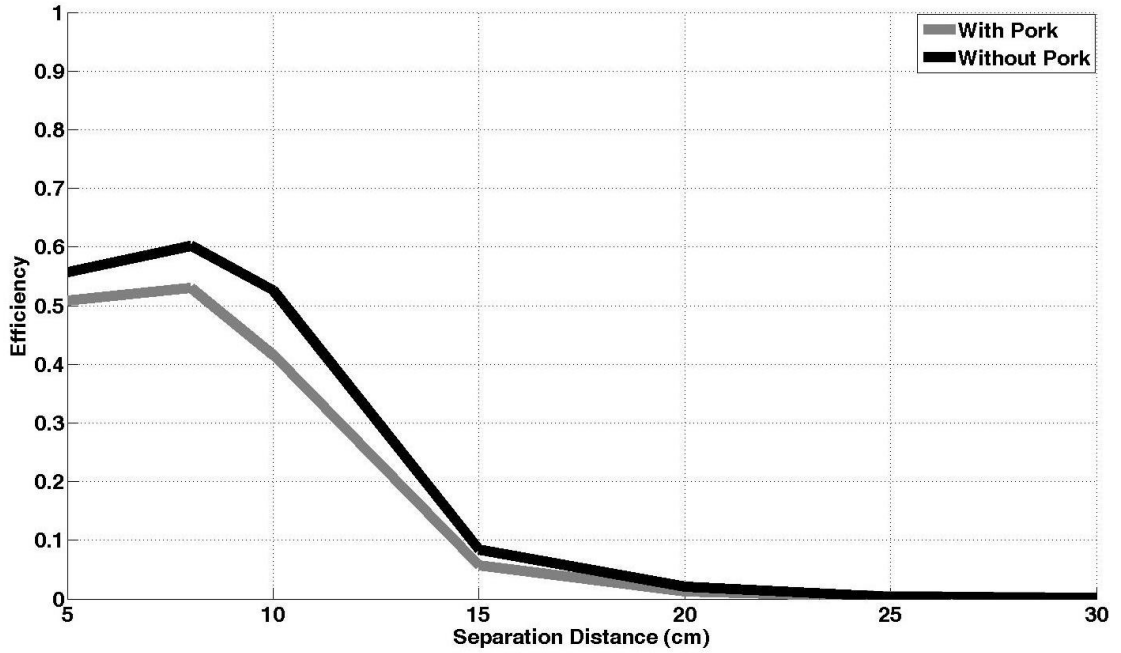


Figure 3-9: Measured power efficiency of design #3 at different distances of d.

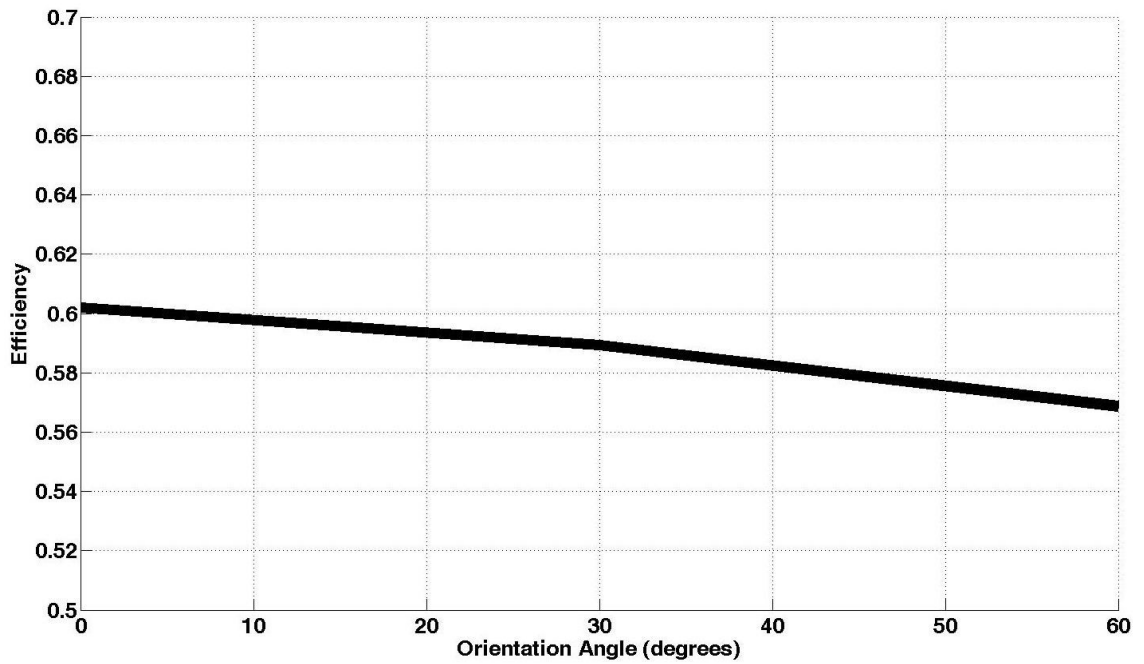


Figure 3-10: Measured power efficiency of design #3 with different orientation angles of receiver coils at a transmission distance of 8 cm.

3.4 Discussion

In this chapter, three wireless power transfer designs using magnetic resonance coupling are studied with different sizes of transmitting and receiving coils. With the radius of receiving coils reduced to 2.5 cm while the transmission efficiency retains higher than 50% in a relatively large transmission distance range, the proposed system can be applied to small electronic and implantable devices, such as pacemakers. Experimental results with the biological objects validated the effectiveness of the proposed wireless power transfer system when implanted.

Chapter 4 **FULLY-PLANAR MCR-WPT FOR SMALL ELECTRONIC DEVICES**

In this chapter, a fully planar wireless power transfer (WPT) system via strongly coupled magnetic resonances is studied. Both the transmitter and the receiver are planarized with the use of coplanar printed spiral coils (PSC) and a printed loop. Comparisons are made in both quality factor and power transfer efficiency of the design with self-resonant printed spirals and with capacitor-loaded printed spirals are made. In addition, the effects of ferrite material and conductive objects on the proposed system are investigated.

An equivalent circuit model of the proposed capacitor-loaded planar WPT system is derived to facilitate the design, and a flowchart is provided for the optimization of the system with given size constraints. To realize high power transmission efficiency, analyses are made of the quality factor of the individual loop or resonator, the mutual coupling between resonators, and the frequency-splitting phenomenon of the system. The effect of the input impedance of the system on the power transmission efficiency is also analyzed. Additionally, techniques are applied to decrease the parasitic resistance and to increase the quality factor of the PSC resonators, and this in turn further improves the transmission efficiency of the proposed planar WPT systems.

4.1 Theory

In the previous chapter, higher power transmission efficiencies over considerably larger transmission distances were realized with non-planar MCR-WPT system. Generally in WPT systems, coils [48] and spirals [35] are widely used as the resonators to create magnetic resonances. A comparison between different topologies in an MCR-WPT system was presented in [51], while in [52], self-resonant helical antennas and capacitor-loaded helical antennas were investigated. Self-resonant resonators in a magnetic resonant coupling WPT system can be considered as electrically very small antennas with very low radiation efficiency and a large reactive electric and magnetic energy which contributes to the coupling between transmitter and receiver [53]. The self-resonant WPT usually has a small self-capacitance. They are sensitive to external objects and hard to tune to a target common resonant frequency of both transmitters and receivers.

To address this issue, a coil resonator using coaxial-like capacitor to adjust a resonant frequency was proposed in [54]. Thus far, most work on magnetic resonant coupling WPT systems uses three-dimensional circular wire loops, spiral loops or helical antennas for the transmitters and receivers. Those coils are often bulky and require precise fabrication to maintain a high quality factor of the coil. This, in turn, poses technical difficulties for the WPT systems to be applied to small electronic devices, and implanted medical devices. Compared to three-dimensional coils, printed spiral coils (PSCs) are more effective as a candidate for a low profile, small-footprint and easy-to-fabricate WPT system. However, only a few studies have investigated the use of PSCs in MCR-WPT systems [21, 22].

In order to yield a maximum power transfer at a given operating distance, the coupling efficiency between the receiver and transmitter resonators should be maximized. As well, and the two coupling coefficients between the source coil the transmitting resonator coil and between the receiving resonator coil and the load coil need to be optimized. To planarize a four-coil WPT system, both the distances between the source and transmitting resonator coils and the distance between the load and receiving resonator need to be substantially reduced. However, the close distance between the coils may cause impedance mismatch between them and consequently degrade the power transmission efficiency of the coupled resonant WPT system. This leads to immense technical difficulties regarding the miniaturization and planarization of the WPT system.

The total quality factor of the spiral resonator is composed of two components defined as [51]:

$$\frac{1}{Q_e} = \frac{1}{Q_C} + \frac{1}{Q_L} \quad (4-1)$$

where Q_C is the quality factor of the spiral capacitor and Q_L is the quality factor of the spiral inductor. For a magnetic resonant coupling WPT, the maximum power transmission efficiency can be achieved at the resonance where the total quality factor is satisfied [51]:

$$Q_e = \frac{1}{M} \quad (4-2)$$

where Q_e is the total quality factor of the spiral resonator and M is the coupling efficiency. In a self-resonant spiral resonator, as the capacitor comes from the parasitic capacitances between the turns, the quality factor of the capacitor is very low, typically several orders of magnitude smaller than the quality factor of the inductor [51]. As a result, the total quality factor of a self-resonant spiral resonator is dominated by the quality factor of the capacitor. Lumped capacitors can be used that have high quality factors. Hence, the quality factor of the capacitor in a spiral resonator can be increased by using the lumped capacitors. Consequently, the higher power transmission efficiency can be achieved as the total quality factor of the spiral resonator is increased. In other words, in comparison to the self-resonant WPT system, a larger proportion of the input power can be delivered from the source in the capacitor-loaded MCR-WPT design.

To obtain an optimal design, the equivalent circuit model of the planarized MCR-WPT system is derived, as shown in Figure 4-1. The complete circuit model of the system with all mutual inductances taken into account is considered in the planar design.

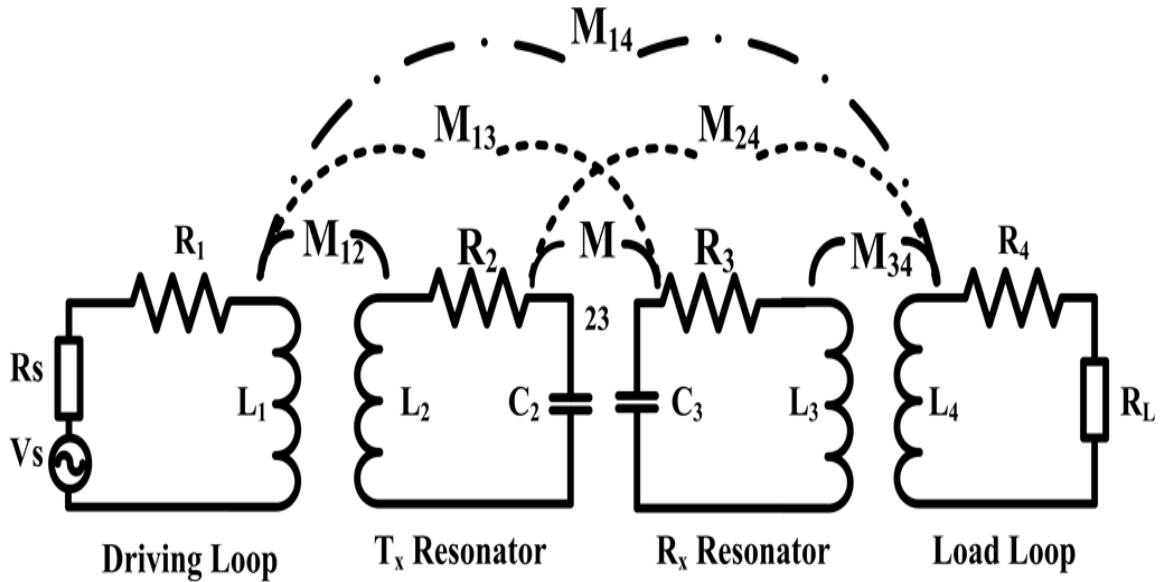


Figure 4-1: Equivalent circuit model of the planarized MCR-WPT system

According to Equation 1 of [55], the self-inductances of rectangular PCSs can be calculated as:

$$L = \frac{1.27\mu_0 n^2 r_{avg}}{2} \left(\ln\left(\frac{2.07}{\varphi}\right) + 0.18\varphi + 0.13\varphi^2 \right) \quad (4-3)$$

where

$$\varphi = \frac{(r_0 - r_i)}{(r_0 + r_i)} \quad (4-4)$$

where φ is the fill factor and n is the number of PCS turns, μ_0 is the permeability of space, r_0 and r_i are the outer and inner radii of the coil, respectively, and

$$r_{avg} = \frac{(r_0 + r_i)}{2} \quad (4-5)$$

The length of the gap can be found from [5]

$$l_g = 4(2r_0 - W_r \cdot n)(n-1) - 4s \cdot n(n+1) \quad (4-6)$$

where W_r and s is the width of the resonator coil in Figure 4-2. The capacitance of a rectangular PSC on a FR4 substrate can be evaluated as [5]

$$C = (0.9\epsilon_{air} + 0.1\epsilon_{sub}) \epsilon_0 \frac{t}{s} l_g \quad (4-7)$$

where ϵ_{air} and ϵ_{sub} are 1 and 4.4 respectively. As suggested by [56], the resistance of a PSC due to the skin effect is given by

$$R_{skin} = R_{dc} \left(\frac{t}{\delta(1 - e^{-t/\delta}) \left(1 + \frac{t}{W_r}\right)} \right) \quad (4-8)$$

where R_{dc} is the dc resistance, t is the thickness of the conductive trace, and δ is the skin depth. According to [57], the resistance of a PSC due to the proximity effect can be defined as

$$R_p = R_{dc} (\beta f + \sigma f^2) \quad (4-9)$$

where f is the frequency, and β and σ are fitting coefficients to be determined empirically. The series resistance of the PCSs can be determined by taking into account the dc resistance, the skin effect, and the proximity effect, that is

$$R_s = R_{skin} + R_p \quad (4-10)$$

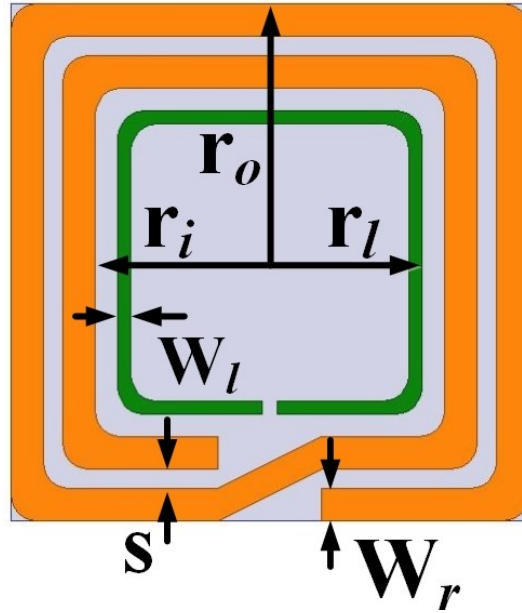


Figure 4-2: The structure of planar MCR-WPT design

In a typical MCR-WPT system, the distance between any two coils is comparable to the radius of the coils. Neumann's equation can be expressed to find the mutual inductance between planar inductors [58].

$$M = \frac{\mu_0}{4\pi} \oint \oint \frac{d\mathbf{l}_1 \cdot d\mathbf{l}_2}{r} \quad (4-11)$$

where $R = \sqrt{a^2 + b^2 + z^2 - 2ab \cos(\varphi_1 - \varphi_2)}$. M can be expressed as:

$$M = \frac{\mu_0 ab}{4\pi \sqrt{a^2 + b^2 + z^2}} \int_{\varphi=0}^{\varphi=2\pi} \frac{\cos(\varphi_1 - \varphi_2)}{\sqrt{1 - \frac{2ab}{a^2 + b^2 + z^2} \cos(\varphi_1 - \varphi_2)}} d\varphi_1 \quad (4-12)$$

For conventional WPT systems, due to the large distance between the transmitter and resonator compared to the radius of the coil, a simplified Neumann's equation for a rectangular shaped coil can be thus applied to the seventh order as follows:

$$M = \left(\frac{4}{\pi}\right)^2 \sum_{i=1}^{i=n_1} \sum_{j=1}^{j=n_2} M_{ij} \text{ and}$$

$$M_{ij} = \frac{\mu_0 \pi a_i^2 b_j^2}{2(a_i^2 + b_j^2 + z^2)^{3/2}} \left(1 + \frac{15}{32} \gamma_{ij}^2 + \frac{315}{1024} \gamma_{ij}^4\right)$$

$$a_i = r_{out_1} - (n_i - 1)(w_1 + s_1) - \frac{w_1}{2}, \quad (4-13)$$

$$b_j = r_{out_2} - (n_j - 1)(w_2 + s_2) - \frac{w_2}{2}$$

$$\gamma_{ij} = \frac{2a_i b_j}{(a_i^2 + b_j^2 + z^2)}$$

However, in our design, the driving/load loop and transmitter/receiver resonator are printed on the same side of the substrate in order to realize the complete planarization of the system. The distance between the two coils is therefore zero, and applying the simplified equation reveals a sizable error in calculating M_{12} and M_{34} . Hence, (4-13) is expanded up to 30th order for more precise evaluation of the mutual inductance, thereby reducing the error. The new equation for mutual inductance can be expressed as

$$M = \left(\frac{4}{\pi}\right)^2 \sum_{i=1}^{i=n_1} \sum_{j=1}^{j=n_2} M_{ij} \text{ and}$$

$$M_{ij} = \frac{\mu_0 \pi a_i^2 b_j^2}{2(a_i^2 + b_j^2 + z^2)^{3/2}} \left(1 + \frac{15}{32} \gamma_{ij}^2 + \frac{315}{1024} \gamma_{ij}^4 + \frac{15015}{65536} \gamma_{ij}^6 + \dots + 0.6028 \gamma_{ij}^{28} \right) \quad (4-14)$$

where r_{out_1} and r_{out_2} are outer radii of PCSs and z is the distance between two PCSs. (4-14) is more accurate than the simplified equation. For instance, with the assumption of $\gamma_{ij}=0.9$, the error in the simplified equation would be 19.75%, whereas with (4-14), the error is reduced to 0.52%.

With the four-port network analysis based on the circuit model shown in Figure 4-1, the current in each coil could be obtained as

$$\begin{bmatrix} I_1 \\ I_2 \\ I_3 \\ I_4 \end{bmatrix} = \begin{bmatrix} Z_{11} & (j\omega M_{12}) & (j\omega M_{13}) & (j\omega M_{14}) \\ (j\omega M_{12}) & Z_{22} & (j\omega M_{13}) & (j\omega M_{24}) \\ (j\omega M_{13}) & (j\omega M_{13}) & Z_{33} & (j\omega M_{34}) \\ (j\omega M_{14}) & (j\omega M_{24}) & (j\omega M_{34}) & Z_{44} \end{bmatrix}^{-1} \begin{bmatrix} V_s \\ 0 \\ 0 \\ 0 \end{bmatrix}$$

$$Z_{11} = \left(R_s + R_1 + j\omega L_1 + \frac{1}{j\omega C_1} \right)$$

$$Z_{22} = \left(R_2 + j\omega L_2 + \frac{1}{j\omega C_2} \right) \quad (4-15)$$

$$Z_{33} = \left(R_3 + j\omega L_3 + \frac{1}{j\omega C_3} \right)$$

$$Z_{44} = \left(R_4 + R_L + j\omega L_4 + \frac{1}{j\omega C_4} \right)$$

where C_1 and C_4 are the parasitic capacitances of the driving loop and the load loop, respectively. By solving the above matrix equation, the ratio between the voltage obtained at the load and the source voltage (V_{load}/V_{source}) can be calculated. The transmission efficiency of the proposed WPT system can then be evaluated as [13]:

$$\eta = |S_{21}|^2 = \frac{V_{Load}^2 / R_{Load}}{V_{Source}^2 / (4R_{Source})} \quad (4-16)$$

where both R_{source} and R_{Load} are assumed to be 50Ω in this work. To obtain the equivalent input impedance of the MCR-WPT, the following expression, as suggested by [36], is

$$Z_{in} = j\omega L_1 + \frac{(\omega M_{12})^2}{Z_{22} + \frac{(\omega M_{23})^2}{Z_{33} + \frac{(\omega M_{34})^2}{Z_{44}}}} \quad (4-17)$$

where $Z_{22} = R_2 + j\omega L_2 + 1/(j\omega C_2)$, $Z_{33} = R_3 + j\omega L_3 + 1/(j\omega C_3)$.

4.2 Self-Resonant and Capacitive-Loaded Planar MCR-WPT

Here we propose a fully planarized MCR- WPT system with both the source/load loop and the transmitting /receiving resonator coil printed on the same side of an FR4 substrate. Figure 4-3 shows the two design variations, one with the self-resonant PSC and the other with a capacitor-loaded PSC of the same dimension. In the current stage, a three-turn PSC is applied to both designs. Table I lists the design parameters of the proposed planar WPT system. To maximize the quality factor of the PSC resonator, the filling factor, defined as the ratio between width W_3 and spacing s (W_3/s), is optimized. Another critical design parameter is the radius of the source loop that affects the distance between the source loop and the PSC resonator and is optimized for impedance matching.

As shown in Figure 4-3(c), a 32 pF lumped capacitor is connected to the two ends of the spiral strip from the back of the substrate in the proposed planar capacitor-loaded WPT

design. Figure 4-4 shows the power transmission efficiency of the self-resonant and capacitor-loaded WPT system. In the self-resonant MCR-WPT system, E- and H- field stored energies are identical at the resonant frequency and convey energy. Conversely, in the capacitor-loaded MCR-WPT system, the E-field is concentrated in the capacitor and power is conveyed by the H-field [52]. The simulated results show that the capacitor-loaded WPT system exhibits higher power transmission efficiency than the self-resonant WPT system, as the transmission distance is increased.

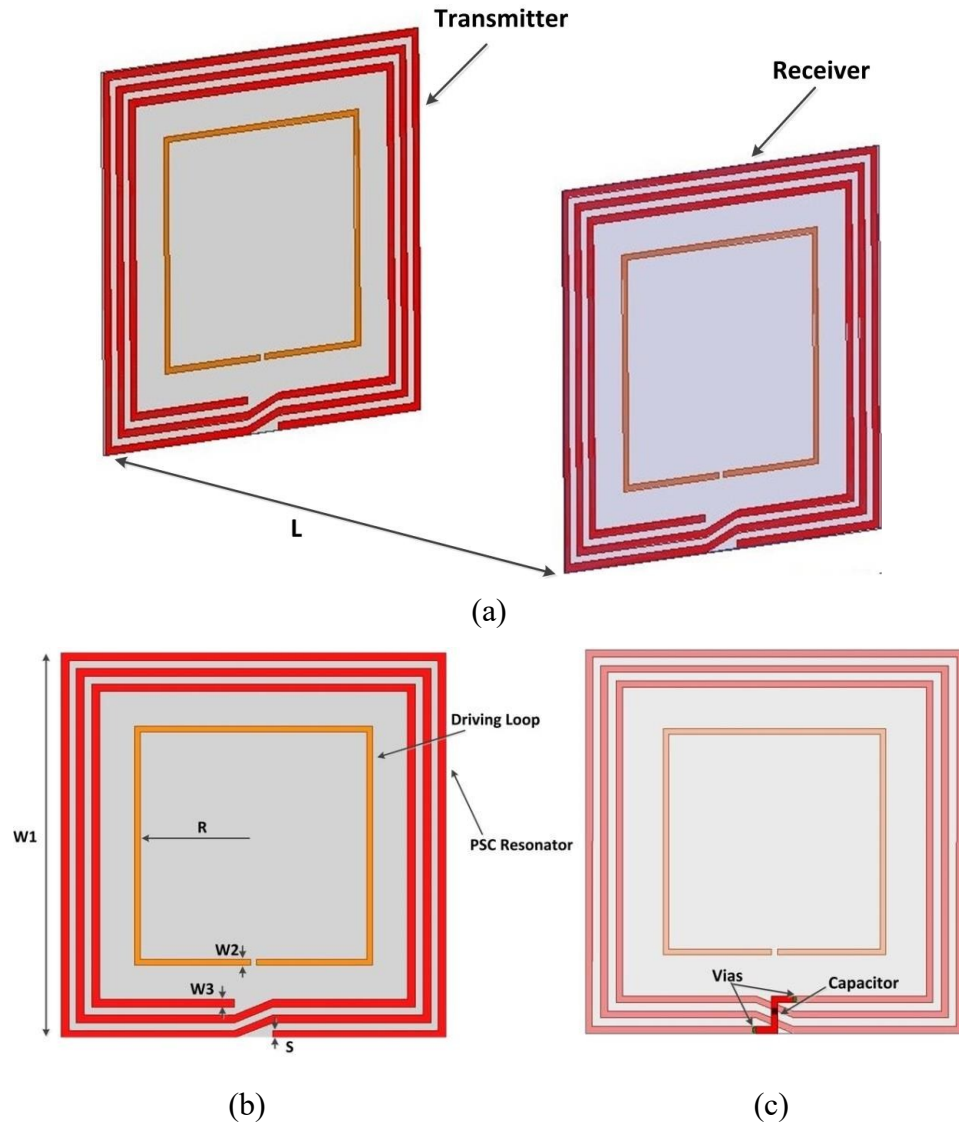


Figure 4-3: (a) Overview of the proposed planar WPT system, (b) the front-view of the transmitter design in the planar WPT system with self-resonant PSC, (c) the back-view of the transmitter design in the planar WPT system with capacitor-loaded PSC.

Table 4-1: Design parameters

W_1 (mm)	200	R (mm)	59
W_2 (mm)	3	L (mm)	200
W_3 (mm)	3.3	Capacitor (pF)	35
S (mm)	4		

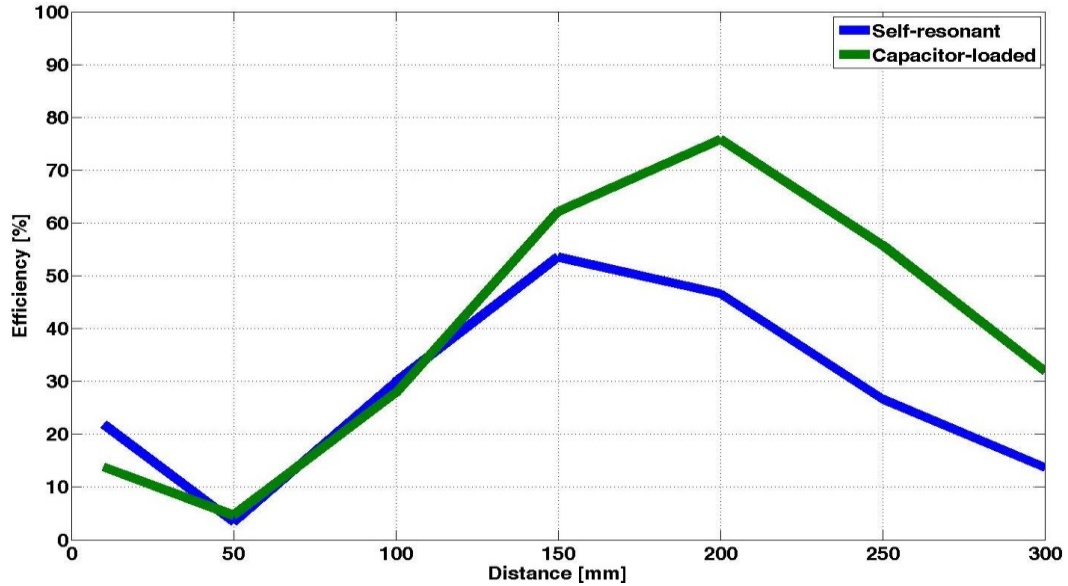


Figure 4-4: Simulated power transmission efficiency of the planar WPT with self-resonant and capacitor-loaded PSC resonators over various transmission distances.

The proposed planar WPT system with the capacitor loaded PSC was fabricated and tested. As shown in Figure 4-5, the PCS resonators, source and load loops are printed on an FR4 substrate with a thickness of 1.6 mm. Figure 4-6 plots the measured power transmission efficiencies of the design over various transmission distances at the resonant frequency of 13.56 MHz, where the simulation results are included for comparison. As shown, the measured results are in good agreement with the simulation results. The measured peak transmission efficiency and the simulated one of the proposed system are about 74.1% and 76%, respectively, at the transmission distance of 200 mm. The slight difference is most likely caused by fabrication errors.

Figure 4-7 shows the measured power transmission efficiency of the capacitor-loaded WPT as a function of operating frequency over a distance of 10 mm to 500 mm between the transmitter and receiver. As depicted, when the distance between the two PCS resonators is reduced, the resonant coupling WPT system becomes over-coupled, and two

local maximum power transmission efficiencies occur at two distinct frequencies: one corresponding to the odd coupling mode between resonators, and the other corresponding to the even coupling mode.



(a)

(b)

Figure 4-5: (a) The fabricated planar capacitor-loaded WPT system, (b) measurement setup.

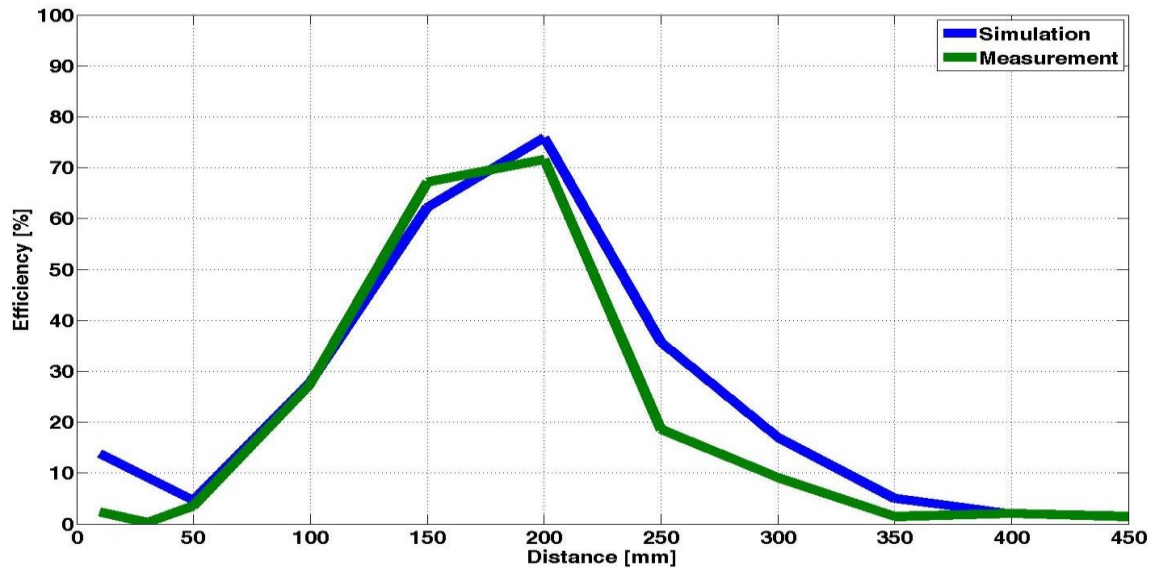


Figure 4-6: Measured and simulated power transmission efficiency of the capacitor-loaded WPT system at 13.56 MHz.

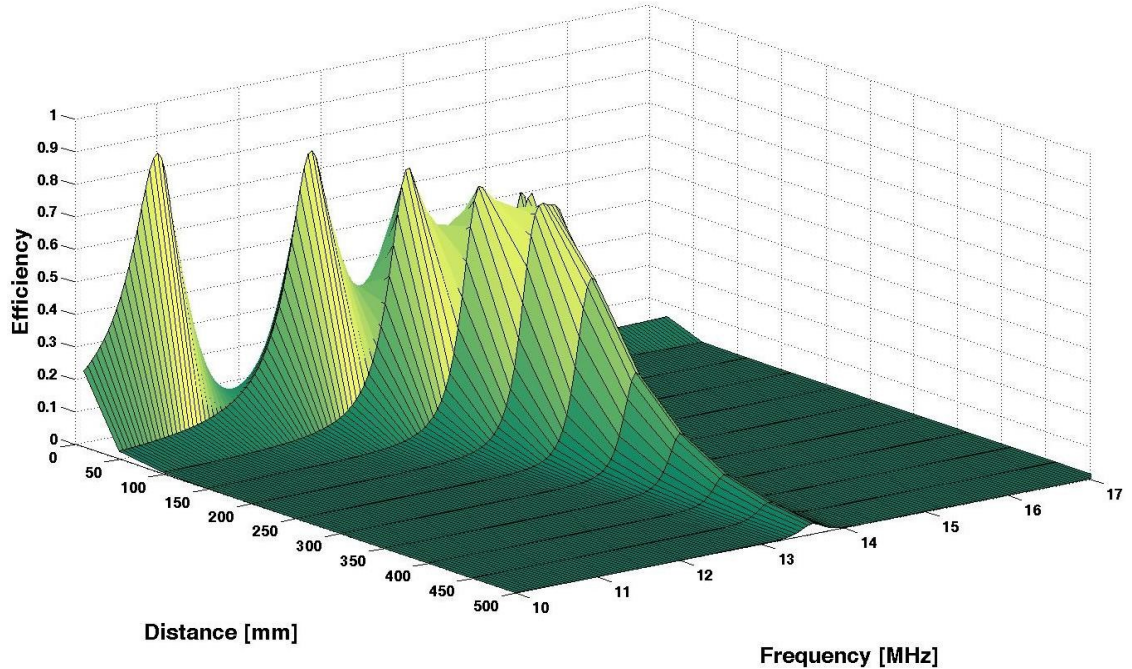


Figure 4-7: Measured power transmission efficiency of the capacitor-loaded WPT system as a function of distance and operating frequency.

4.2.1 Effect of Ferrite Material

According to [59], the power transmission efficiency of the proposed planar WPT system can be further improved if the leakage of the magnetic field can be minimized. To reduce the magnetic field leakage, ferrite plates are applied to the proposed WPT structure as magnetic reflectors. Two rectangular ferrite plates ($\mu_r=2500$, $\tan\delta/\mu_r=5\times 10^{-6}$ (@0.1 MHz)) are placed behind the transmitter and receiver sets respectively, at a distance of D . The geometrical size of the ferrite plates and the distance of D are optimized to yield maximum improvement of the power transmission efficiency. As thin ferrite sheets tend to be fragile, a ferrite plate with a thickness of 7 mm was used for structural purposes. The size of the plate is $350\times 350\times 7$ mm³ and the optimum distance of D was found to be 7 mm. Figure 4-8 illustrates the power transmission efficiency of the WPT system after the application of ferrite plates. The maximum power transmission efficiency of the capacitor-loaded WPT system increased from 76% to 82.8% at a distance of 200 mm in the presence of ferrite plates. Table 4-2 also lists the maximum power transmission efficiency of the

self-resonant WPT system with and without ferrite plates. However, ferrite materials are expensive and make the WPT system bulky and hard to implement.

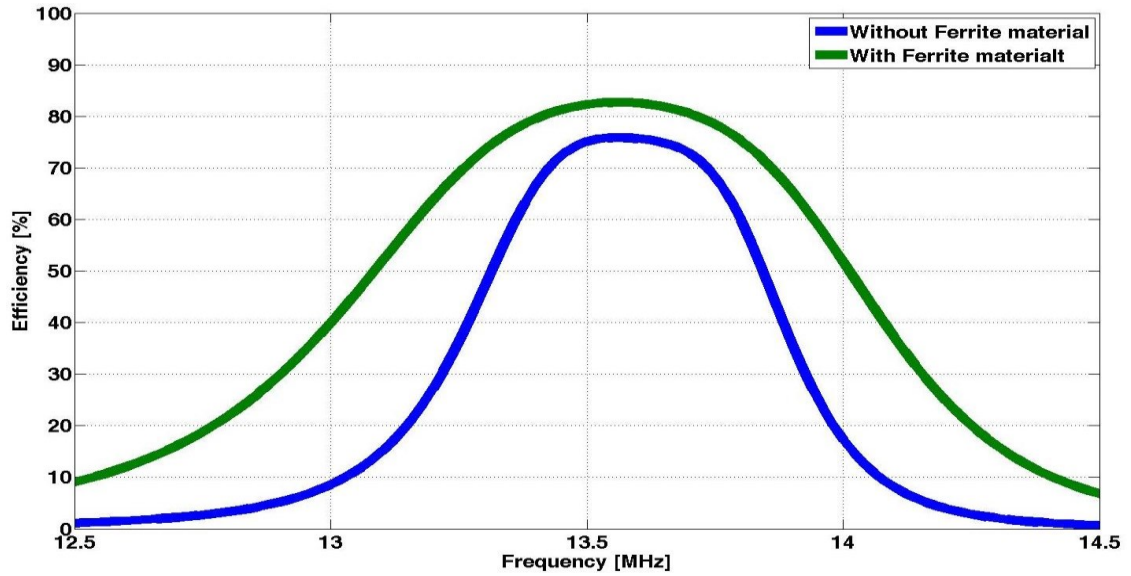


Figure 4-8: Simulated power transmission efficiency of the capacitor-loaded WPT system at a distance of 200 mm with and without ferrite plates.

Table 4-2: The maximum power transmission efficiency of the proposed planar structures

	Capacitor-Loaded	Self-resonant
Proposed PSC model	76%	46.5%
With ferrite material	82.8%	62%
With PEC	22%	4.7%

4.2.2 Effects of Conductive Objects

The effects of conductive objects that are in close proximity to the proposed planar WPT designs with self-resonant PSC and capacitor-loaded PSC are also investigated. The ferrite plates are replaced with a copper plate of the same thickness. The results indicate that the power transmission efficiency and the resonant frequency of the self-resonant WPT system is more sensitive to surrounding conductive objects compared to the capacitor-loaded WPT system.

As shown in Table 4-2, at a transmission distance of 200 mm, the maximum power transmission efficiency of the planar self-resonant WPT system is reduced from 82.8% to 22%, while the transmission efficiency of the capacitor loaded WPT system is reduced from 62% to 4.7%. This observation can be explained by the electric field spatial distribution of two designs. Specifically, with the capacitor-loaded PSC resonator, the electric field is mostly trapped within the lumped capacitor and the magnetic field coupling dominates the field coupling between the transmitter and receiver. In the WPT system with the self-resonant PSC resonator, however, both the electric and magnetic field coupling exist between the transmitter and the receiver [52], leading to more substantial efficiency degradation when the copper plates are inserted.

4.3 Optimization of Planar MCR-WPT System

To design a practical MCR-WPT system for small electronic devices, the size of the WPT coils needs to be reduced. First, the size of the proposed planar WPT system is reduced from 200 mm to 100 mm. However, when the coils are resized, there is less room for driving and load loops. Therefore, the critical parameters of the MCR-WPT system need to be optimized to achieve the highest feasible transmission efficiency. To do that, with an accurate equivalent circuit model of the proposed planar WPT system, we need to analytically study and analyze the input impedance of the system, the quality factor of individual loops and resonators, the mutual coupling between resonators, and the frequency-splitting phenomenon of the WPT. With a systematic design procedure, the critical design parameters, including the number of turns for the PSC, the dimensions of driving and load loops, and the dimensions of the resonators are derived to yield the optimum transmission efficiency of the planar WPT system with specific size constraints.

As the proposed planar MCR-WPT system aims to provide the efficient wireless power transfer to small portable electronic devices, the maximum dimension of both the transmitter and receiver of the system is constrained to 10 cm, and is designed to exhibit maximum power transmission efficiency at a distance of 10 cm. As discussed in [35], to maintain a sufficient quality factor of the load loop, the Q_{Load} has to be greater than $1/Q_{Resonator}^{1/2}$; therefore, the inner radius of a PSC resonator is limited in order to leave sufficient space for the driving and load loops.

Another critical design factor is the input impedance of the whole system, which greatly depends on mutual coupling. The parameter of r_l (Figure 4-2) has a significant effect on the frequency-splitting phenomenon, as the extremely large impedance angle and relatively low amplitude can reduce the efficiency [36]. Therefore, for each design, an optimal radius of the driving and load loops needs to be defined for maximum efficiency. Figure 4-9 illustrates the systematic procedure used in this work for the analytical design of the planar MCR-WPT system.

The number of turns of the PCS resonators starts at one for optimized efficiency, and gradually increases up to seven. Furthermore, the initial geometric parameters of the PSC are defined to be $r_o=50$, $r_l=20$, $W_r=1$, $W_l=1$ and $s=1$ mm. The optimization is then performed with a MATLAB program using Particle Swarm Optimization scheme to optimize the other physical dimensions for the highest transmission efficiency analytically. By running the optimization processes with PSC resonators of different numbers of turns, we found that the 2-turn PCS resonator gives the highest peak of transmission efficiency. Although, with increasing the number of turns the quality factor of the resonator can be improved, but due to the limited size of the radius of the driving loop/load loop, a strong impedance mismatching occurs. The design parameters of the planar WPT design with 2-turn PCS resonators are then fine-tuned with HFSS v15 to further improve the efficiency prior to fabrication. Table 4-3 shows the finalized design parameters of the proposed planar WPT system with 2-turn PCS resonators.

Table 4-3: Design parameters, RLC values

	2-turn WPT	2-turn WPT with parallel paths
W_r (mm)	4	2.5
W_l (mm)	6.3	6.3
r_o (mm)	50	50
r_l (mm)	29.5	29.5
s (mm)	3.7	3.7
L_2 (μ H)	0.61	0.58
C_2 (pF)	220	240
R_s (Ω)	0.19	0.15
Q_2 (unloaded) @13.56 MHz	274	328
SRF (MHz)	134.25	130.2

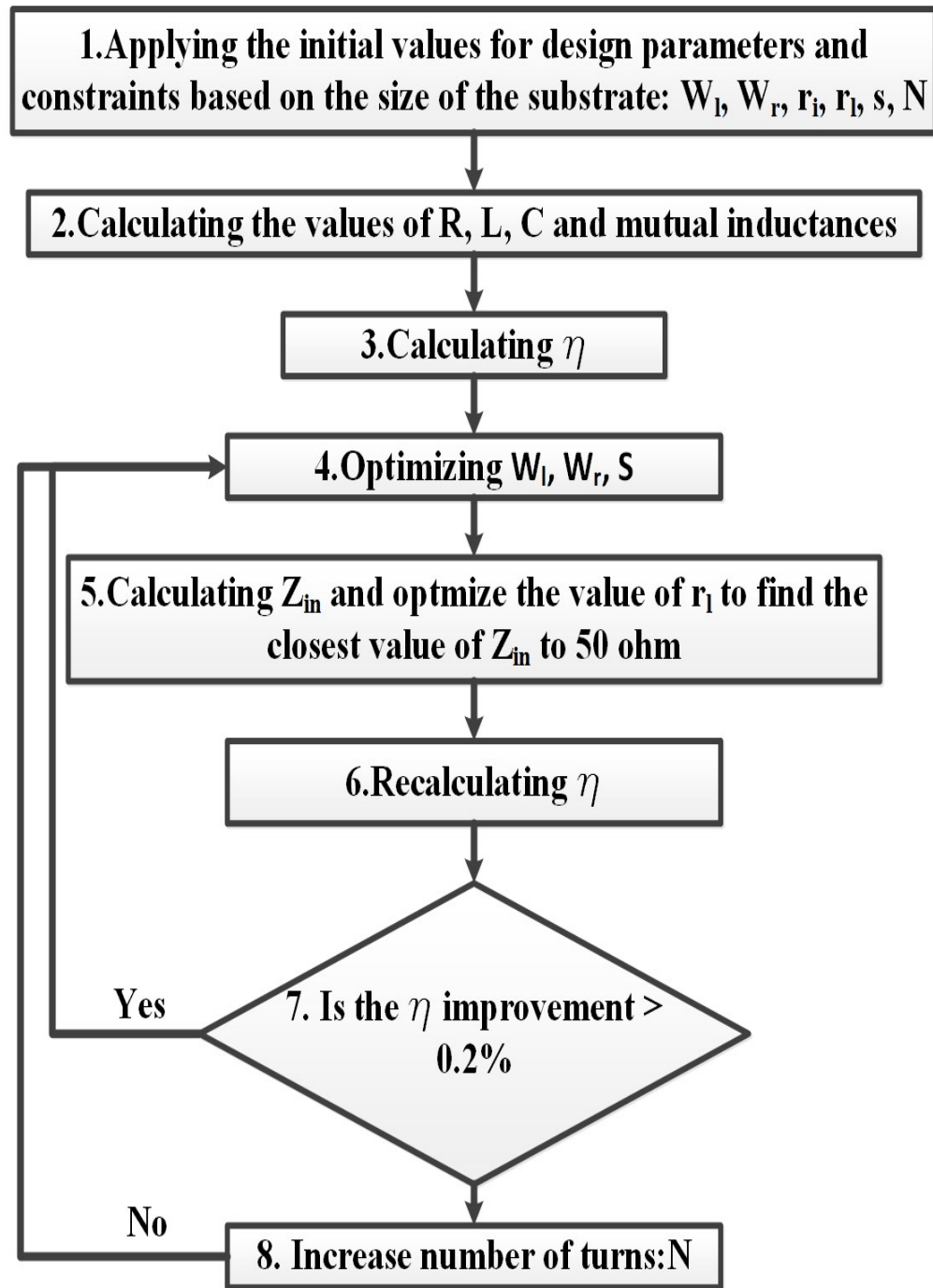


Figure 4-9: PSCs design flowchart.

4.3.1 Efficiency Improvement by Auxiliary Strips

A dual-spiral resonator was proposed in [60] to further increase the quality factor of the resonators. However, it has been observed in this present work that the quality factor of the

resonator decreases dramatically as the space between two interconnected spiral coils reduces. As the objective of this research endeavor is to design a complete planar MCR-WPT system for wireless power transfer to small electronic devices, the PSC resonators were printed on the FR4 PCB board with a thickness of 1.6 mm to form the planar transmitter and receiver. In order to increase the Q factor of the resonator without sacrificing the low axial profile of the planar WPT system, two identical auxiliary strips are applied to the backside of transmitter and receiver, respectively, and then connected to the resonators on the opposite side of the substrate through vias.

Figure 4-10(b) shows the layout of the auxiliary strips where the size of W_b and s_b are the same as the size of W_r and s . As seen in Table 4-3, after being loaded with parallel paths, the resistance of the resonator due to the proximity effect decreases from 0.19Ω to 0.15Ω (21% reduction), and consequently the unloaded Q -factor of the planar WPT system increases from 274 to 328.

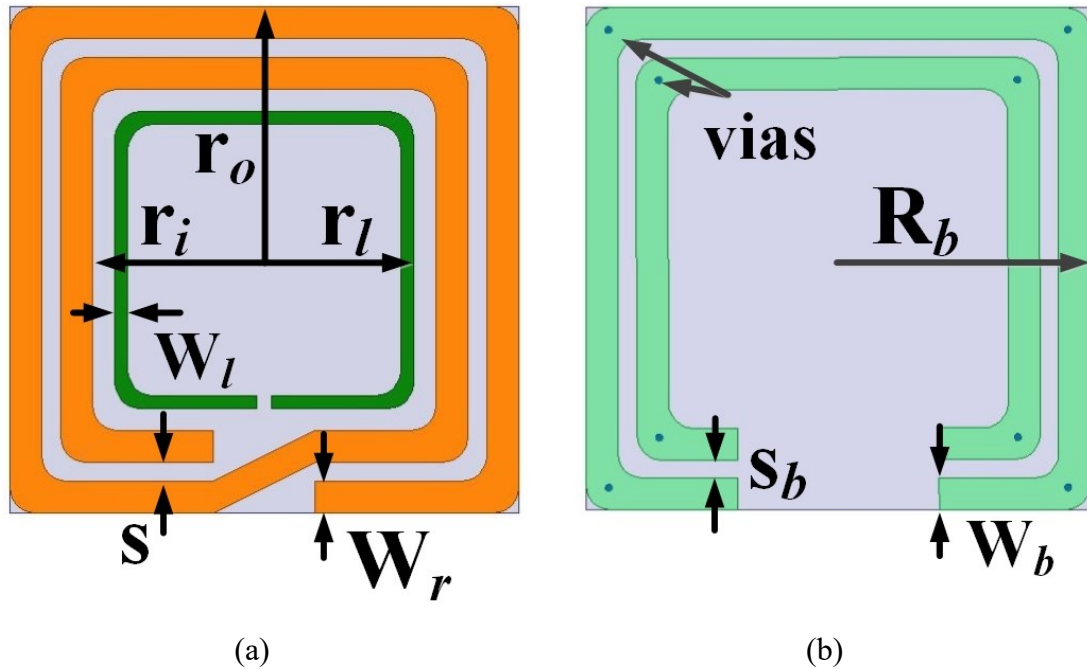


Figure 4-10: (a) Geometry of the proposed PSC, (b) geometry of the auxiliary strips on the bottom side of the substrate

Figure 4-11 shows the photo of the proposed planar MCR-WPT system with 2-turn resonators after fabrication. Figure 4-12 presents the calculated, simulated and measured

efficiency of the MCR-WPT system with and without parallel paths, at a transmission distance of 10 cm. As shown, the proposed planar WPT systems operate at 13.56 MHz, and the experimental results are in good agreement with both the analytical results from the RLC equivalent circuit and the simulated ones from HFSS.

The results indicate that, the proposed planar WPT system is able to provide efficient power transmission with efficiency higher than 77 %. Moreover, with the parallel paths, the maximum power efficiency of the system is further improved by 4.41%. Table 4-4 gives a comparison of the maximum power transmission efficiency of the planar WPT system with and without parallel paths, and Figure 4-13 presents the maximum power transmission efficiency of the proposed WPT systems at different transmission distances.

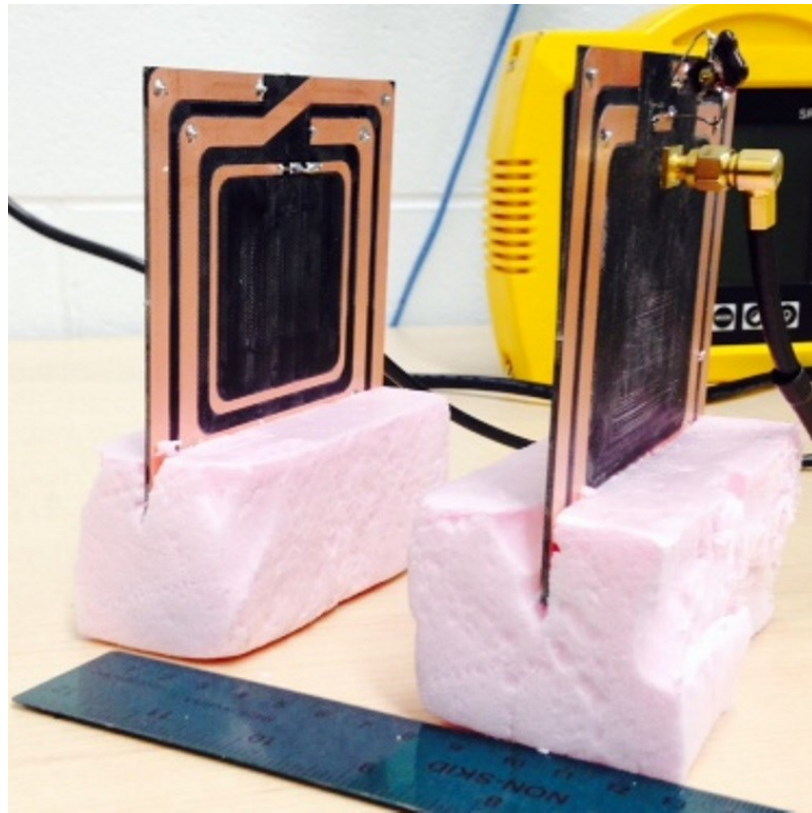


Figure 4-11: Geometry of the proposed PSC with auxiliary strips on the backside of the substrates.

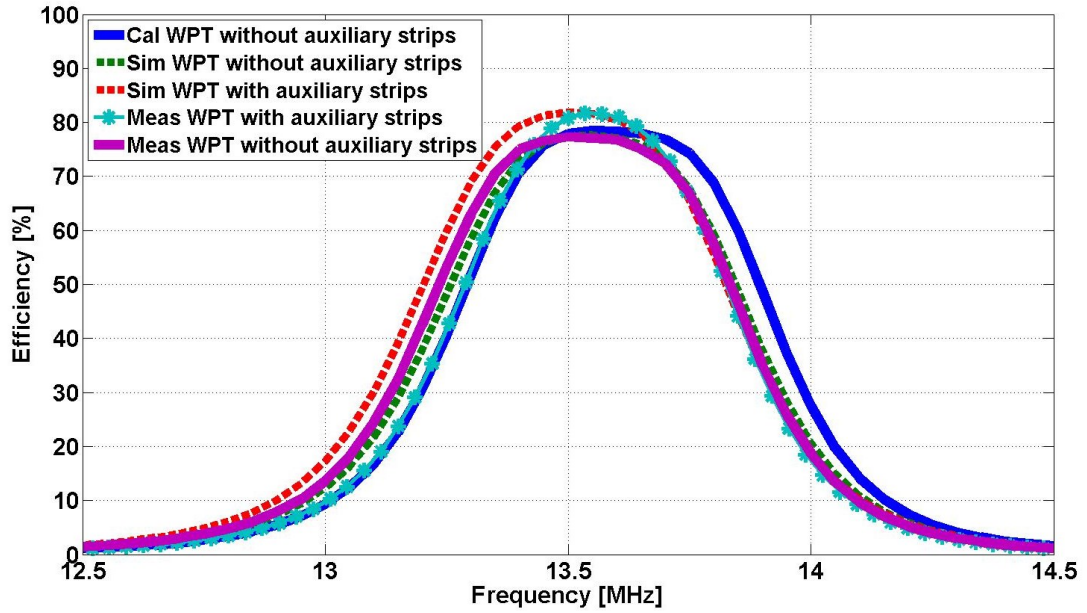


Figure 4-12: Analytical, simulated, and measured transmission efficiency of the proposed planar MCR-WPT system at a distance of 10 cm.

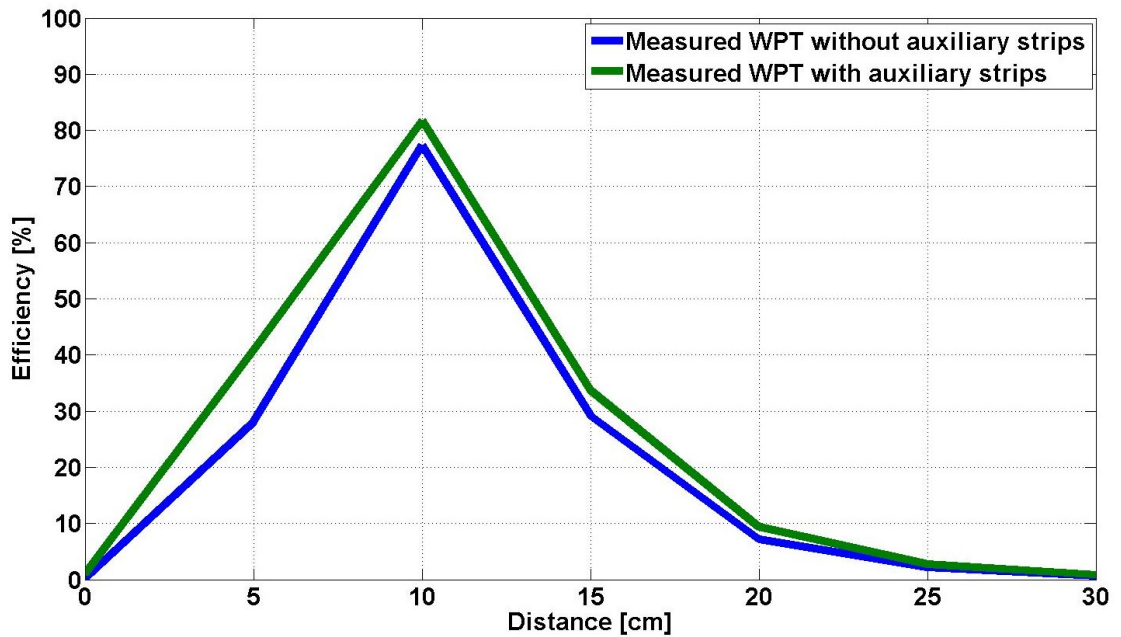


Figure 4-13: Measured transmission efficiency at different transmission distances.

Table 4-4: The maximum transmission efficiency of the proposed WPT system with auxiliary strips

	2-turn WPT	2-turn WPT with parallel paths
Calculated	78.46%	-
Simulated	77.51%	81.87%
Measured	77.27%	81.68%

4.3.2 Multilayer Planar MCR-WPT system

To further, improve the transmission efficiency of planar MCR-WPT systems, an additional resonator with the same dimension is added to the transmitter/ receiver substrate. As shown in Figure 4-14, two PCS resonators with the same dimension are printed on the opposite side of the substrate. In the presence of the second resonator, the mutual coupling between the two resonators rises and the resonance frequency of the WPT system shifts upward. The value of the lumped capacitor is then fine-tuned to adjust the resonance to the desired frequency at 13.56 MHz. A comparison of the quality factor between the 2-layer resonator and the conventional resonator reveals that the quality factor of the 2-layer resonator is increased from 274 to 363. In order to further increase the quality factor of the MCR-WPT system, a conductive shorting wall is applied to the outer edge of the substrate to connect both resonators together. By applying the shorting walls on the all four sides of the substrate, the resistance of the resonators due to proximity effect decreases and the quality factor of the PSC resonators increases from 363 to 416.

To further investigate the effect of the multi-layer resonator on the transmission efficiency of the MCR-WPT system, a 3-layer transmitter/receiver resonator is proposed. In this design, as shown in Figure 4-15, two PSC resonators are printed on the opposite sides of the first substrate, whereas the driving/load loop and the third PSC resonator are printed on the top and bottom surfaces of the second substrate, respectively. To yield a compact and low profile structure, two substrates are stacked together with conductive shorting walls applied to the outer edges of structure to attach all three PSC resonators together. With such a layout, the quality factor of the proposed MCR-WPT system is increased to 435.

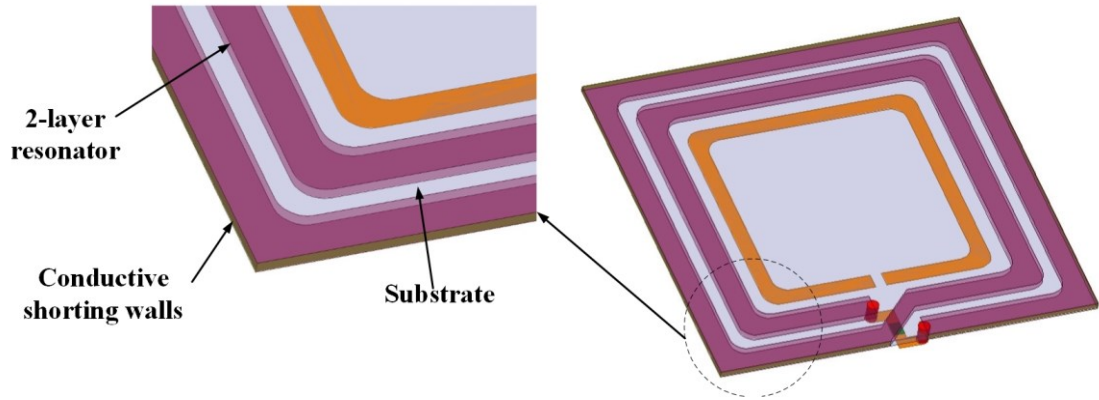


Figure 4-14: Geometry of the proposed planar MCR-WPT systems with 2-layer PSC resonator using a conductive shorting wall

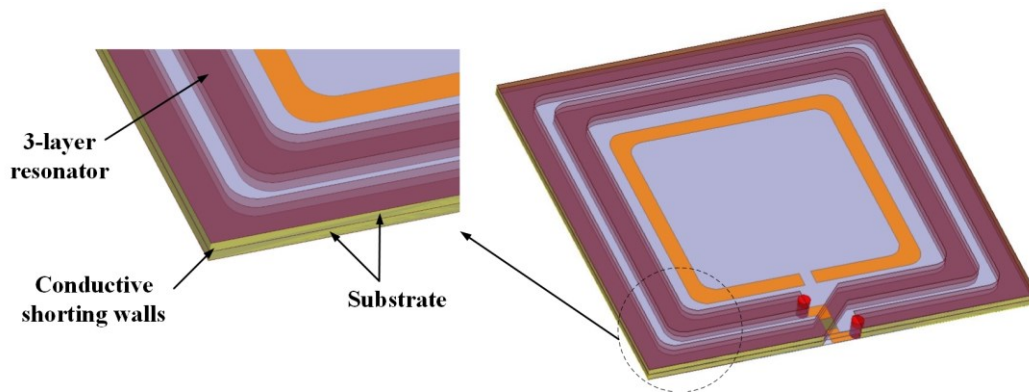
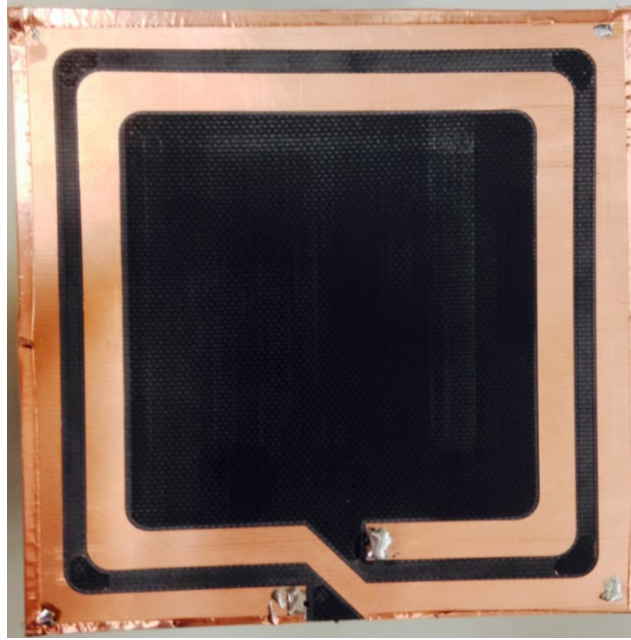
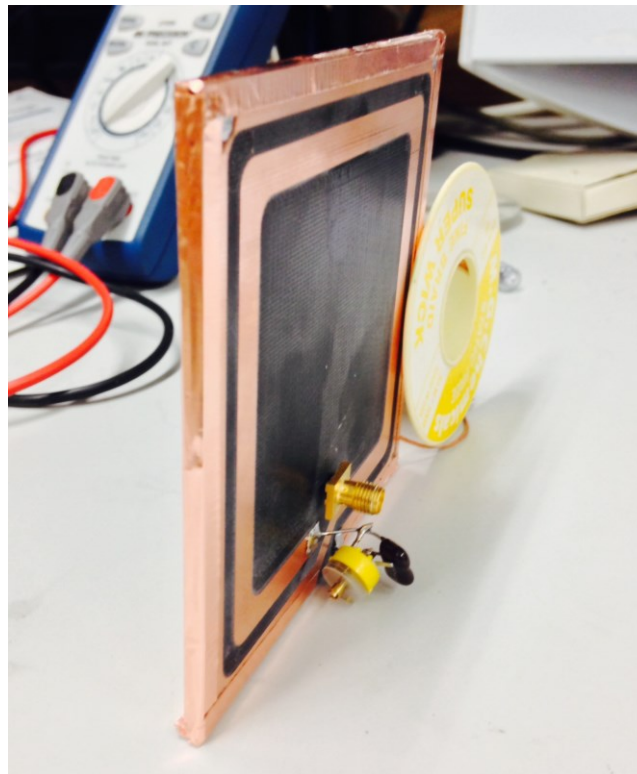


Figure 4-15: Geometry of the proposed planar MCR-WPT systems with 3-layer PSC resonator using a conductive shorting wall

The PSC resonators are printed on FR4 substrates with a thickness of 1.6 mm, and the planar MCR-WPT system is designed to operate at 13.56 MHz. The design parameters of the conventional planar WPT are $w_r=4$ mm, $w_l=6.3$ mm, $s=3.7$ mm, $r_i=29.5$ mm and $n=2$, and the lumped capacitor is chosen to be 220 pF. For the 2-layer and 3-layer, PCS resonator, the lumped capacitor is fine-tuned to 240 pF and 250 pF, respectively, to have the resonance frequency at 13.56 MHz. Figure 4-16 shows the fabricated planar MCR-WPT system with 3-layer PCS resonators with conductive shorting walls.



(a)



(b)

Figure 4-16: Fabricated 3-layer PSC resonator with conductive shorting walls; a) top view, b) side view.

Figure 4-17 depicts the simulated and measured transmission efficiency of the conventional planar MCR-WPT and the proposed MCR-WPT with 3-layer resonator. The measurement results reveal that, the transmission efficiency of the proposed planar MCR-WPT with 3-layer PSC resonator is improved from 77.27% to 84.38% in comparison to the conventional planar MCR-WPT, at a nominal distance of 10 cm.

Table 4-5 shows the maximum transmission efficiency of the conventional planar MCR-WPT and the proposed MCR-WPT with different layers of resonators. As depicted, the transmission efficiency of the planar MCR-WPT is increased from 77.27% to 79.75% by adding another layer of PCS resonator, and the efficiency is further increased to 82.67% by adding shorting walls.

Figure 4-17 shows the measured transmission efficiency at different distances between transmitter and receiver at 13.56 MHz. The proposed planar WPT system with 3-layer PSC resonator with shorting walls offers higher transmission efficiency than the conventional planar WPT system at distances larger than 7.5 cm. However, the transmission efficiency in over-coupled region remains almost the same.

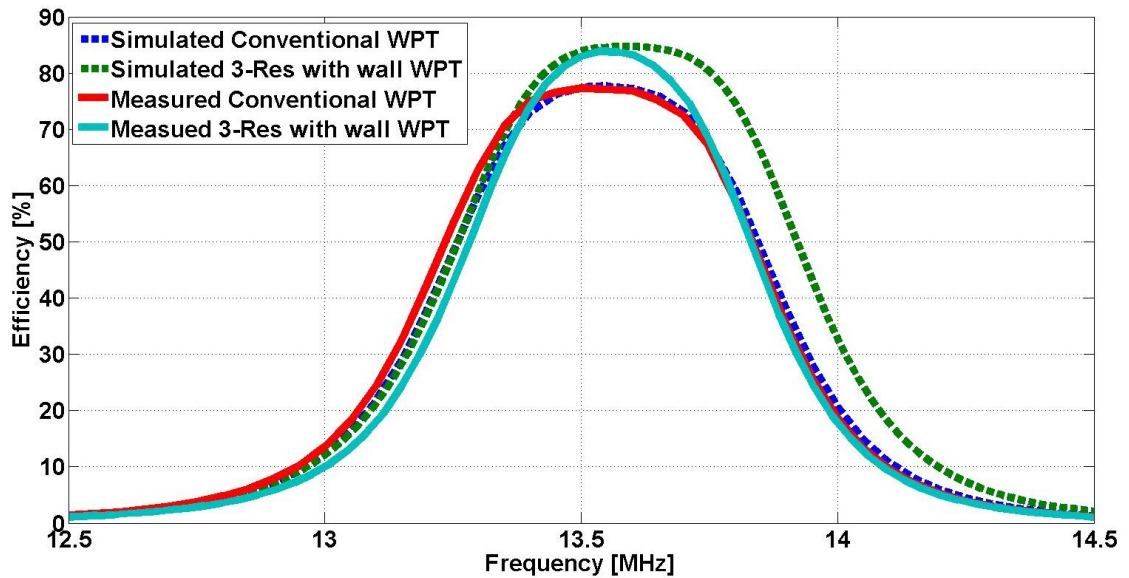


Figure 4-17: Transmission efficiency of conventional planar MCR-WPT and proposed planar MCR-WPT at a nominal distance of 10 cm.

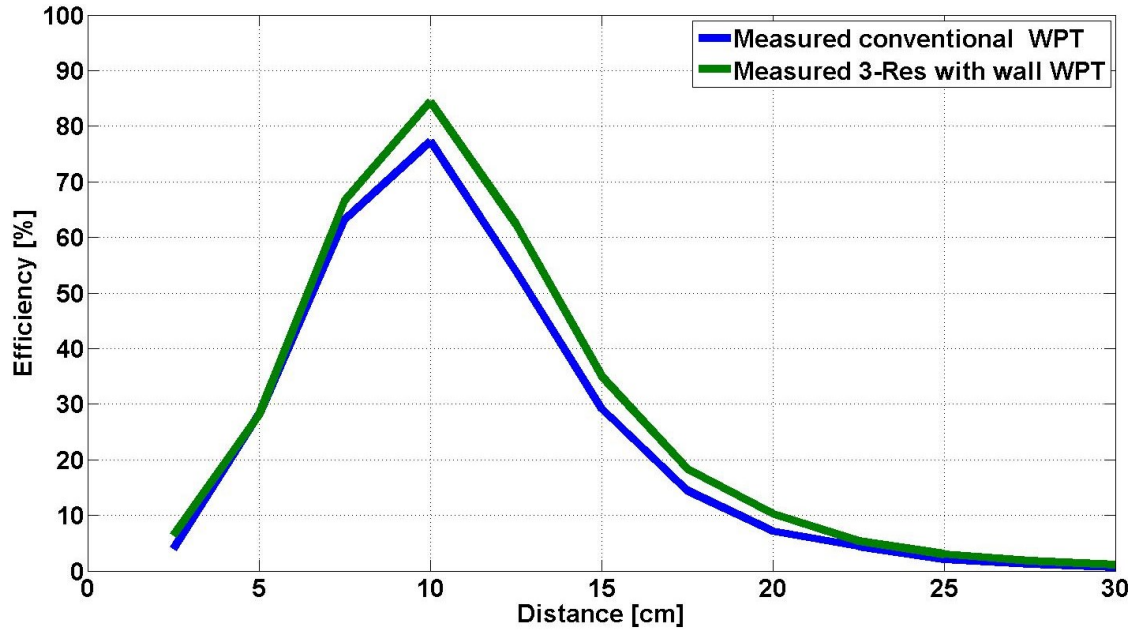


Figure 4-18: Measured transmission efficiency against distance at 13.56 MHz.

Table 4-5: Maximum transmission efficiency of the proposed multilayer MCR-WPT systems

	Simulated (%)	Measured (%)
Conventional	77.51	77.27
2-layer resonator	80.49	79.75
2-layer resonator with wall	83.29	82.67
3-layer resonator	82.43	82.01
3-layer resonator with wall	84.71	84.38

4.3.3 Asymmetrical MCR-WPT System

To make the WPT-MCR system more practical for small electronic devices, a size constraint of 50 mm × 50 mm for the receiving side and 100 mm × 100 mm for the transmitting side is applied. Therefore, all parameters of the MCR-WPT system for an asymmetrical structure are re-designed and optimized. In addition, to increase the quality factor of the resonator, the auxiliary strips technique is applied to both the transmitting and receiving resonators. A nominal transmission distance can be calculated by

$$D = \sqrt{r_{o_Tx} \times r_{o_Rx}} \quad (4-18)$$

where r_{o_Tx} and r_{o_Rx} are the radii of transmitting and receiving resonators, respectively. The transmission distance of 70 mm is chosen with regard to the size constraint of both resonators. To further increase the transmission efficiency of the WPT system, a matching circuit is designed for both source and load loops as shown in Figure 4-19. Table 4-6 gives the optimized parameters for the asymmetrical planar MCR-WPT system with and without matching circuit. Figure 4-20 shows the transmission efficiency of the WPT system versus distance.

The results indicate that, the proposed asymmetrical planar WPT system is able to provide efficient power transmission with efficiency higher than 78.46 % and 74.37% with and without matching circuit, respectively. Figure 4-21 shows the transmission efficiency of the asymmetrical planar MCR-WPT system with one when the receiver is moved along the xy plane parallel to the transmitter at $D=70$ mm. In addition, the receiver is moved along the φ and θ directions as shown in Figure 4-22. The transmission efficiency results in Figure 4-23 depicts that the transmission efficiency of the system is very stable with different orientation angles and varies from 76.91% to 78.75%.

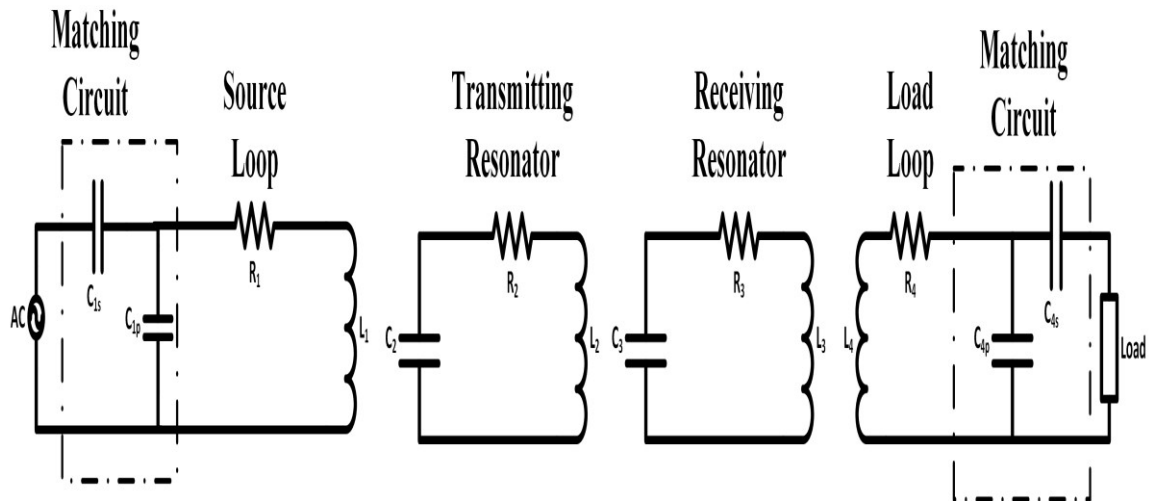


Figure 4-19: Equivalent circuit model of the MCR-WPT system with matching circuit

Table 4-6: Design parameters, *RLC* values of asymmetrical WPT system.

	Without matching circuit	With matching circuit
$W_{r\ Tx}$ (mm)	6.3	6.3
$W_{l\ Tx}$ (mm)	2.9	2.9
$r_{o\ Tx}$ (mm)	50	50
$r_{l\ Tx}$ (mm)	24	24
$S\ Tx$ (mm)	3.2	3.2
$W_{r\ Rx}$ (mm)	3.4	3.4
N_{Tx}	3	3
$W_{l\ Rx}$ (mm)	1	1
$r_{o\ Rx}$ (mm)	25	25
$r_{l\ Rx}$ (mm)	15.8	15.8
$S\ Rx$ (mm)	1.4	1.4
N_{Rx}	2	2
C_2 (pF)	150	135
C_3 (pF)	527	427
C_{1p} (pF)	-	380
C_{1s} (pF)	-	188
C_{4s} (pF)	-	382
C_{4p} (pF)	-	414

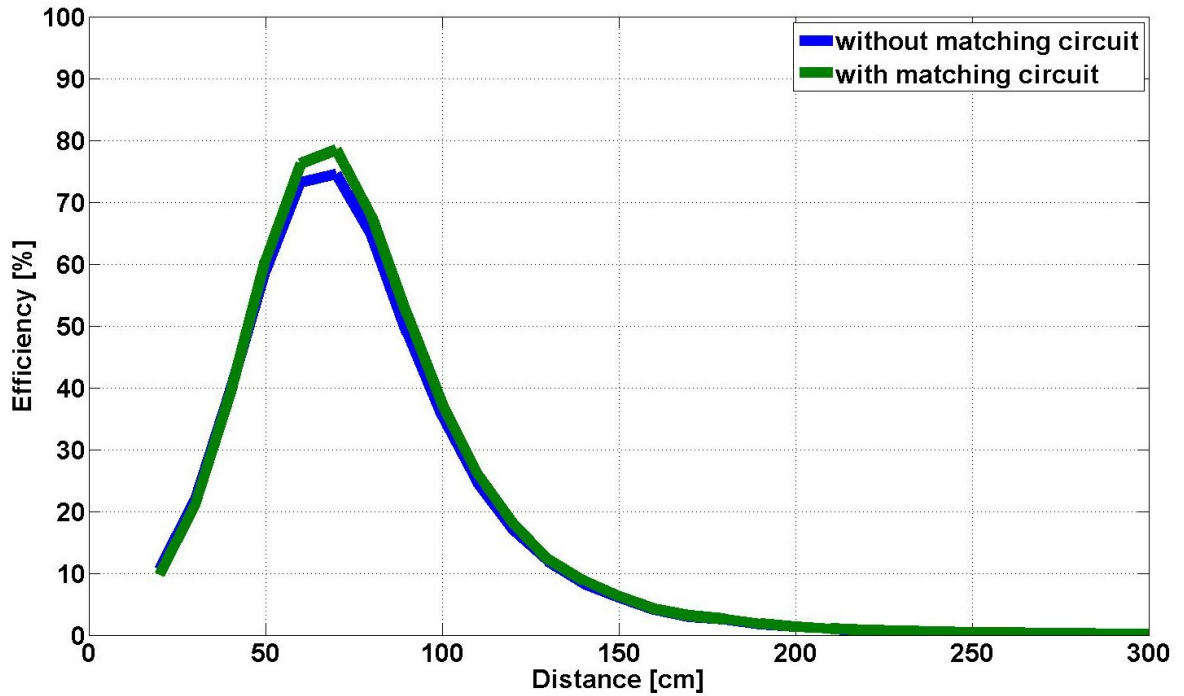


Figure 4-20: Transmission efficiency of asymmetrical MCR-WPT system against distance at 13.56 MHz.

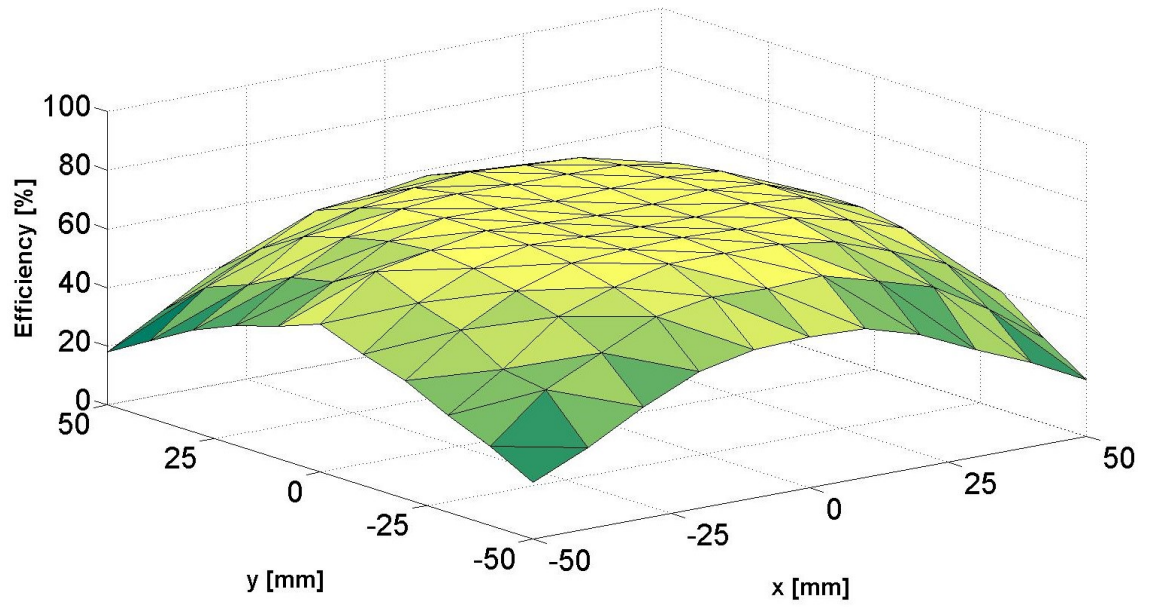


Figure 4-21: Transmission efficiency of asymmetrical planar MCR-WPT system.

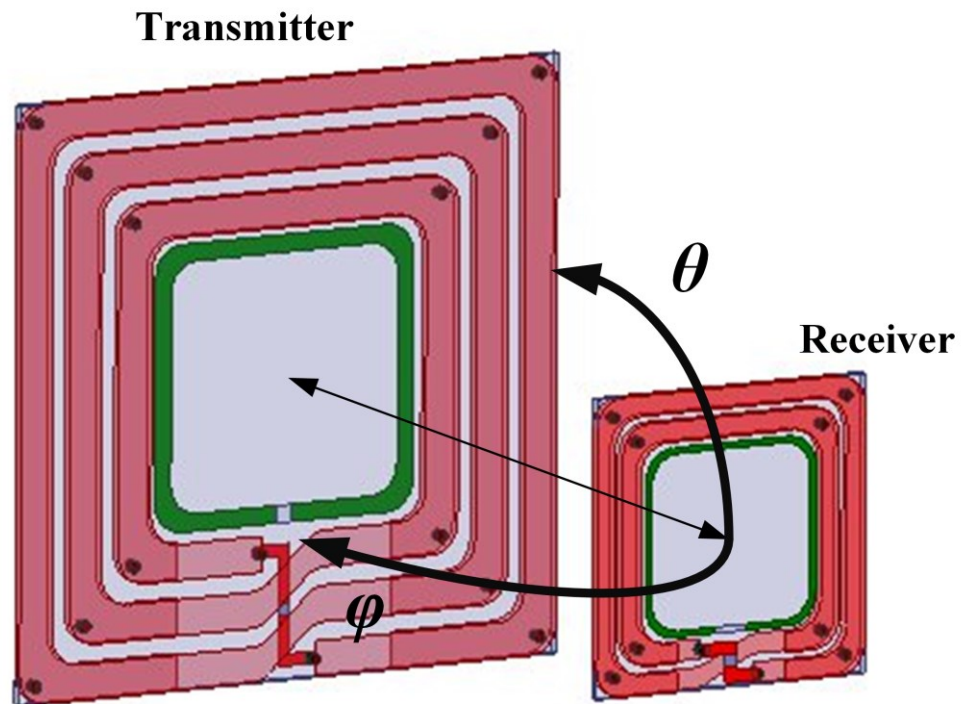


Figure 4-22: Geometry of asymmetrical MCR-WPT system with different orientation angles of the receiver at a transmission distance of 7 cm.

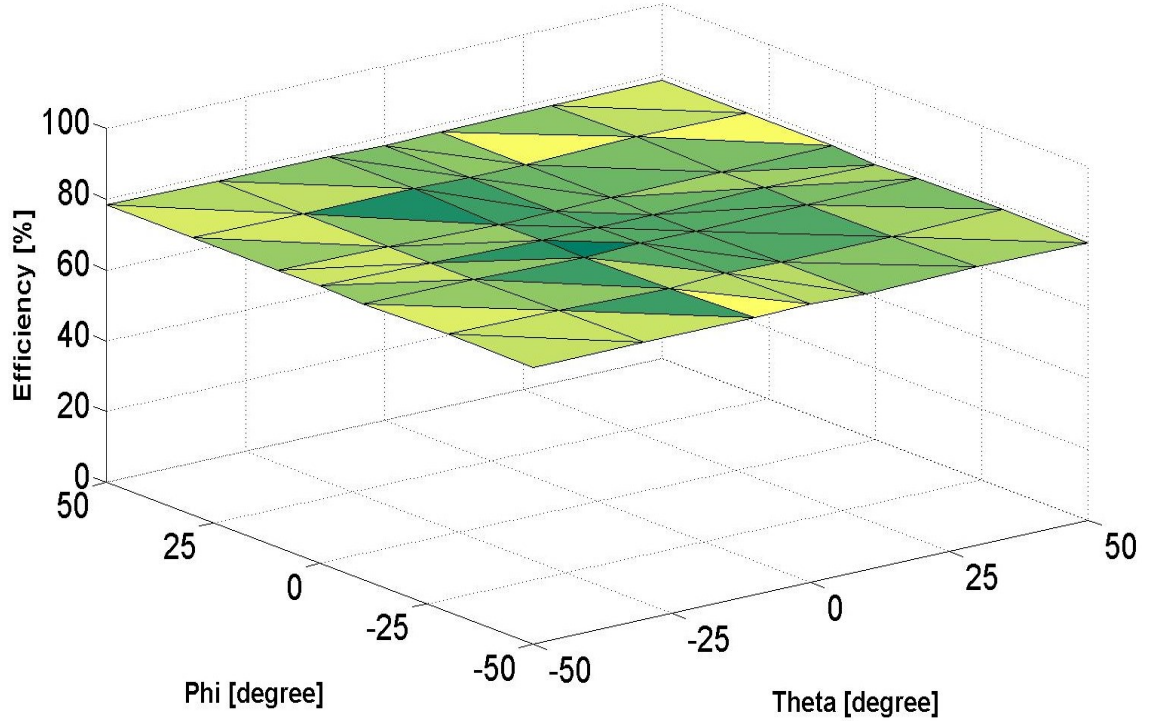


Figure 4-23: Transmission efficiency of asymmetrical MCR-WPT system with different orientation angles of the receiver at a transmission distance of 7 cm.

4.4 Discussion

In this chapter, a novel planar WPT system is presented for wireless power transfer via coupled magnetic resonances. In the proposed design, both the transmitter coil set and the receiver coil set are planarized, with the transmitting/receiving resonator coil and the source/load loop printed on the same layer of a dielectric substrate. The planar structure and high power transmission efficiency make the proposed design a practical candidate as WPT systems for small portable electronic devices and implantable medical devices. The results show that with capacitor-loaded PSC resonators tuned to resonate at 13.56 MHz, the power transmission efficiency can exceed 74% at a transmission distance of 200 mm.

In addition, it is demonstrated that with ferrite sheets applied to the proposed design as magnetic reflectors, the transmission efficiency can be further improved. The sensitivity of the proposed WPT system in the presence of conductive objects is also discussed, as is a comparison of different planar WPT designs with PSCs of different numbers of turns, in

terms of both efficiency and input impedance. The comparison reveals that with a 2-turn PCS resonator, the maximum power transmission efficiency of the proposed planar WPT system can be as high as 77.27% at a transmission distance of 10 cm. Moreover, with parallel paths created with auxiliary strips, the quality factor of the PSC resonators can be further improved and maximum power transmission efficiency increased to 81.68%.

In addition, four designs with different layers of resonators and with/without shorting walls were investigated. In the 3-layer planar MCR-WPT system, two substrates were stacked together to construct a low profile structure, and by adding shorting walls, the quality factor of the MCR-WPT system was increased to 435. Consequently, the transmission efficiency of the proposed system was increased from 77.27% to 84.38% at a distance of 10 cm, in comparison with the conventional planar WPT system.

Finally, a receiver with the dimension of 50 mm × 50 mm was proposed and investigated. It was compact and had a low profile and high transmission efficiency. The proposed planar WPT system can be a good candidate for wireless energy transfer to small electronic devices.

A novel magnetically coupled resonant wireless power transfer (MCR-WPT) system using an array of printed spiral resonators is presented to expand the receiving area. First, the effect of a misalignment of a receiver coil on a conventional transmitting array is discussed. Then by replacing the conventional MCR-WPT array with a novel feeding structure, the transmission efficiency of the misaligned receiver is investigated. An optimization scheme is derived by the combined use of HFSS/Q3D, Designer/ADS and MATLAB to improve the transmission efficiency of the WPT designs. With the proposed optimization strategy, both the memory requirement and CPU cost in computer aided designs and simulations are significantly reduced in comparison with conventional full-wave electromagnetic modeling. The proposed MCR-WPT array system is able to provide consistent transmission efficiency when the receiver is axially misaligned with the transmitter. Additionally, the transmission efficiency of the MCR-WPT system is significantly improved in both over-coupled and under-coupled regions.

5.1 Background

One major issue related to the implementation of the MCR-WPT system is the rapid decrease in transmission efficiency due to a misalignment. To address this issue, a transmit coil array is proposed in [61]. However, depending on the position of the receiving coil, a frequency tracking system is required. This is due to the frequency-splitting phenomenon caused by mutual coupling between arrayed transmitting coils [18]. A transmission coil array is proposed to maintain higher transmission efficiency in a wider receiving area, and an adaptive matching network is used to improve the WPT system performance in axial-misalignment condition [17].

In addition, the staggered repeater coil array is stacked with the transmitter coil array to increase the transmission efficiency due to the misalignment [19]. However, the distance between the transmitter and receiver coils is about 37% of the diameter of the receiver, while the transmission efficiency is shown to be up to 50% of the axial-misalignment. In a practical MCR-WPT system, a simple and easy-to-implement WPT system with

transmission efficiency that is less sensitive to axial-misalignment and distance is always more desirable.

5.2 Conventional MCR-WPT Array System

A conventional transmit coil array of 2×2 elements consisting of one transmitting MCR-WPT resonator and three repeaters is depicted in Figure 5-1. The planar MCR-WPT array with the resonator coil size of $10 \times 10 \text{ cm}^2$ and identical repeaters is printed on a substrate and a driving loop and open loops are printed on the backside of the substrate for the resonator and repeaters respectively. The receiver consists of a $10 \times 10 \text{ cm}^2$ spiral resonator with parallel path printed on the two sides of the substrate and a driving loop printed on the backside of the same substrate, as depicted in Figure 4-10. In the conventional MCR-WPT array system, because of the coupling between transmitting resonator coil and repeater coils, a frequency-splitting phenomenon takes place and decreases the transmission efficiency. In order to decrease the mutual coupling, d should be increased; however, when increases: (a) the size of the transmit coil array will be increased, and (b) the transmission efficiency decreases significantly when the receiver coil is misaligned.

A simulation of a conventional MCR-WPT array of 2×2 with one transmitting resonator and three repeaters is conducted. The resonant frequency of the transmitting resonator/repeaters and receiving resonator are fine-tuned at 13.56 MHz. Figure 5-2 shows the transmission efficiency of the MCR-WPT array system with a different gap between the transmitting resonator and the repeaters when the receiving coil is aligned with the transmitting resonator at a distance of 10 cm. It shows that increasing the gap increases efficiency.

Figure 5-3, however, illustrates that when the receiving resonator is aligned with one of the repeaters at 13.56 MHz, the transmission efficiency drastically decreases due to the frequency-splitting phenomenon. Figure 5-4 shows the measured transmission efficiency of the conventional MCR-WPT array system when the receiver is moving along the xy plane parallel to the transmitter at $d=100 \text{ mm}$. As illustrated, the transmission efficiency varies drastically when the receiver is moved. For instance, when the receiver is located at $P_1=(x,y)=(-52.5 \text{ mm}, 52.5 \text{ mm})$, the transmission efficiency is about 70%. On the other hand, when the receiver is located at $P_2=(52.5 \text{ mm}, 52.5 \text{ mm})$, $P_3=(-52.5 \text{ mm}, -52.5 \text{ mm})$,

$P_4=(52.5 \text{ mm}, -52.5 \text{ mm})$, and $P_5=(0 \text{ mm}, 0 \text{ mm})$ the transmission efficiency decreases to 2.1%, 5.9%, 55.2% and 3.9 %, respectively.

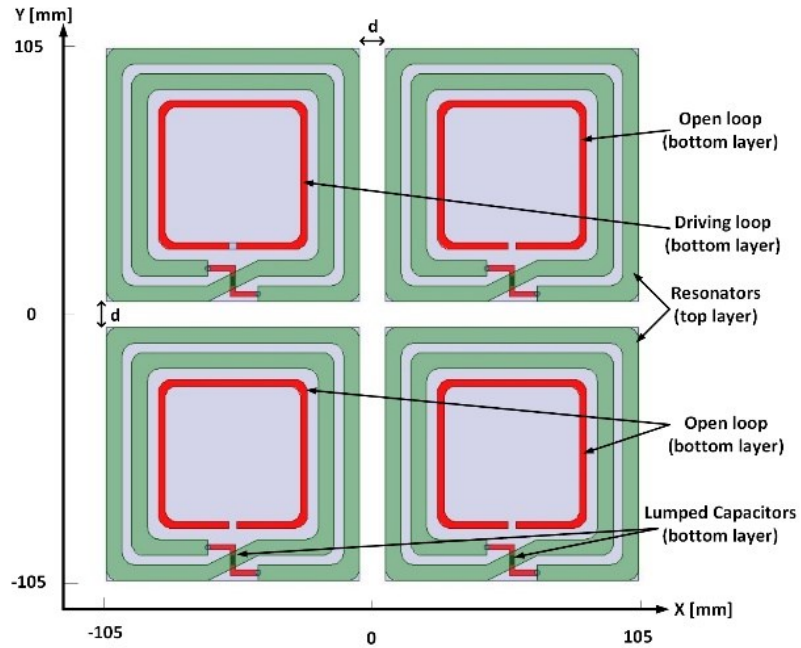


Figure 5-1: Conventional MCR-WPT array transmitter with one resonator and three repeaters.

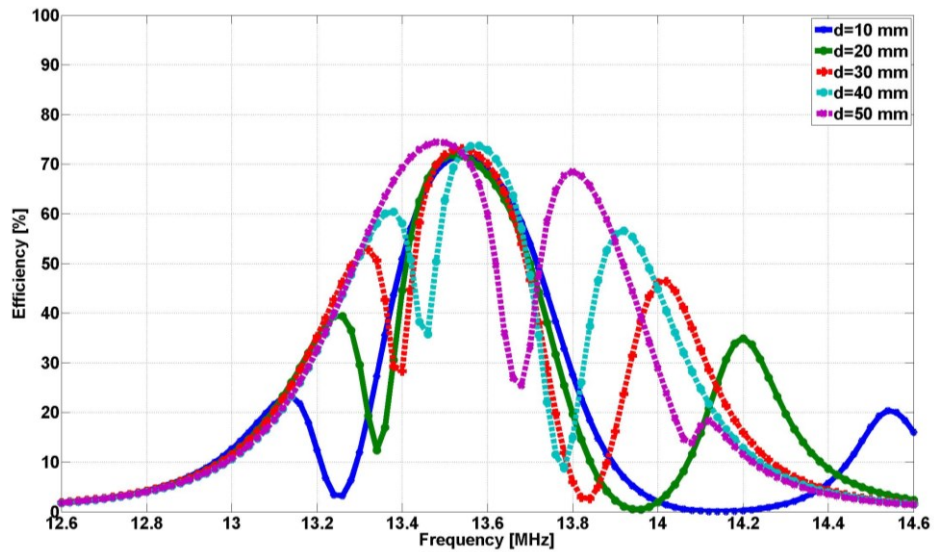


Figure 5-2: Simulated transmission efficiency of conventional planar MCR-WPT array system at a distance of 10 cm aligned with resonator.

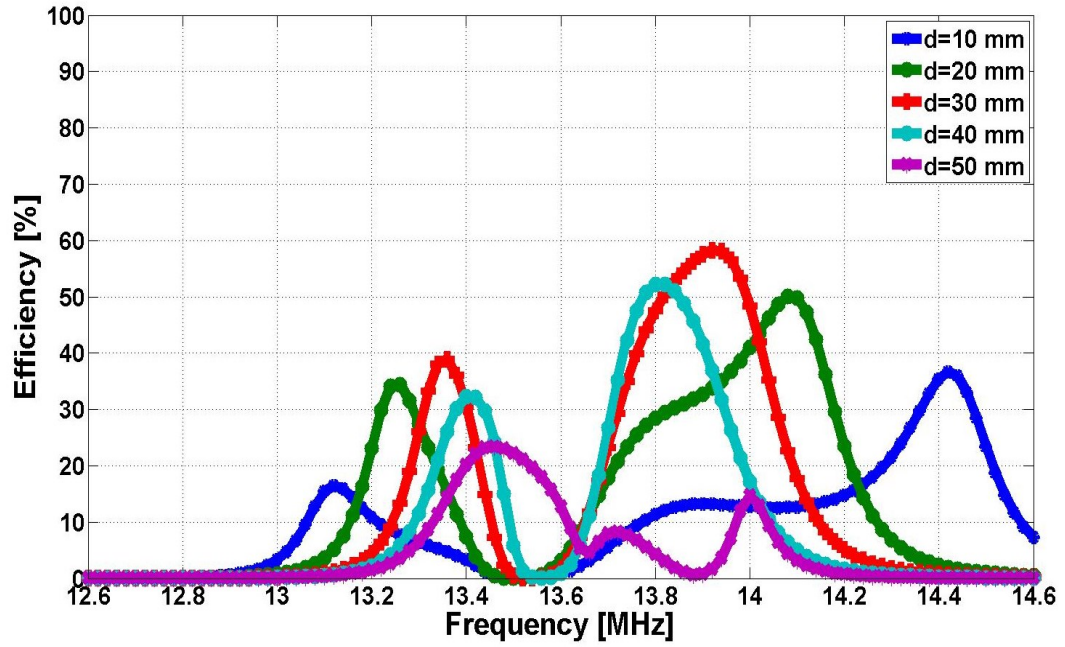


Figure 5-3: Simulated transmission efficiency of conventional planar MCR-WPT array system at a distance of 10 cm aligned with repeater.

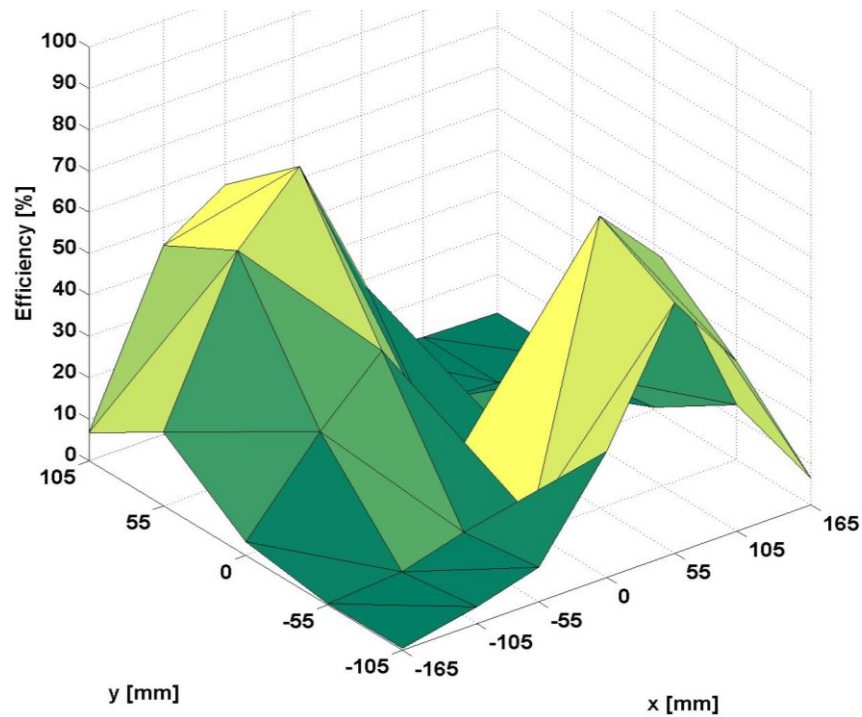


Figure 5-4: Measured transmission efficiency of conventional planar MCR-WPT system with one T_x resonator and three repeaters.

5.3 Position-Free MCR-WPT Array System

A conventional inductively coupled feed MCR-WPT system consists of a driving loop, a transmitter resonator, a receiver resonator and a load loop. When the distance is changed between a transmitter and a receiver, the mutual coupling between the transmitter and receiver resonators changes as well. Specifically, it causes mismatching and could increase the reflected power while decreasing the transmission efficiency. In the proposed design, the typical multi-turn resonator is replaced with an array of smaller multi-turn resonators, which are designed to have the same overall size as the typical transmitter resonator.

Figure 5-5(a) shows the transmitter design of a typical planar MCR-WPT system with a $10 \times 21 \text{ cm}^2$ resonator printed on a substrate and a driving loop printed on the backside of the substrate. The proposed design is depicted in Figure 5-5(b), where two multi-turn resonators with a size of $10 \times 10 \text{ cm}^2$ are placed with 10 mm spacing. The driving loop is printed on the backside of the substrate to inductively couple with the array of 1×2 resonators. By using the array of resonators for the transmitting side, a uniform magnetic field is obtained and the transmission efficiency is improved when axial-misalignment occurs.

To further improve the performance of the MCR-WPT system, an array of 2×2 is proposed and used at the transmitting side. As can be seen in Figure 5-6, the conventional multi-turn resonator with a size of $21 \times 21 \text{ cm}^2$ is replaced with four smaller multi-turn resonators with a size of $10 \times 10 \text{ cm}^2$ (Figure 5-7) each. The gap between resonators is chosen to be 10 mm, which is the worst-case scenario for the conventional MCR-WPT array system with regard to Figure 5-3. The lumped capacitors are then fine-tuned at the resonant frequency of the MCR-WPT system at 13.56 MHz and the novel single driving loop is studied for the proposed structure.

When the center of the receiver is perfectly aligned with the center of the transmitter, the current induced on all of the resonators is clockwise. As shown in Figure 5-8, when the center of receiver is perfectly aligned with the center of the transmitter of the conventional MCR-WPT, the coupling factor significantly increases. When they move closer together due to resonant frequency splitting (as mentioned above), the performance of the system drops significantly. However, with the proposed MCR-WPT coil array of 2×2 , the results

show that the coupling factor at Pr_1 and Pr_2 are less sensitive to the distance between the coils. Consequently, the transmission efficiency improves in the under-coupled region.

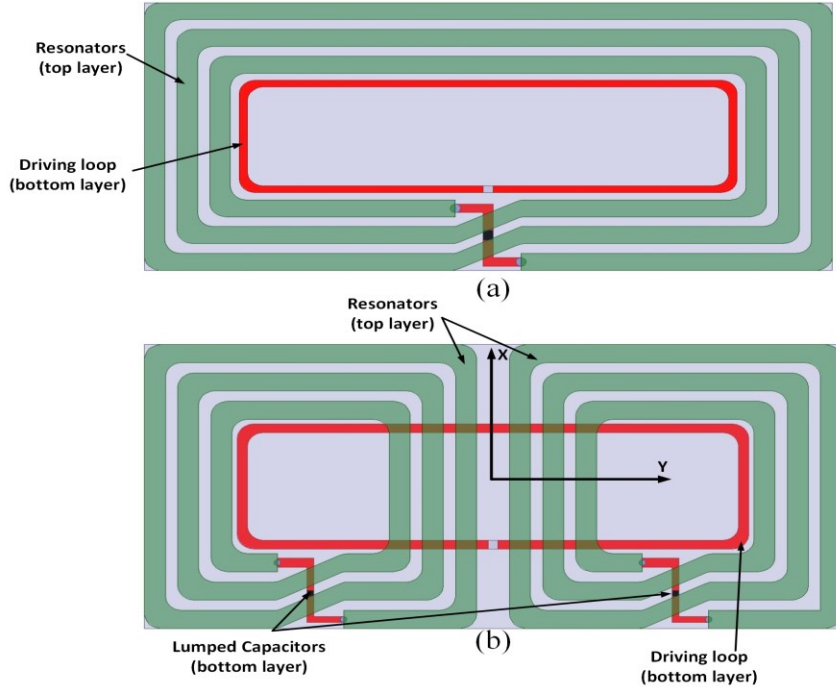


Figure 5-5: (a) Transmitter design of conventional MCR-WPT; (b) transmitter design of the proposed MCR-WPT with an array of 1×2 resonator.

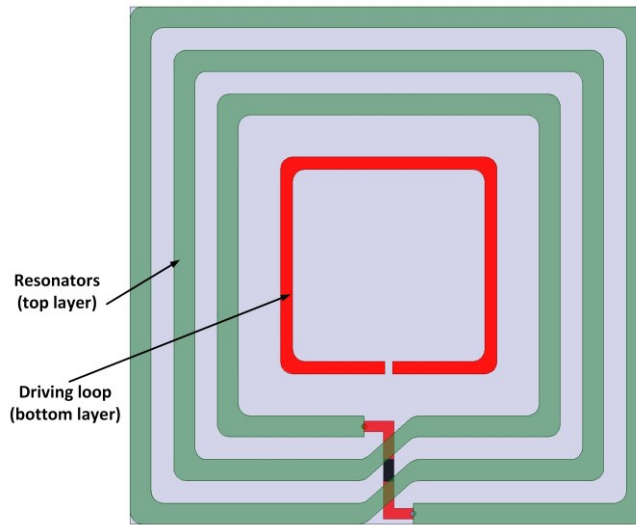


Figure 5-6: Transmitter design of conventional MCR-WPT.

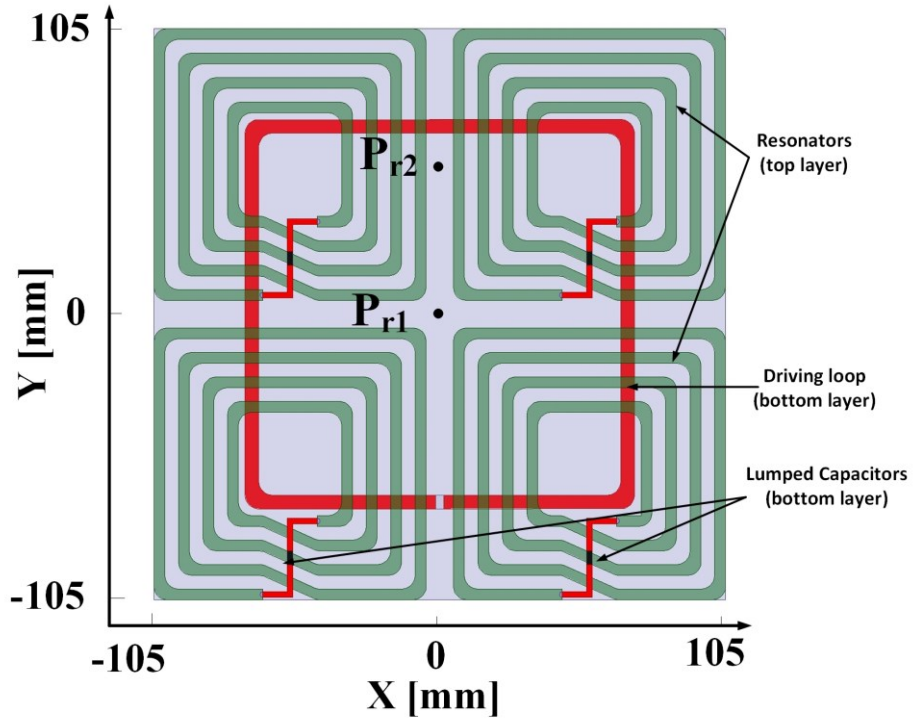


Figure 5-7: Proposed position-free MCR-WPT array system with an array of 2×2 resonator.

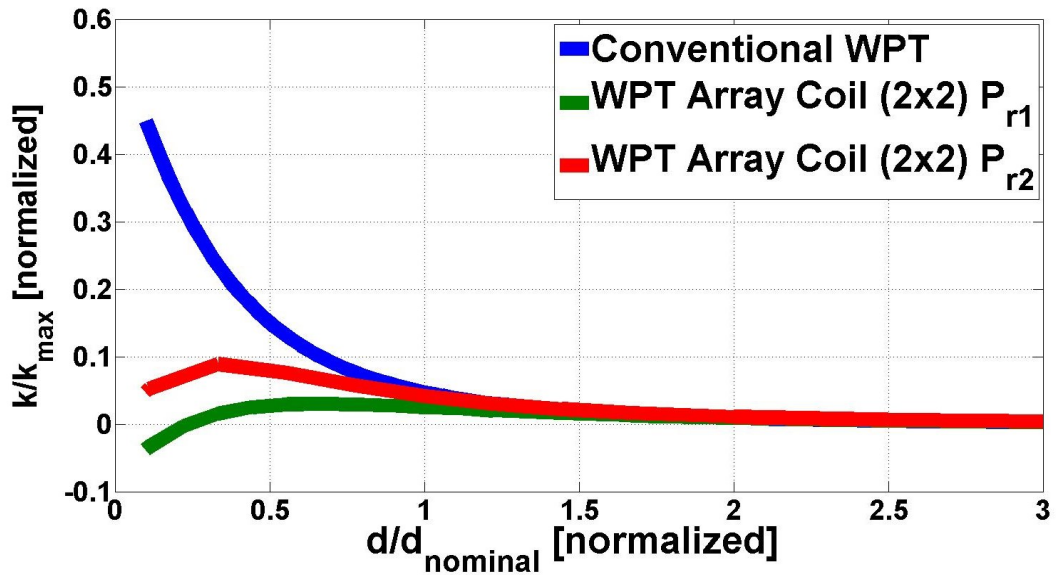


Figure 5-8: Normalized coupling factor between the receiver and transmitter resonators with regard to normalized transmission distance.

5.4 Optimization Scheme

A full-wave electromagnetic simulation of an MCR-WPT array system with multiple transmitting resonators involves a large number of design parameters, and consequently the optimization of the design is often too computationally expensive to carry out. To address this issue, an optimization scheme using the dynamic link between HFSS/Q3D (for extracting RLC and mutual inductance), Designer/ Advanced Design System (ADS) (for solving equivalent circuit model) and MATLAB (for implementation of optimization algorithm) is proposed. A fully planar MCR-WPT system with an integrated transmitter coil array is used. With an accurate equivalent circuit model derived from the WPT system, the critical design parameters, including the number of turns for the resonators, dimensions of driving and load loops, and the dimensions of resonators can be optimized, which in turn yields the optimum performance of the proposed design. By using the proposed structure, the larger feeding loop provides some degrees of freedom for the inner radius of the PCS resonators due to the higher quality factor of the feeding loop. Therefore, a multi-turn resonator with the higher quality factor can be achieved. In addition, the dynamic link between the field-solver and the circuit simulation tools is applied to reduce CPU cost and RAM usage, and the full-wave electromagnetic simulation is applied to validate the design after optimization. Finally, the prototype is fabricated and tested for verification and evaluation.

The planar MCR-WPT system consists of an array of identical transmitting resonators. The equivalent circuit model of the MCR-WPT system is shown in Figure 5-9, where the mutual coupling between any two adjacent coils needs to be taken into account. Direct application of full-wave electromagnetic simulations of the mutual coupling between the coils leads to high computational cost. For the proposed design with $n=7$ (with a 2×2 array of transmitting resonator) as shown in Figure 5-7, the computational time required by the HFSS to run one full-wave simulation with a relatively fine-mesh is around 144 minutes with a Dell computer equipped with i7-3770K 3.5 GHz CPU and 32 GB RAM. To optimize all critical design parameters (e.g. the number of turns of the resonator, the width of each turn, the gap between two adjacent turns, the dimension of driving and load loop) of the

proposed MCR-WPT design, the computational cost and memory requirement with the full-wave electromagnetic simulation will be too expensive for normal computers.

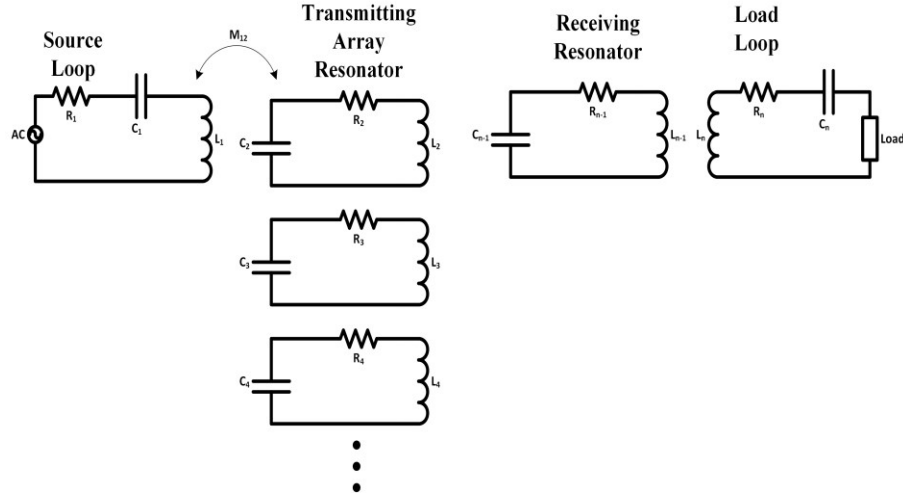


Figure 5-9: Equivalent circuit model of the proposed planar MCR-WPT array.

With the n -port network analysis based on the circuit model shown in Figure 5-9, the current in each coil could be obtained as

$$\begin{bmatrix} I_1 \\ I_2 \\ \vdots \\ I_{n-1} \\ I_n \end{bmatrix} \begin{bmatrix} Z_{11} & j\omega M_{12} & \cdots & j\omega M_{1(n-1)} & j\omega M_{1n} \\ j\omega M_{21} & Z_{22} & \cdots & j\omega M_{2(n-1)} & j\omega M_{2n} \\ \vdots & \vdots & \ddots & \vdots & \vdots \\ j\omega M_{(n-1)1} & j\omega M_{(n-1)2} & \cdots & j\omega M_{(n-1)(n-1)} & j\omega M_{(n-1)n} \\ j\omega M_{n1} & j\omega M_{n2} & \cdots & Z_{nn} & \end{bmatrix}^{-1} \begin{bmatrix} V_s \\ 0 \\ \vdots \\ 0 \\ 0 \end{bmatrix}$$

$$Z_{11} = \left(R_s + R_1 + j\omega L_1 + \frac{1}{j\omega C_1} \right)$$

$$Z_{22} = \left(R_2 + j\omega L_2 + \frac{1}{j\omega C_2} \right)$$

\vdots

$$Z_{(n-1)(n-1)} = \left(R_{n-1} + j\omega L_{n-1} + \frac{1}{j\omega C_{n-1}} \right)$$

$$Z_{nn} = \left(R_n + R_L + j\omega L_n + \frac{1}{j\omega C_n} \right)$$

(5-1)

To overcome this issue, the full-wave simulator HFSS and Q3D, using finite element method and method of moments respectively, is only used to extract the series resistance, parasitic capacitance, self-inductance, and mutual inductance of MCR-WPT coils. Then, by using a dynamic simulation setup between HFSS/Q3D and Designer/ADS, the equivalent circuit model of the system can be solved to obtain the desired transmission efficiency. The design parameters are then implemented in MATLAB. The block diagram of the proposed simulation and optimization process is shown in Figure 5-10. With the proposed method, the total computational time for each simulation with a relatively fine-mesh is reduced to 5 minutes, which is only 3.4% of what was required with a full-wave simulation. Figure 5-11 illustrates the systematic optimization procedure used in this work for the transmitter coil array MCR-WPT system with transmitter coil array.

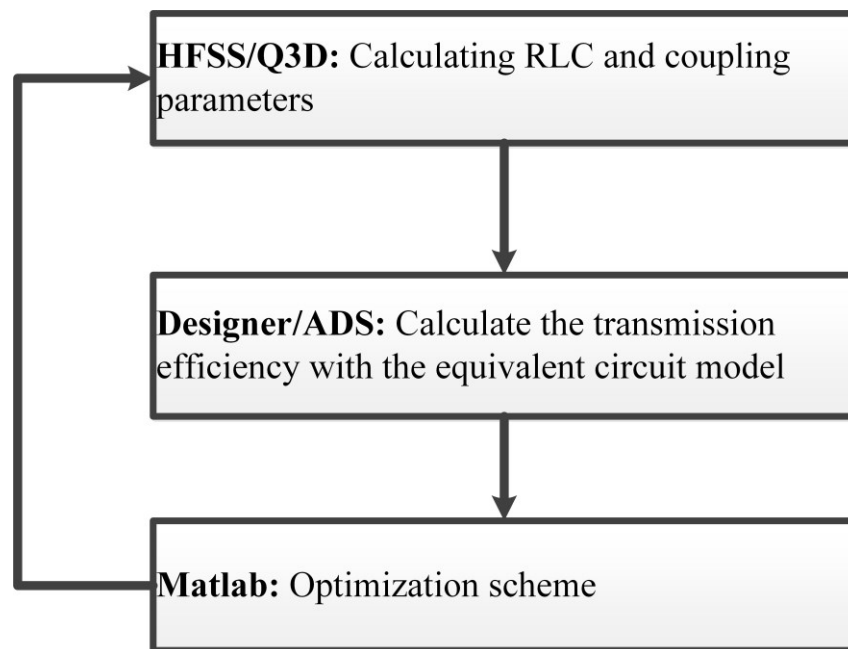


Figure 5-10: Block diagram of simulation and optimization processes.

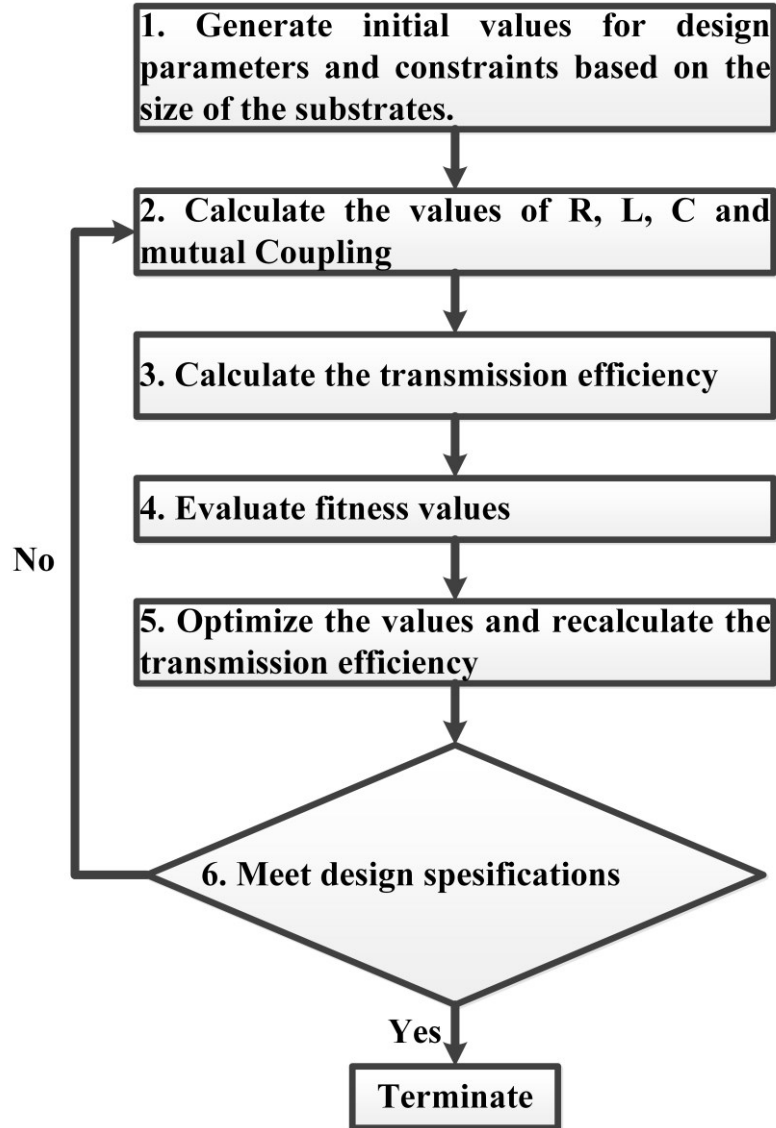


Figure 5-11: Flowchart of optimization algorithm for optimization of proposed MCR-WPT

5.4.1 Simulation and Measurement Results

Figure 5-12 shows the proposed structures using an array of small resonators on the transmitter side and the single resonator printed on FR4 substrates on the receiver side. The system is fine-tuned to 13.56 MHz. As shown in Figure 5-13, the transmission efficiency of the array of 1×2 is improved in the under-coupled region by more than 10% compared with the conventional MCR-WPT system, although in the over-coupled region the transmission efficiency remains unchanged. Figure 5-14 shows the measured and

simulated transmission efficiency of the proposed MCR-WPT system with an array of 2×2 resonator. The simulation results from both Ansys Designer and ADS are plotted for comparison. The results show that with the proposed MCR-WPT design, a transmission efficiency of up to 68% is achieved.

In the proposed array of 2×2 , the transmission efficiency in the under-coupled region is significantly improved. At a distance of 5 cm, the transmission efficiency is increased from 5% of the conventional design to 66% of the array of 2×2 . In addition, the transmission efficiency in the array of 2×2 in the over-coupled region decreases only gradually, which is an advantage of the MCR-WPT system.

It should be noted that there is a difference between the simulated and measured transmission efficiency of the array of 2×2 in the under-coupled region. The main reason for this is the simplified structure that was used in the simulation due the long computation time with HFSS v15. Figure 5-15 shows measured S_{21} of the array of 2×2 , at different distances between the transmitting and receiving coils. It is shown that at different transmission distances, the maximum transmission efficiency remains at 13.56 MHz. Meanwhile, in the over-coupled region, the frequency splitting becomes less severe than in the conventional MCR-WPT.

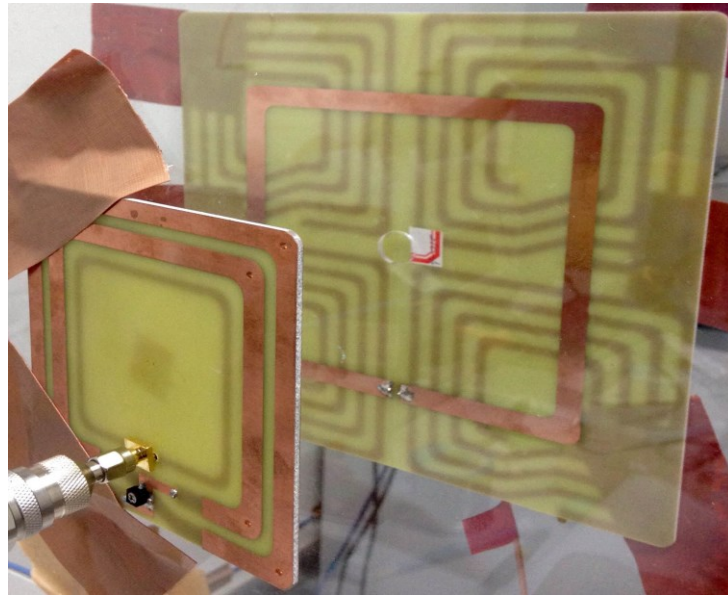


Figure 5-12: Configuration of proposed the array of 2×2 .

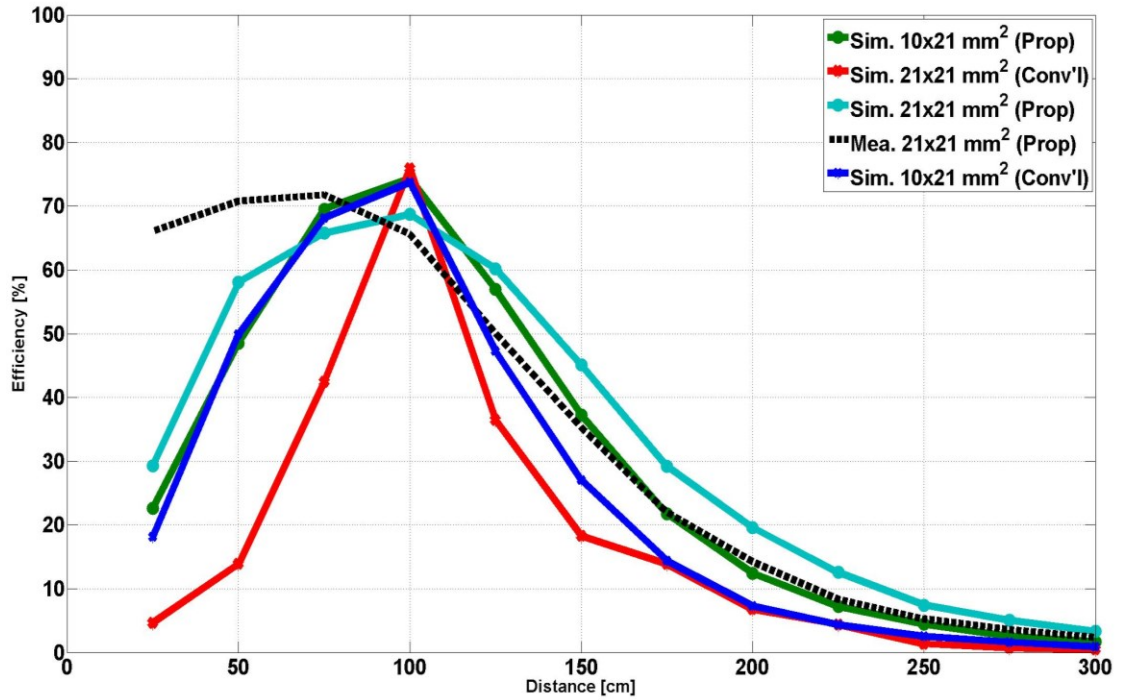


Figure 5-13: Measured and simulated transmission efficiency at a distance of 10 cm in between the transmitter and receiver.

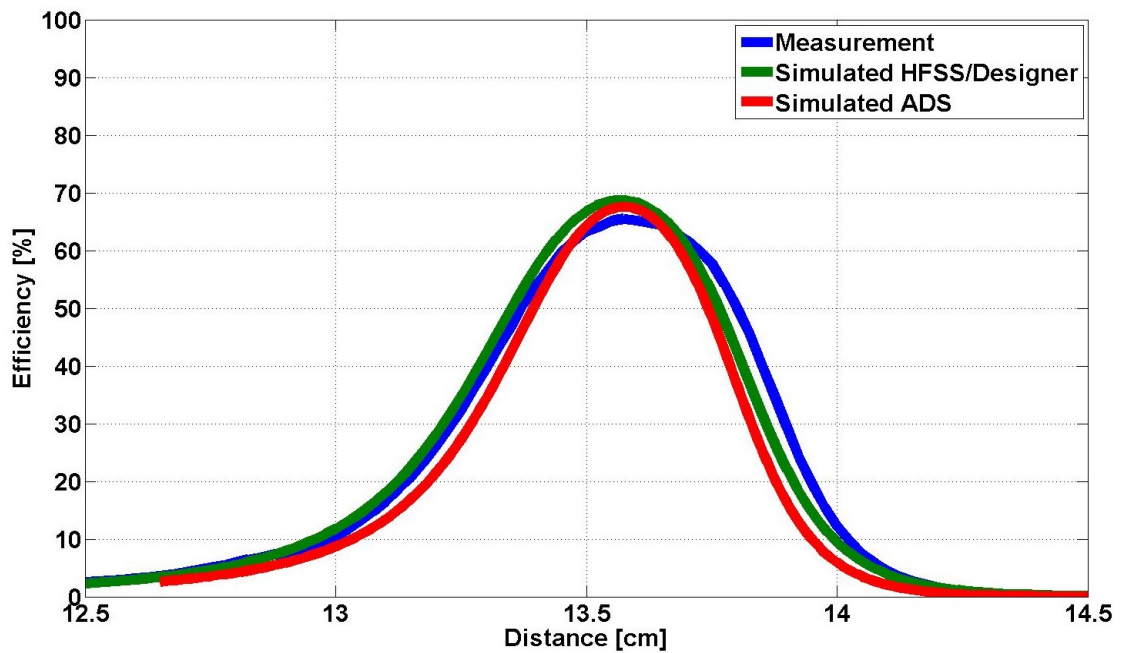


Figure 5-14: Measured and simulated transmission efficiency of proposed MCR-WPT system with transmitting resonator array.

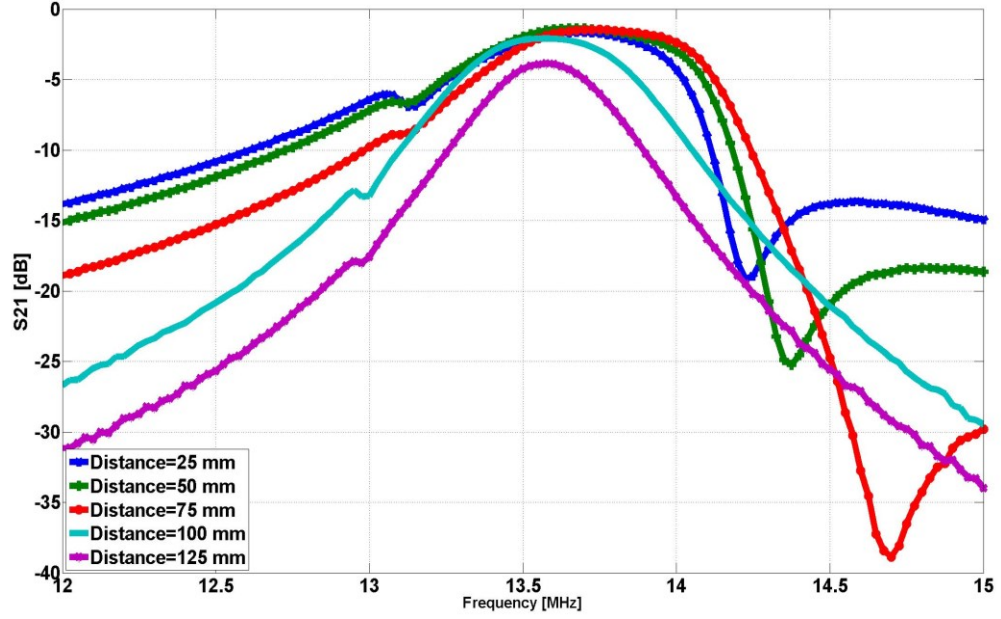


Figure 5-15: Measured S_{21} of the array of 2×2 .

Furthermore, the impact of axial-misalignment in both designs is investigated. Table 5-1 shows the maximum transmission efficiency of the array of 2×2 at a distance of 10 cm between the transmitting and receiving coils at four different positions. It shows that when the Rx coil is displaced by 55 mm, 110 mm and 165 mm away from the positive y-axis, the transmission efficiency is improved by 6.84%, 15.2% and 1.65%, respectively, compared to the typical MCR-WPT system.

Table 5-2 shows the transmission efficiency of the array of 2×2 at a distance of 10 cm. When the receiving coil is displaced away from the positive y-axis by 55 mm, 110 mm and 165 mm, respectively, the transmission efficiency is improved by 7.8%, 34.4%, and 1.97%, respectively, compared to the conventional design. Also, when the receiving coil is fixed in the x-axis at 55 mm and the receiving coil is displaced in the y-axis by 55 mm, 110 mm, 165 mm, the transmission efficiency is improved by 27.16%, 39.92%, and 1.89%, respectively, compared to the conventional design.

Figure 5-16 shows the measured transmission efficiency of the proposed planar multi-resonator MCR-WPT design when the receiver is placed at the same distance from the transmitter coil array ($d=10$ mm). It indicates that with the proposed transmitter design, a

uniform magnetic field distribution is realized on the receiver plane and more consistent transmission efficiency can be achieved when the receiver is moving.

Table 5-1: Transmission Efficiency of the array of 1×2 in axial-misalignment condition

	Simulated (Conventional)	Simulated (Proposed)
(x=0,y=0)	73.72%	74.3%
(x=0,y=55)	63.3%	70.14%
(x=0,y=110)	21.73%	36.93%
(x=0,y=165)	0.7%	2.35%

Table 5-2: Transmission Efficiency of the array of 2×2 in axial-misalignment condition

	Simulated Conventional	Simulated Proposed	Measured Proposed
x=0,y=0	75.9%	68.71%	65.31%
x=0,y=55	50.2%	66.16%	58.4%
x=0,y=110	8.33%	48.63%	42.73%
x=0,y=165	0.13%	6.13%	2.1%
x=55,y=0	58.37	67.08%	59.02%
x=55,y=55	33.23	64.75%	60.39%
x=55,y=110	0.75%	48.52%	40.67%
x=55,y=165	0.06%	5.9%	1.95%

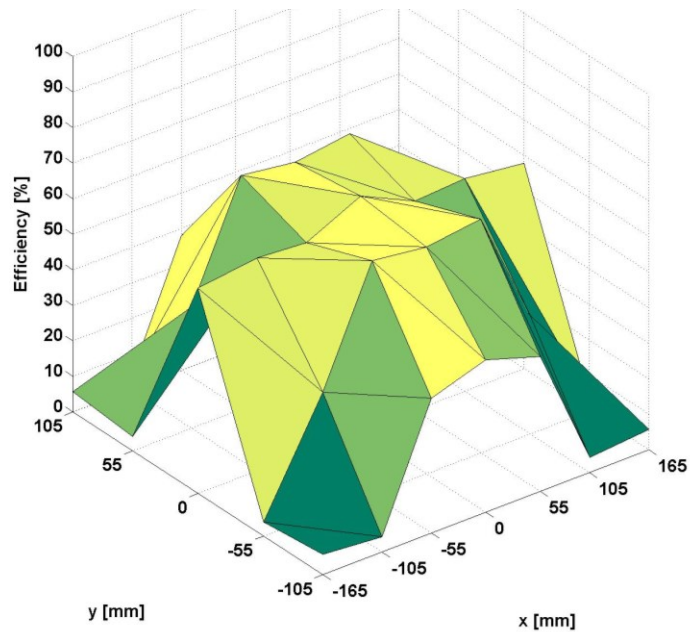


Figure 5-16: Measured transmission efficiency of proposed planar MCR-WPT system with an array of 2×2.

Figure 5-17 shows the magnetic field distribution of the three different WPT systems at the three different locations of $PT_1=(x,y)=(52.5 \text{ mm}, 52.5 \text{ mm})$, $PT_2=(x,y)=(0 \text{ mm}, 52.5 \text{ mm})$, and $PT_3=(x,y)=(-52.5 \text{ mm}, 52.5 \text{ mm})$. Figure 5-17(a)-(c) show the field distribution of the conventional WPT array system, which has one transmitting MCR-WPT resonator and three identical repeaters. It shows that magnetic fields are distributed intensively when the receiver is aligned with the resonator (PT_3) and sparsely near the repeater (PT_1) and the gap between the resonator and the repeater (PT_2).

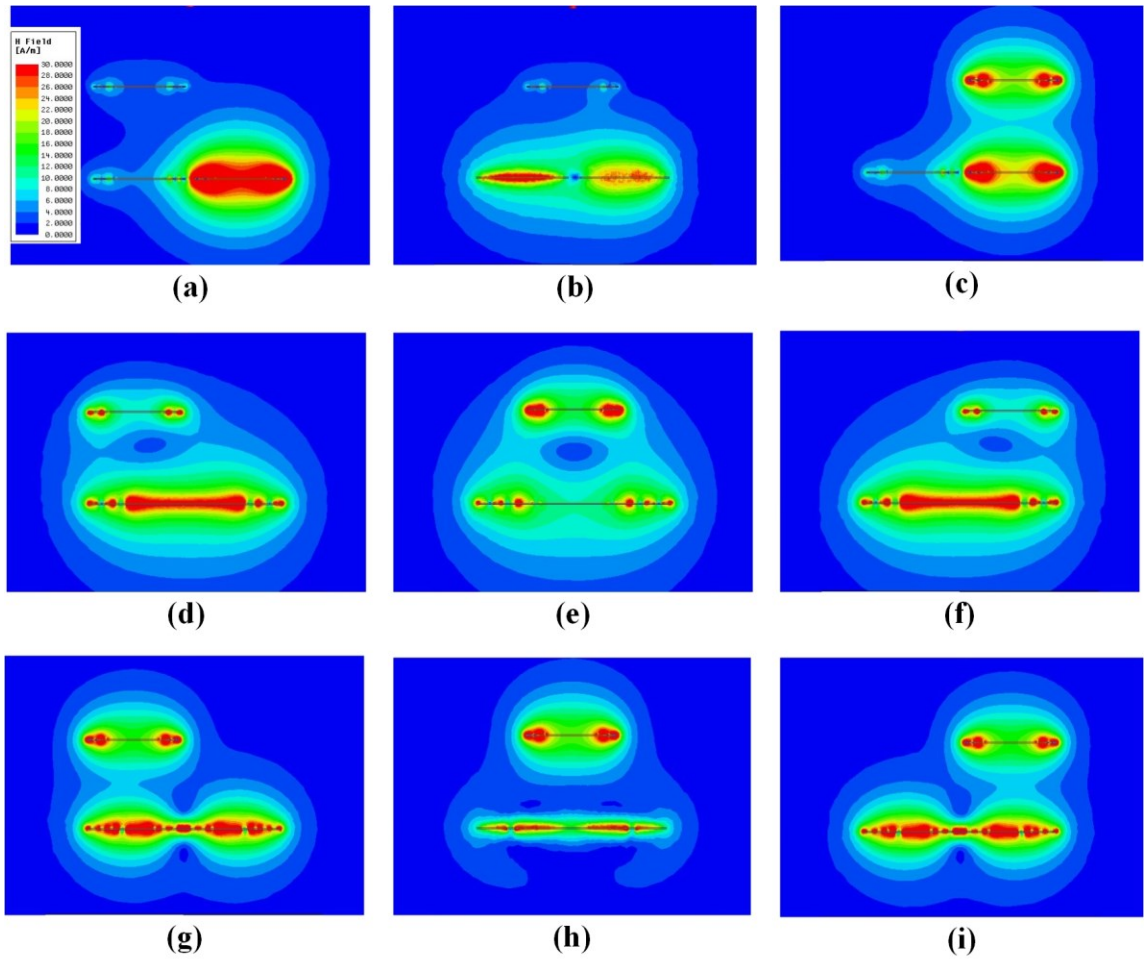


Figure 5-17: Magnetic field distribution of (a)-(c) conventional MCR-WPT array (repeater), (d)-(f) conventional MCR-WPT system, and (g)-(i) proposed MCR-WPT array system.

Figure 5-17(d)-(f) show the magnetic field distribution of the conventional WPT with a single transmitting resonator and Figure 5-17(g)-(i) show the magnetic field distribution of

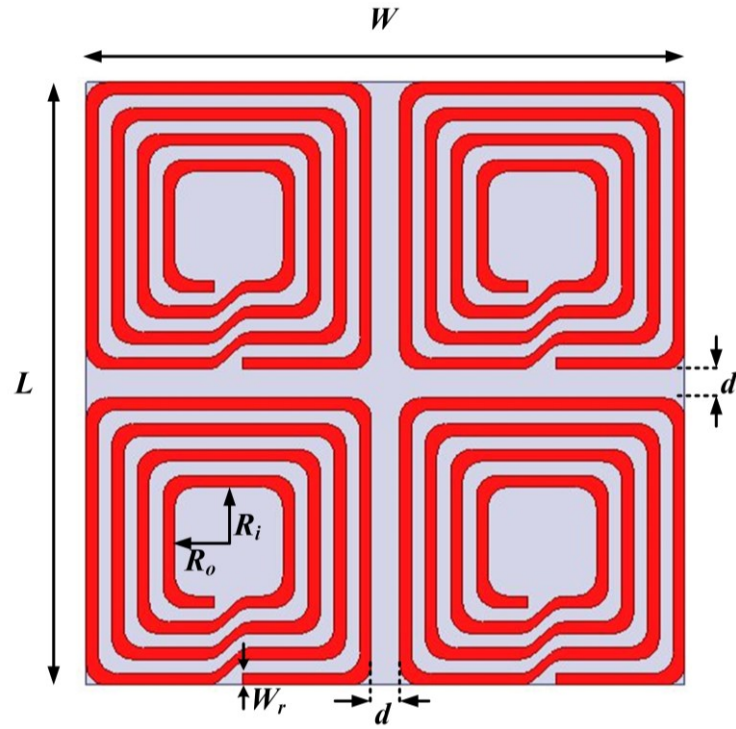
the proposed MCR-WPT array system. In the conventional WPT with a single transmission resonator, the transmitter transfers power mainly when the receiver is aligned at PT_2 rather than PT_1 and PT_3 , which means that the generated field distribution is large at the center and the transmit diversity is small at PT_1 and PT_3 . As a result, there is a little difference in the intensity of the magnetic field when the receiver is aligned at PT_1 and PT_3 . In contrast, in the proposed MCR-WPT array system, the single feeding structure for the array resonator creates a nearly uniformly distributed magnetic field regardless of the misalignment. As can be seen, it is more localized in both transmitting and receiving coils in comparison with the other two WPT systems.

5.5 MCR-WPT Array with Small Receiver

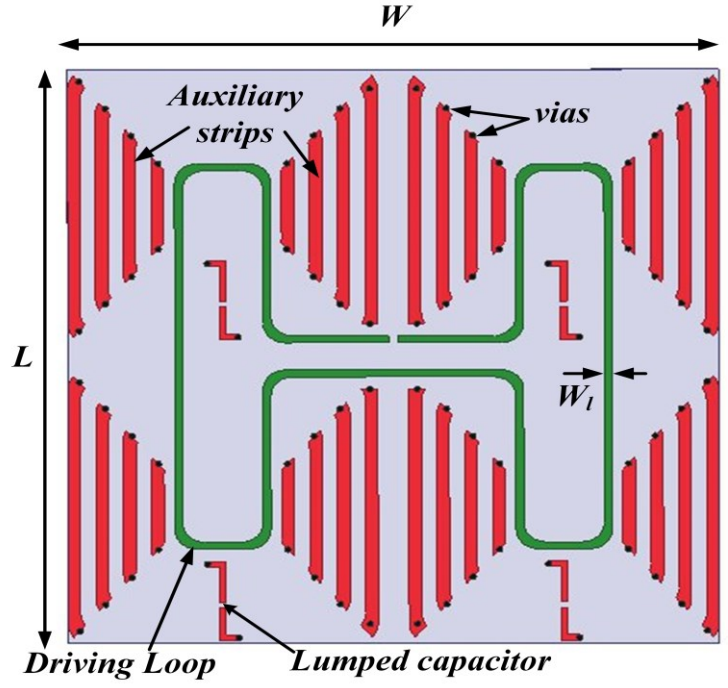
5.5.1 Array of 2×2

To meet the industrial requirements for small electronic devices such as smartphones, the receiving side with a size of $10 \times 7 \text{ cm}^2$ is chosen. Using an optimization scheme, which was previously discussed, the array of 2×2 with four resonators for transmitter is designed and optimized. The distance between resonators is chosen to be 1 cm in order to keep the size of transmitter minimized.

As shown in Figure 5-18, the array is printed on an FR4 substrate and a proper driving loop is designed to induce a uniform magnetic field. In addition, to increase the quality factor of the resonators, auxiliary strips are applied to the structure. However, because of the printed driving loop on the backside of the substrate, a limited space is dedicated to auxiliary strips. Table 5-3 shows the *RLC* parameters of the MCR-WPT array. A matching network is applied to both the transmitter and receiver to further increase the performance.



(a)



(b)

Figure 5-18: Geometry of MCR-WPT array transmitter: (a) top, (b) bottom.

Table 5-3: Design parameters, RLC values of MCR-WPT array

	Transmitter	Receiver
W_r (mm)	4	6.3
W_l (mm)	2.5	2.4
R_o (mm)	19	20.4
R_i (mm)	19	35.4
W (mm)	210	100
L (mm)	210	70
N	4	2
d (mm)	10	-
C (pF)	110	290
C_p (pF)	26	376
C_s (pF)	150	176

As shown in Figure 5-19, the receiver is placed at two different positions $P_1=(x,y)=(0,0)$ and $P_2=(x,y)=(55\text{ mm},55\text{ mm})$ at a distance of 10 cm from the transmitter. Figure 5-20 illustrates the transmission efficiency of the array. It shows that when the receiver is located at P_1 , the transmission efficiency of the array is higher than P_2 in the both over-coupled and under-coupled regions. In the over-coupled region, the transmission efficiency is increased from 20% to 70% when the receiver is moved from P_2 to P_1 . In addition, the overall transmission efficiency is increased by 20% when the receiver is moved from P_2 to P_1 at different distances. This is due to the direction of the current at adjacent resonators at P_1 .

To investigate the performance of the system when it is not aligned with the transmitter array, the receiver is moved along the xy plane parallel to the transmitter at $D=10$ cm. Figure 5-21 illustrates the transmission efficiency of the system showing that the transmission efficiency is independent of the position of the receiver along the xy axis. Transmission efficiency fluctuates between 65% and 70.62%, which is highly desirable. In addition, the receiver moves along the φ and θ directions as shown in Figure 5-22. The transmission efficiency results depict that the transmission efficiency of the system is very stable.

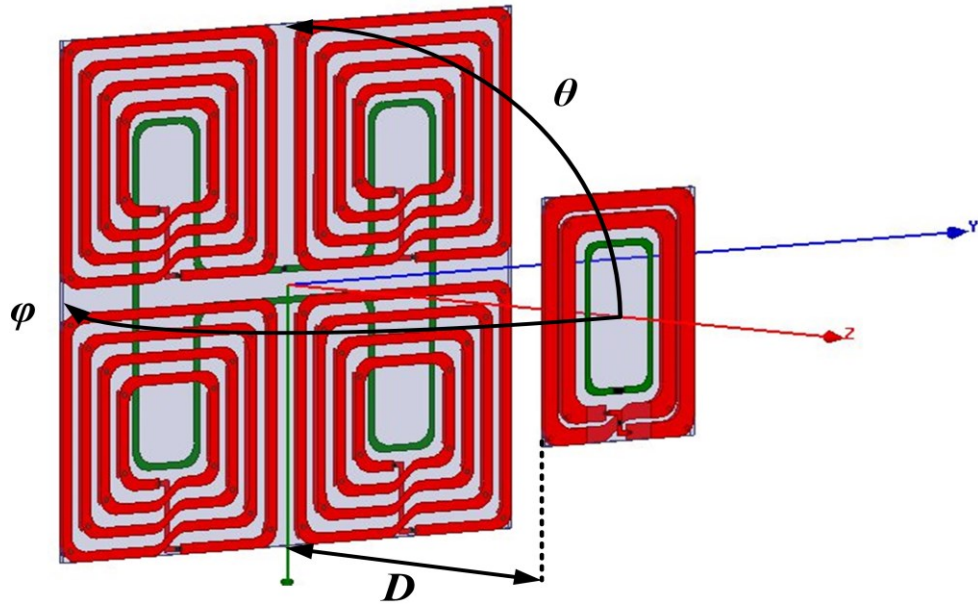


Figure 5-19: Geometry of MCR-WPT array (2×2) with different orientation angles of the receiver at a transmission distance of 10 cm.

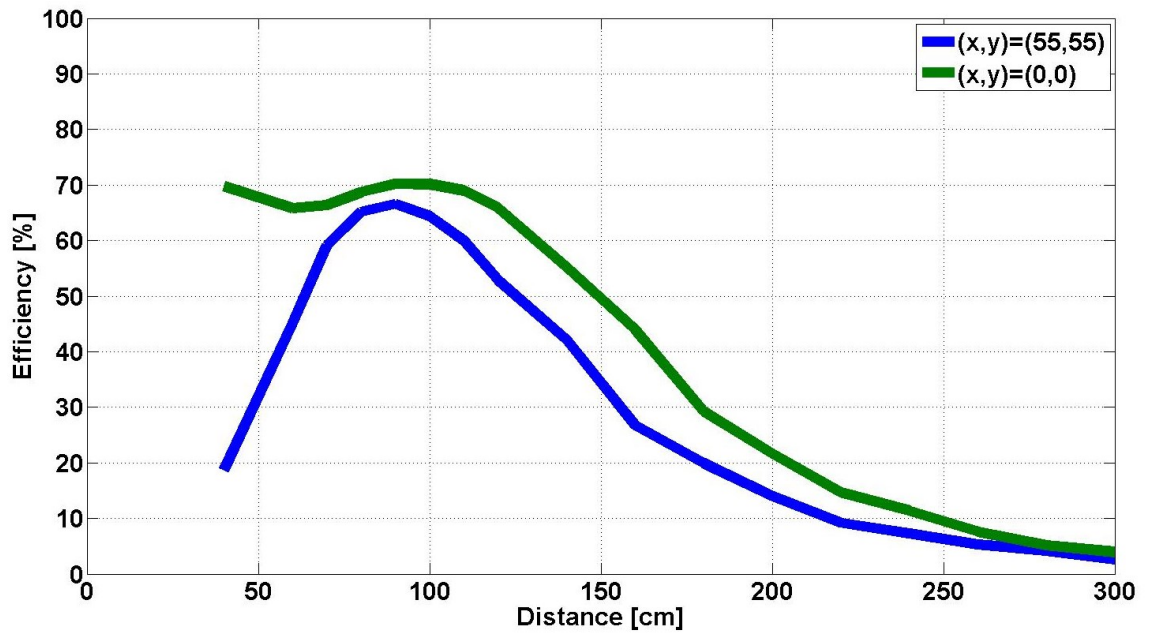


Figure 5-20: Transmission efficiency of MCR-WPT array against distance at 13.56 MHz.

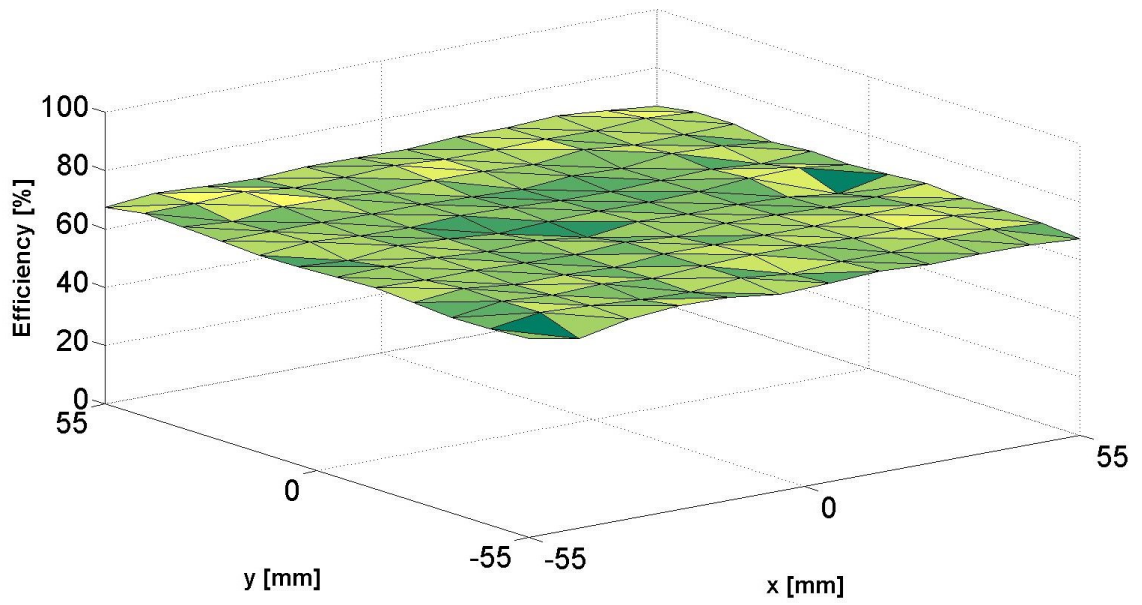


Figure 5-21: Transmission efficiency of MCR-WPT array at a transmission distance of 10 cm.

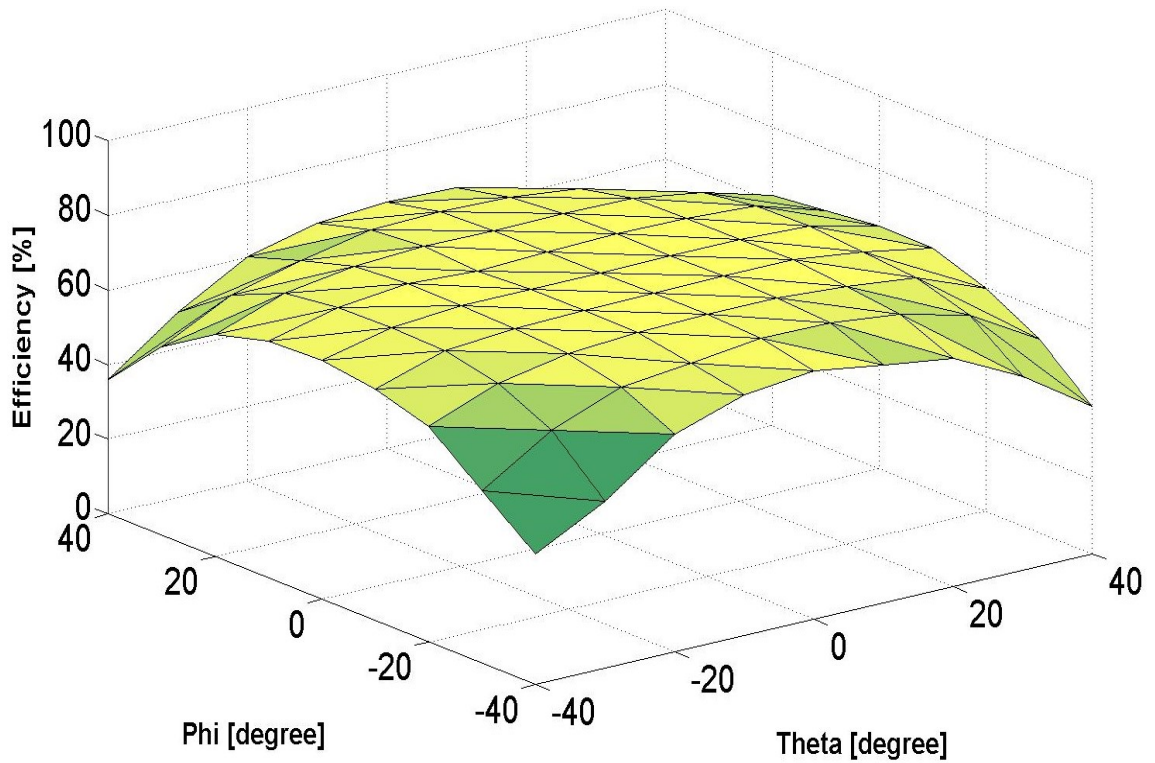


Figure 5-22: Transmission efficiency of MCR-WPT array with different orientation angles of the receiver at a transmission distance of 10 cm.

To verify the performance of the proposed MCR-WPT array coil, it is tested by integrating it into a WPT system that consists of four other subsystems: an amplifier, a rectifier, a DC-to-DC converter and two loads. Figure 5-23 shows the components of the proposed WPT system.

The proposed systems are demonstrated to be more feasible to implement inside walls and under desks for charging small electronic devices anywhere inside its confines. The transmitter charges and power two different electronic devices simultaneously. The receiver coils are placed at a transmission distance of 10 cm from the transmitter array coil. To have a compact and low profile receiver, the rectifier is printed on the receiving substrate. Therefore, the integrated receiver coil with the rectifier can be used for portable devices conveniently.

The proposed system transfer 6 W of power to a smartphone and a speaker with the received voltage of 4.242 V and 5.10 V, respectively. Then, the performance of the system with the axial-misalignment is investigated and it confirms that the overall efficiency does not drop when the receivers are moving at a transmission distance of 10 cm.

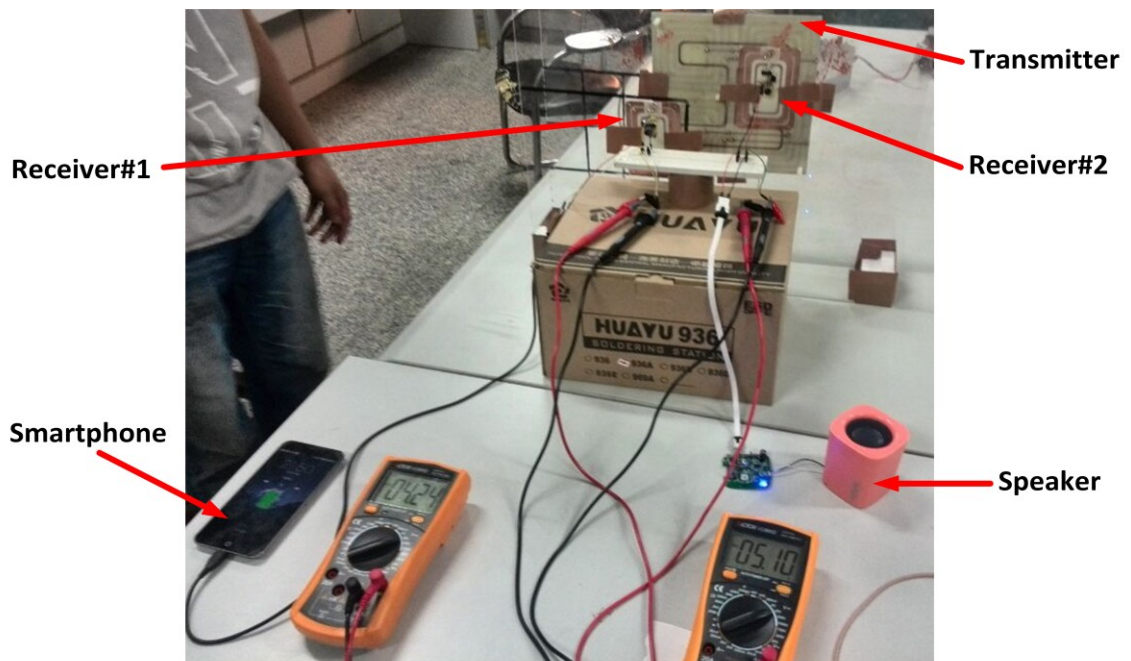


Figure 5-23: Picture of the developed MCR-WPT array system for multiple charging electronic devices.

5.5.2 Array of 3×3

To make the MCR-WPT system more feasible and practical for reaching small electronic devices, the transmitter of the MCR-WPT system should be large enough to cover the desired area. For example, to wirelessly power two electronic devices such as a tablet and a smartphone simultaneously, the proposed array of 2×2 cannot satisfy the requirements. We should also keep in mind that the mutual inductances of the different resonators of the array transmitter would be different when the array transmitter has $n \times n$ resonators where $n \geq 3$. Therefore, the complexity of the feeding structure and different mutual inductances at different resonators should be considered.

Figure 5-24 shows the geometry of the transmitting array of 3×3 which has 9 resonators (R_1, \dots, R_9). First, the same approach developed in the previous section for designing the array transmitter of 2×2 by using the same value of the lumped capacitor for all transmitting resonators, is applied here. Table 3-1 shows all parameters of the MCR-WPT array system for the transmitter and the receiver. To fine-tune the value of the lumped capacitor for the transmitting resonators to resonate at 13.56 MHz, 142 pF is chosen.

However, as depicted in Figure 5-25, when moving the receiver to different locations at a transmission distance of 90 mm, the transmission efficiency of the MCR-WPT array system varies. For instance, when the receiver moves from P_5 to P_3 at 10 cm away from the transmitter, the transmission efficiency drops from 69.75% to 42.52%. This is caused by the unequal mutual inductance between each resonator R_i and adjacent resonators for different i when the transmitter array has $n \times n$ resonators (where $n > 2$). So when R_1 is adjacent to R_2 and R_4 , R_2 is adjacent to R_1 , R_3 and R_5 , and R_5 is adjacent to R_2 , R_4 , R_6 and R_8 . Therefore, capacitors with different values need to be applied to different resonators to yield the same resonant frequency.

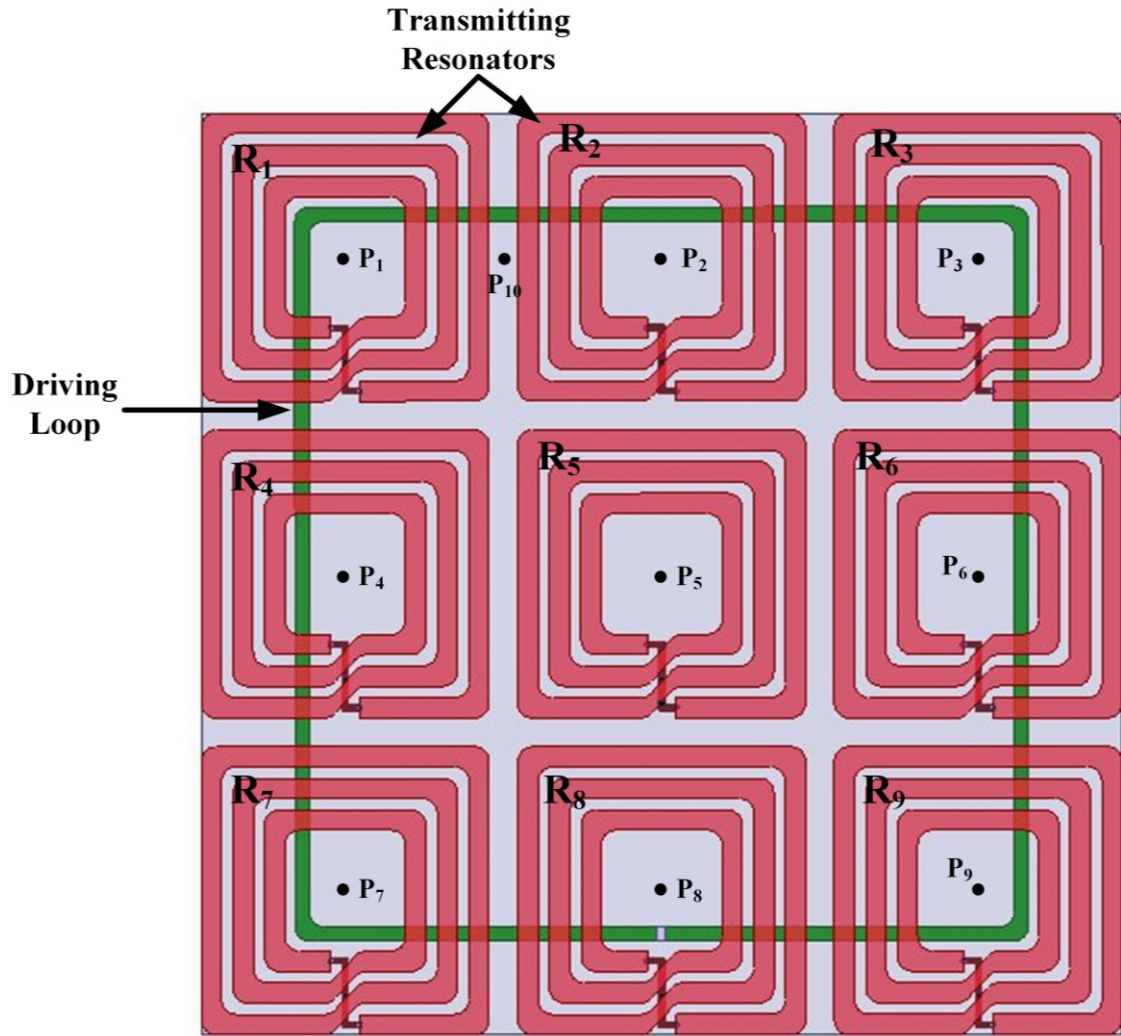


Figure 5-24: Geometry of transmitting array of 3×3

Table 5-4: Parameters of MCR-WPT array system with nine transmitting resonators

	Transmitter	Receiver
W_r (mm)	4	6
W_l (mm)	3.5	2.5
R_o (mm)	21	20
R_i (mm)	21	35
W (mm)	320	100
L (mm)	320	70
N	3	2
D (mm)	10	-
C (pF)	142	271
C_p (pF)	101	434
C_s (pF)	45	177

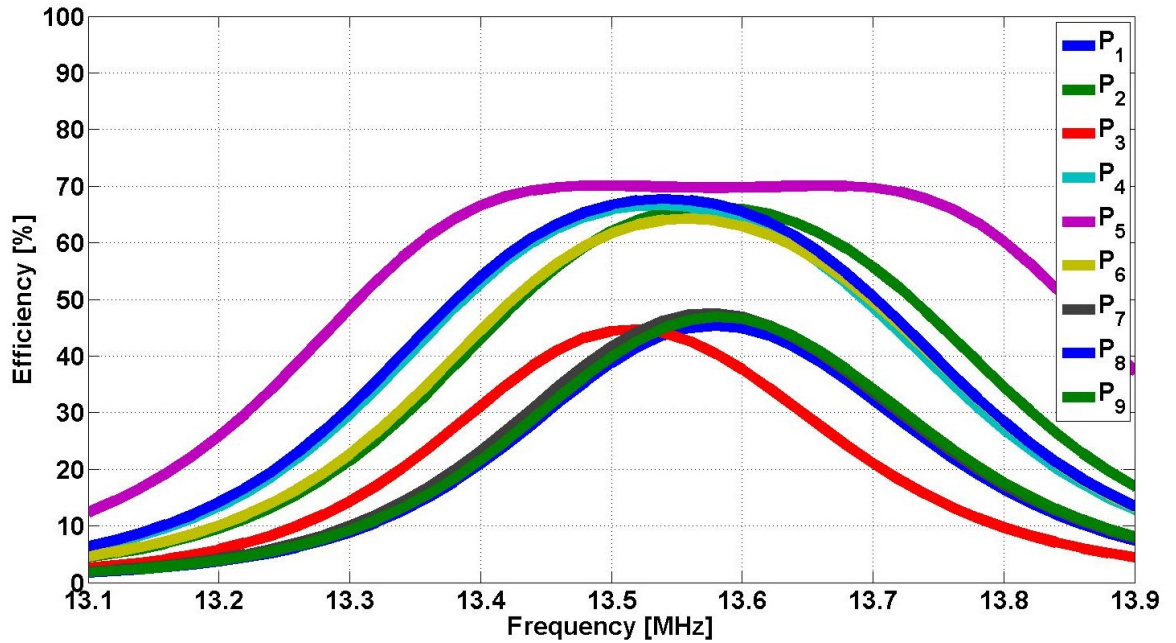


Figure 5-25: Transmission efficiency of MCR-WPT array system with 9 transmitting resonators at a distance of 90 mm.

Three sets of resonators are chosen with the same mutual inductances. The first set is the transmitting resonators, which are adjacent to two other resonators including R_1 , R_3 , R_7 and R_9 . The second set is the transmitting resonators, which are adjacent to three other resonators, including R_2 , R_4 , R_6 and R_8 . Moreover, the third set is R_5 , which is adjacent to four other resonators.

Each set of resonators is fine-tuned with a different lumped capacitor. The optimization scheme ran on Ansoft Designer to optimize all the capacitors and the transmitter and receiver matching networks to achieve the maximum efficiency at $P_1, P_2 \dots P_9$.

Figure 5-26 illustrates the transmission efficiency of the system using optimized capacitors given in Table 5-5. The transmission efficiency is between 63.06% and 69.13%, which means when the receiver is moving at any position of $P=(x,y)$ on the xy plane at a distance of 90 mm, the lowest transmission efficiency is 6.07% below the maximum achievable efficiency. This feature makes the MCR-WPT array system with the array of 3×3 more feasible and attractive.

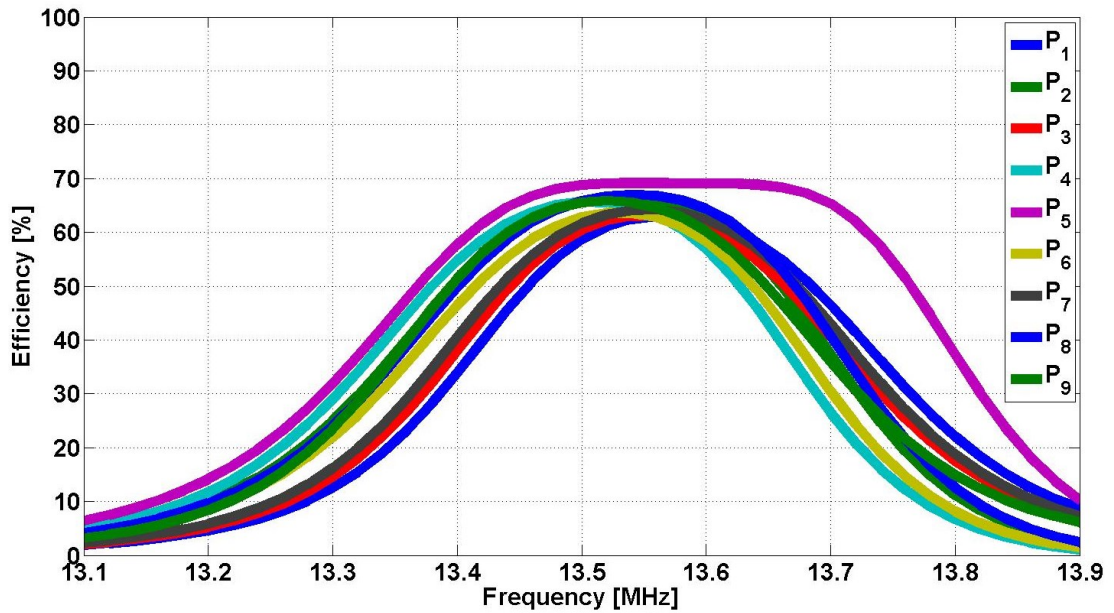


Figure 5-26: Transmission efficiency of MCR-WPT array system with 9 transmitting resonators using different lumped capacitors at a distance of 90 mm.

Table 5-5: Value of capacitors for MCR-WPT array system with nine resonators

	Design with fixed capacitors	Design with varied capacitors
C_{R1}	142 pF	154 pF
C_{R2}	142 pF	140 pF
C_{R3}	142 pF	154 pF
C_{R4}	142 pF	140 pF
C_{R5}	142 pF	110 pF
C_{R6}	142 pF	140 pF
C_{R7}	142 pF	154 pF
C_{R8}	142 pF	140 pF
C_{R9}	142 pF	154 pF
C_{Rx}	271 pF	291 pF
C_{Txp}	101 pF	95 pF
C_{Txs}	44 pF	41 pF
C_{Rxp}	434 pF	400 pF
C_{Rxs}	177 pF	170 pF

As shown in Figure 5-27, the array is printed on an FR4 substrate and the driving loop is designed to cover eight out of nine resonators, inducing a uniform magnetic field. In addition, to increase the quality factor of the receiving resonator, auxiliary strips are applied

to the receiver. However, because of the printed driving loop on the backside of the substrate, the auxiliary strips are not applied to the transmitting resonators.

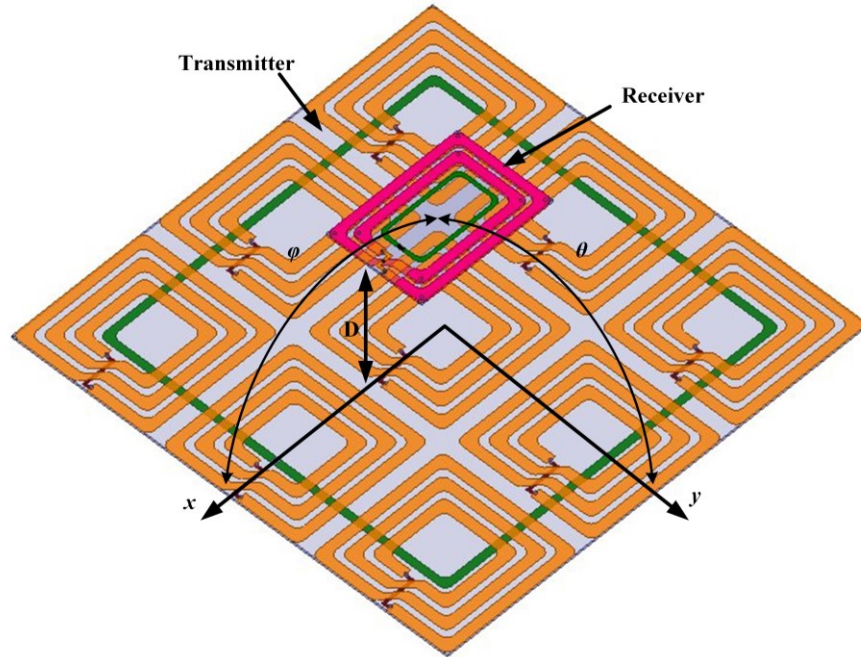


Figure 5-27: MCR-WPT array system with an array of 3×3 transmitting resonators.

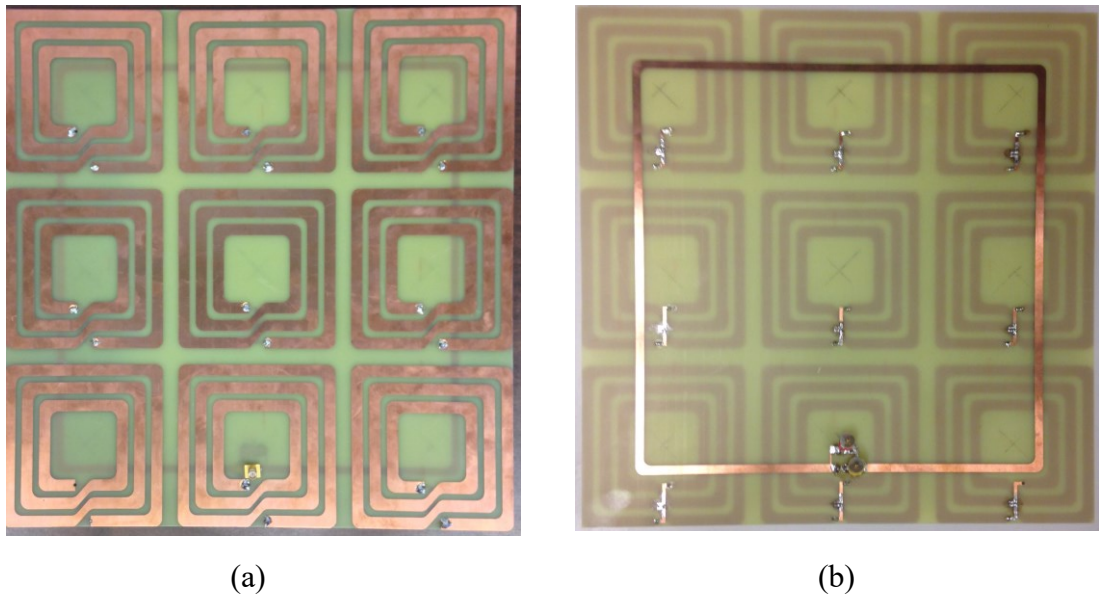


Figure 5-28: Picture of MCR-WPT array system with an array of 3×3 transmitting resonators: (a) top layer, (b) bottom layer.

Figure 5-29 shows the transmission efficiency of the system versus the transmission distance. It depicts that the transmission efficiency at P_1 , P_5 and P_{10} in the under-coupled region is dropped gradually. Meanwhile, in the over-coupled region, P_{10} performs better than the other points. Figure 5-28 shows the fabricated transmitting array coil.

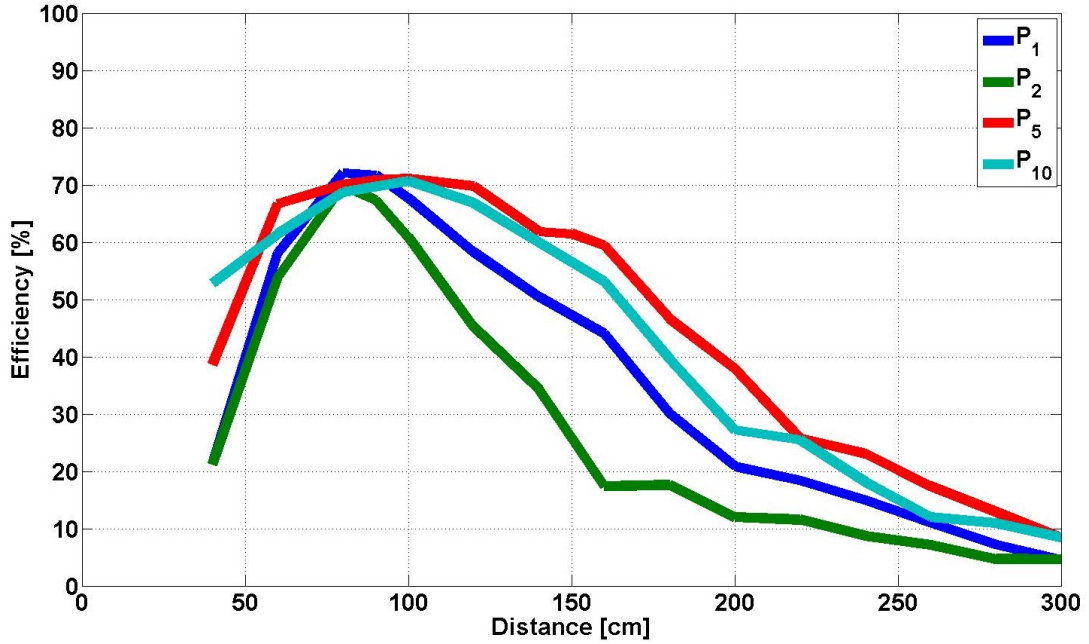


Figure 5-29: Transmission efficiency of MCR-WPT array system with an array of 3×3 transmitting resonators versus transmission distance.

To further investigate the performance of the system when it is not aligned with the transmitter array, the receiver is moved along the xy plane parallel to the transmitter at 9 cm. Figure 5-30 shows the transmission efficiency of the system. It shows that the transmission efficiency is independent of the position of the receiver along the xy axis, and that the transmission efficiency fluctuates between 63.05% and 69.13%, which is very desirable. In addition, the receiver is moved along the φ and θ directions as shown in Figure 5-31. The transmission efficiency results depict that the transmission efficiency of the system ($\theta=0$ degree and $\varphi=0$ degree) is highly stable and is between 68.74% and 71.72%.

By sacrificing the simplicity of the structure and applying auxiliary strips to the transmitting resonators through the addition of another substrate, we can improve the

transmission efficiency of the system. As shown in Figure 5-32, to have enough room to add the auxiliary strips to the transmitting resonators, the resonators are printed on top of the substrate and the auxiliary substrates are printed on the backside of the substrate. The driving loop is then printed on the second substrate and both substrates are stacked together to have a unified transmitter with an overall thickness of 3.2 mm.

Figure 5-32 depicts the transmission efficiency of the system with auxiliary strips. It shows that the transmission efficiency varies from 64.45% to 72.75%, which is about 2% more than the single-layer one. Figure 5-33 shows the transmission efficiency of the proposed MCR-WPT coil array with an array of 3×3 when the receiver is moved.

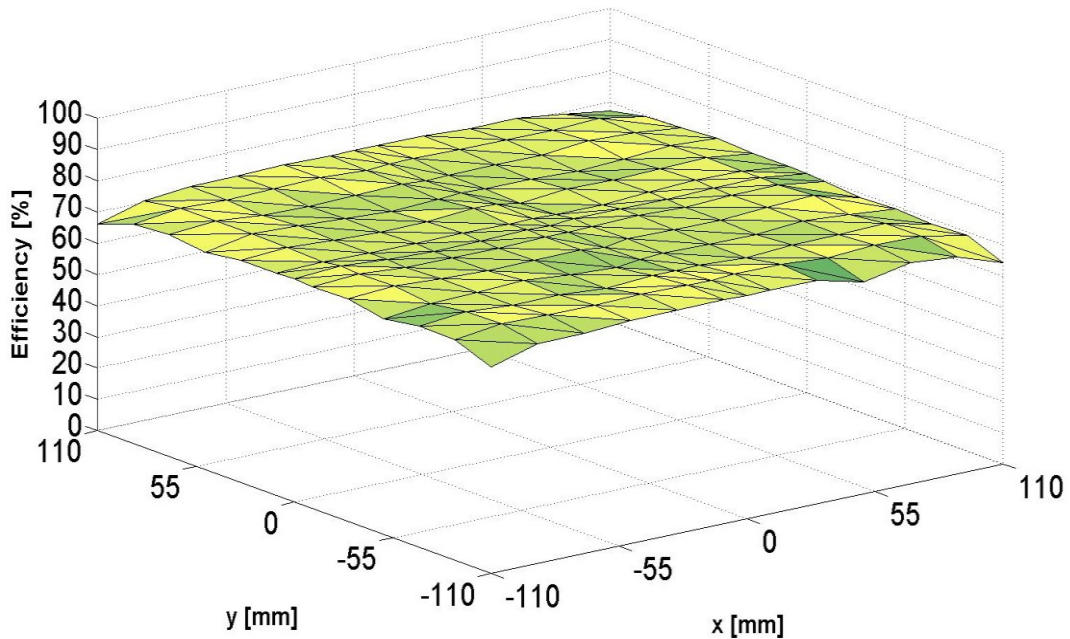


Figure 5-30: Transmission efficiency of MCR-WPT array system with an array of 3×3 transmitting resonators at a distance of 90 mm

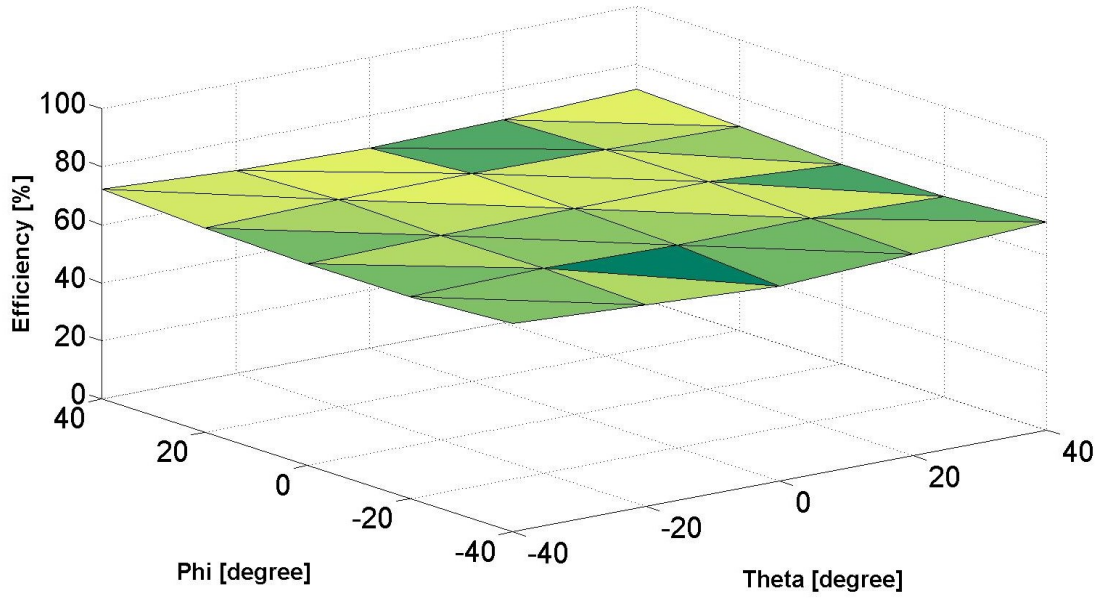


Figure 5-31: : Transmission efficiency of MCR-WPT array system with an array of 3×3 transmitting resonators with different orientation angles of the receiver at the transmission distance of 9 cm.

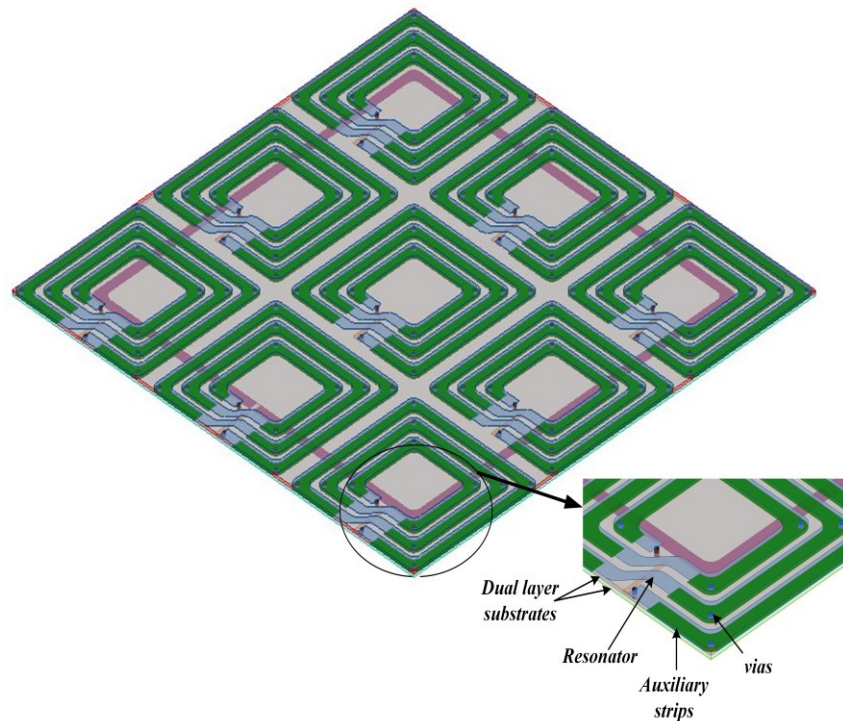


Figure 5-32: Geometry of the MCR-WPT array system with an array of 3×3 transmitting resonators using auxiliary strips.

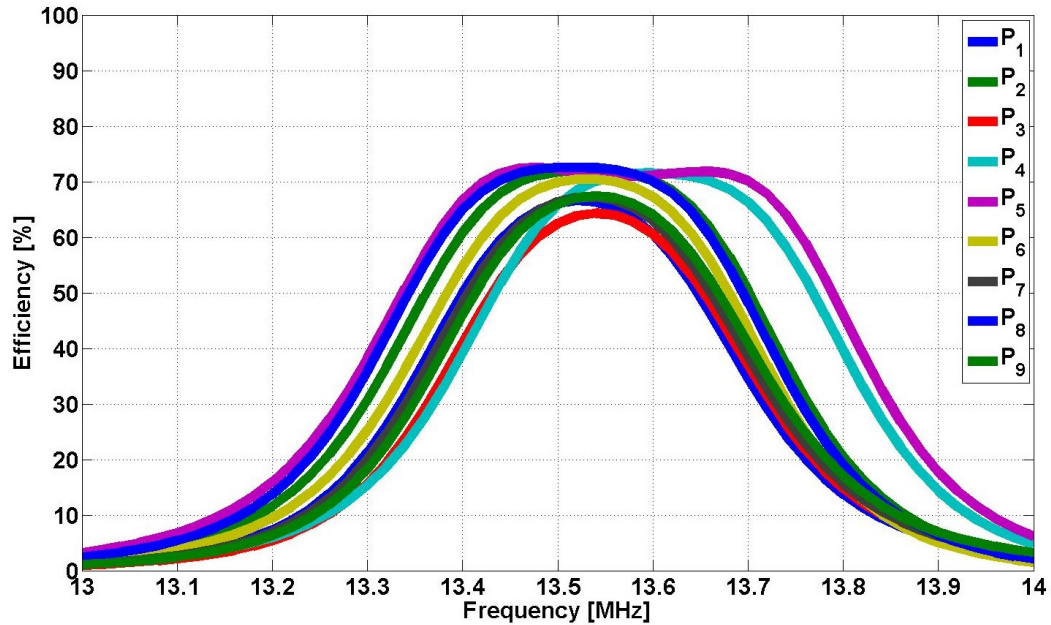


Figure 5-33: Transmission efficiency of MCR-WPT array system with an array of 3×3 .

5.6 Discussion

An efficient and effective strategy is presented to model and optimize the fully planar MCR-WPT system with the transmitting resonator array we recently proposed. The computational cost of the proposed design strategy is only 3.4% of that with the full-wave electromagnetic simulation method. A novel, simple, and easy-to-fabricate design is presented to improve the transmission efficiency of an MCR-WPT system when an axial-misalignment occurs. The conventional transmission resonator is replaced by an array of smaller resonators and a single driving loop. The proposed designs show that the transmission efficiency of the MCR-WPT system is significantly improved in the axial-misalignment condition. Higher transmission efficiency is obtained in both over- and under-coupled regions without any frequency tracking and adaptive matching techniques. Thus, it is a good candidate for practical WPT applications where transmission efficiency needs to be less sensitive to axial-misalignments and transmission distances.

6.1 Conclusion

This dissertation presented a detailed analytical method of an MCR-WPT system and proposed several MCR-WPT designs with different size constraints for transmitting and receiving coils. The planar structure and high power transmission efficiency rendered the proposed designs practical candidates for charging small portable electronic devices. The results showed that with capacitor-loaded PSC resonators that are tuned to resonate at 13.56 MHz, the power transmission efficiency can be as high as 74% at a transmission distance of 200 mm.

In addition, a comparison of various planar WPT designs with PSCs of different numbers of turns in terms of both efficiency and input impedance was made. The results revealed that with a 2-turn PCS resonator with optimized geometric parameters, the maximum power transmission efficiency of the proposed planar WPT system could be as high as 77.27% at a transmission distance of 10 cm. Moreover, with the parallel paths created with auxiliary strips, the quality factor of PSC resonators can be further improved, and the maximum power transmission efficiency can increase to 81.68%.

As well, four designs with different layers of resonators with and without shorting walls were investigated. In the 3-layer planar MCR-WPT system, two substrates were stacked together to construct a low-profile structure; by adding shorting walls, the quality factor of the MCR-WPT system increased to 435. Consequently, the transmission efficiency of the proposed system increased from 77.27% to 84.38% at a distance of 10 cm compared to a conventional planar WPT system. A receiver with a size of 50 mm × 50 mm was studied to yield a compact, low profile, and highly efficient planar MCR-WPT design.

Furthermore, an efficient and effective strategy was investigated to model and optimize the fully planar MCR-WPT system with transmitting resonator array. It was shown that the computational cost of the proposed design strategy was only 3.4% of that with the full-wave electromagnetic simulation method.

To improve the transmission efficiency of an MCR-WPT system when the receiver is axially misaligned with the transmitter, a novel and easy-to-fabricate design was presented. The conventional transmission resonator was replaced by an array of smaller resonators

and a single driving loop. The proposed designs show that the transmission efficiency of the MCR-WPT system is significantly improved under scenarios of axial-misalignment. In addition, higher transmission efficiency was also observed in both over- and under-coupled regions without any frequency tracking and adaptive matching techniques. Finally, a planar transmitting array consisting of nine resonators (array of 3×3) was proposed with different lumped capacitors optimized for different transmitter resonators to realize uniform magnetic field distribution at the receiver and consequently a position-free WPT system.

In conclusion, the planar MCR-WPT systems and position-free planar MCR-WPT array systems proposed in this work were proven candidates for wireless charging of small electronic devices.

6.2 Future Work

The focus of the thesis was on studying of planar MCR-WPT system for small electronic devices and on investigating an array transmitter to cover a larger area. My aim was also to improve transmission efficiency when the receiver is laterally and axially misaligned.

In the first part of the work, a planar MCR-WPT was studied, and several techniques, such as auxiliary strips and short-walls were presented to improve the performance. In the optimization scheme, the number of turns was limited to 2 to 7 turns. More work can be done on the optimization scheme, such as adding more parameters and different geometries like circle-shaped or hexagonal-shaped resonators. In addition, the use of ferrite materials with different implementations can be further investigated. The research can include shielding and take all of the other parts of an electronic device into consideration to investigate their effects on transmission efficiency of WPT systems.

As well, more work can be carried out to extend the transmission distance of the system. The effect of different techniques in the over- and under-coupled regions can be done to further improve performance.

Different resonator feeding structures for the planar MCR-WPT array system can be investigated to increase the transmission efficiency of laterally, axially and angularly misaligned receiver. The array of $n \times n$ with $n \geq 3$ can be investigated and the proper feeding loop can be examined.

Finally, more discussions should be entered into regarding the entire system, including the rectifier, amplifier and other sub-systems. An attempt should be made to integrate all subsystems into a single board in order to design an easy-to-implement MCR-WPT system for small electronic devices.

REFERENCES

- [1] A. Karalis, J. D. Joannopoulos, and M. Soljačić, "Efficient wireless non-radiative mid-range energy transfer," *Annals of Physics*, vol. 323, no. 1, pp. 34-48, 1 2008.
- [2] C. S. Wang, O. H. Stielau and G. A. Covic, "Design considerations for a contactless electric vehicle battery charger," *Industrial Electronics, IEEE Transactions on*, vol. 52, no. 5, pp. 1308-1314, 2005.
- [3] T. Imura, H. Okabe and Y. Hori, "Basic experimental study on helical antennas of wireless power transfer for Electric Vehicles by using magnetic resonant couplings," in *Vehicle Power and Propulsion Conference, 2009. VPPC '09. IEEE*, 2009, pp. 936-940.
- [4] J. Shin, S. Shin, Y. Kim, S. Ahn, S. Lee, G. Jung, S. J. Jeon and D. H. Cho, "Design and implementation of shaped magnetic-resonance-based wireless power transfer system for roadway-powered moving electric vehicles," *Industrial Electronics, IEEE Transactions on*, vol. 61, no. 3, pp. 1179-1192, 2014.
- [5] A. K. RamRakhyani, S. Mirabbasi, and M. Chiao, "Design and optimization of resonance-based efficient wireless power delivery systems for biomedical implants," *Biomedical Circuits and Systems, IEEE Transactions on*, vol. 5, no. 1, pp. 48-63, 2011.
- [6] K. Na, H. Jang, H. Ma, and F. Bien, "Tracking optimal efficiency of magnetic resonance wireless power transfer system for biomedical capsule endoscopy," *Microwave Theory and Techniques, IEEE Transactions on*, vol. 63, no. 1, pp. 295-304, 2015.
- [7] J. Zhao, G. Xu, C. Zhang, Y. Li, X. Zhang, Q. Yang, Y. Li, and H. Yu, "The design and research of a new kind small size resonator used in magnetic coupling resonance wireless energy transmission system," *Magnetics, IEEE Transactions on*, vol. 48, no. 11, pp. 4030-4033, 2012.
- [8] J. W. Kim, H. C. Son, K. H. Kim, and Y. J. Park, "Efficiency analysis of magnetic resonance wireless power transfer with intermediate resonant coil," *Antennas and Wireless Propagation Letters, IEEE*, vol. 10, pp. 389-392, 2011.
- [9] J. Lee, Y. Lim, H. Ahn, J. D. Yu, and S. O. Lim, "Impedance-matched wireless power transfer systems using an arbitrary number of coils with flexible coil positioning," *Antennas and Wireless Propagation Letters, IEEE*, vol. 13, pp. 1207-1210, 2014.
- [10] Y. Zhao, V. Vutipongsatorn, and E. Leelarasmee, "Improving the efficiency of wireless power transfer systems using metamaterials," in *Electrical Engineering/Electronics, Computer, Telecommunications and Information Technology (ECTI-CON), 2013 10th International Conference on*, 2013, pp. 1-4.

- [11] B. Wang, W. Yezauris, and K. H. Teo, "Wireless power transfer: Metamaterials and array of coupled resonators," *Proceedings of the IEEE*, vol. 101, no. 6, pp. 1359-1368, 2013.
- [12] J. Park, Y. Tak, Y. Kim, Y. Kim, and S. Nam, "Investigation of adaptive matching methods for near-field wireless power transfer," *Antennas and Propagation, IEEE Transactions on*, vol. 59, no. 5, pp. 1769-1773, 2011.
- [13] T. P. Duong, and J. W. Lee, "Experimental results of high-efficiency resonant coupling wireless power transfer using a variable coupling method," *Microwave and Wireless Components Letters, IEEE*, vol. 21, no. 8, pp. 442-444, 2011.
- [14] J. Kim, W.S. Choi and J. Jeong, "Loop switching technique for wireless power transfer using magnetic resonance coupling," *Progress In Electromagnetics Research*, vol. 138, pp. 197-209 2013.
- [15] B. C. Park, and J. H. Lee, "Adaptive impedance matching of wireless power transmission using multi-loop feed with single operating frequency," *Antennas and Propagation, IEEE Transactions on*, vol. 62, no. 5, pp. 2851-2856, 2014.
- [16] W. Lee, W. I. Son, K. Oh and J. W. Yu, "Contactless energy transfer systems using antiparallel resonant loops," *Industrial Electronics, IEEE Transactions on*, vol. 60, no. 1, pp. 350-359, 2013.
- [17] S. G. Lee, H. Hoang, Y. H. Choi, and F. Bien, "Efficiency improvement for magnetic resonance based wireless power transfer with axial-misalignment," *Electronics Letters*, vol. 48, no. 6, pp. 339-340, 2012.
- [18] K. Miwa, J. Kaneda, N. Kikuma, H. Hirayama, and K. Sakakibara, "Consideration of use of arrayed transmitting coils in wireless power transfer with magnetically coupled resonance," in *Antennas and Propagation (ISAP), 2012 International Symposium on*, 2012, pp. 451-454.
- [19] K. Mori, Hyunkeun Lim, S. Iguchi, K. Ishida, M. Takamiya, and T. Sakurai, "Positioning-free resonant wireless power transmission sheet with staggered repeater coil array (SRCA)," *Antennas and Wireless Propagation Letters, IEEE*, vol. 11, pp. 1710-1713, 2012.
- [20] K. Miwa, H. Mori, N. Kikuma, H. Hirayama, and K. Sakakibara, "A consideration of efficiency improvement of transmitting coil array in wireless power transfer with magnetically coupled resonance," in *Wireless Power Transfer (WPT), 2013 IEEE*, 2013, pp. 13-16.
- [21] M. Kiani, and M. Ghovanloo, "The circuit theory behind coupled-mode magnetic resonance-based wireless power transmission," *Circuits and Systems I: Regular Papers, IEEE Transactions on*, vol. 59, no. 9, pp. 2065-2074, 2012.

- [22] K. Chen, and Z. Zhao, "Analysis of the double-layer printed spiral coil for wireless power transfer," *Emerging and Selected Topics in Power Electronics, IEEE Journal of*, vol. 1, no. 2, pp. 114-121, 2013.
- [23] M. M. Falavarjani, M. Shahabadi, and J. Rashed-Mohassel, "Design and implementation of compact WPT system using printed spiral resonators," *Electronics Letters*, vol. 50, no. 2, pp. 110-111, 2014.
- [24] N. Tesla, "System of transmission of electrical energy," 03/20 1900. <https://www.google.com/patents/US645576>.
- [25] W. C. Brown, "The history of wireless power transmission," *Solar Energy*, vol. 56, no. 1, pp. 3-21, 1996.
- [26] W. C. Brown, "Experiments involving a microwave beam to power and position a helicopter," *Aerospace and Electronic Systems, IEEE Transactions on*, vol. AES-5, no. 5, pp. 692-702, 1969.
- [27] W. C. Brown, "Free-space microwave power transmission study, phase 3," *NASA STI/Recon Technical Report N*, vol. 76 1975.
- [28] Y. Jang, and M. M. Jovanovic, "A contactless electrical energy transmission system for portable-telephone battery chargers," *Industrial Electronics, IEEE Transactions on*, vol. 50, no. 3, pp. 520-527, 2003.
- [29] B. Choi, J. Nho, H. Cha, T. Ahn, and B. Choi, "Design and implementation of low-profile contactless battery charger using planar printed circuit board windings as energy transfer device," *Industrial Electronics, IEEE Transactions on*, vol. 51, no. 1, pp. 140-147, 2004.
- [30] S. Y. R. Hui, and W. C. Ho, "A new generation of universal contactless battery charging platform for portable consumer electronic equipment," in *Power Electronics Specialists Conference, 2004. PESC 04. 2004 IEEE 35th Annual*, 2004, pp. 638-644 .
- [31] P. Raval, D. Kacprzak, and A.P. Hu, "A wireless power transfer system for low power electronics charging applications," in *Industrial Electronics and Applications (ICIEA), 2011 6th IEEE Conference on*, 2011, pp. 520-525.
- [32] K. Phaebua, D. Torrungrueng, and C. Phongcharoenphanich, "Design of planar rectangular spiral antennas for the wireless vehicle battery charging system," in *Microwave Conference Proceedings (APMC), 2013 Asia-Pacific*, 2013, pp. 1172-1174.
- [33] S. Y. R. Hui, W. Zhong, and C. K. Lee, "A critical review of recent progress in mid-range wireless power transfer," *Power Electronics, IEEE Transactions on*, vol. 29, no. 9, pp. 4500-4511, 2014.

- [34] A. Kurs, A. Karalis, R. Moffatt, J. D. Joannopoulos, P. Fisher, and M. Soljacic, "Wireless power transfer via strongly coupled magnetic resonances," *Science*, vol. 317, no. 5834, pp. 83-86, 2007.
- [35] A. P. Sample, D. A. Meyer, and J. R. Smith, "Analysis, experimental results, and range adaptation of magnetically coupled resonators for wireless power transfer," *Industrial Electronics, IEEE Transactions on*, vol. 58, no. 2, pp. 544-554 2011.
- [36] Y. Zhang, Z. Zhao, and K. Chen, "Frequency splitting analysis of magnetically-coupled resonant wireless power transfer," in *Energy Conversion Congress and Exposition (ECCE), 2013 IEEE*, 2013, pp. 2227-2232.
- [37] K. E. Koh, T. C. Beh, T. Imura, and Y. Hori, "Impedance matching and power division using impedance inverter for wireless power transfer via magnetic resonant coupling," *Industry Applications, IEEE Transactions on*, vol. 50, no. 3, pp. 2061-2070, 2014.
- [38] T. Imura, "Equivalent circuit for repeater antenna for wireless power transfer via magnetic resonant coupling considering signed coupling," in *Industrial Electronics and Applications (ICIEA), 2011 6th IEEE Conference on*, 2011, pp. 1501-1506.
- [39] C. K. Lee, W. X. Zhong, and S. Y. R. Hui, "Effects of magnetic coupling of nonadjacent resonators on wireless power domino-resonator systems," *Power Electronics, IEEE Transactions on*, vol. 27, no. 4, pp. 1905-1916, 2012.
- [40] W. Zhong, C. K. Lee, and S. Y. R. Hui, "General analysis on the use of tesla's resonators in domino forms for wireless power transfer," *Industrial Electronics, IEEE Transactions on*, vol. 60, no. 1, pp. 261-270, 2013.
- [41] J. H. Kim, B. C. Park, and J. H. Lee, "New analysis method for wireless power transfer system with multiple n resonators," *Journal of Korean Institute of Electromagnetic Engineering and Science*, vol. 13, no. 3, pp. 173-177, 2013.
- [42] S. D. Huang, Z. Q. Li, and Y. Li, "Transfer efficiency analysis of magnetic resonance wireless power transfer with intermediate resonant coil," *Journal of Applied Physics*, vol. 115, no. 17, pp. 17A336-17A336-3, 2014.
- [43] J. B. Pendry, "Negative refraction," *Contemporary Physics*, vol. 45, no. 3, pp. 191-202, 2004.
- [44] B. Wang, K. H. Teo, T. Nishino, W. Yerazunis, J. Barnwell, and J. Zhang, "Experiments on wireless power transfer with metamaterials," *Applied Physics Letters*, vol. 98, no. 25, pp. 254101-254101-3, 2011.
- [45] D. Ahn, M. Kiani, and M. Ghovanloo, "Enhanced wireless power transmission using strong paramagnetic response," *Magnetics, IEEE Transactions on*, vol. 50, no. 3, pp. 96-103, 2014.

- [46] X. Zhang, S. L. Ho, and W. N. Fu, "Analysis and optimization of magnetically coupled resonators for wireless power transfer," *Magnetics, IEEE Transactions on*, vol. 48, no. 11, pp. 4511-4514, 2012.
- [47] C. M. Zierhofer, and E. S. Hochmair, "Geometric approach for coupling enhancement of magnetically coupled coils," *Biomedical Engineering, IEEE Transactions on*, vol. 43, no. 7, pp. 708-714, 1996.
- [48] B. L. Cannon, J. F. Hoburg, D. D. Stancil, and S. C. Goldstein, "Magnetic resonant coupling as a potential means for wireless power transfer to multiple small receivers," *Power Electronics, IEEE Transactions on*, vol. 24, no. 7, pp. 1819-1825, 2009.
- [49] J. Choi, J. K. Cho, and C. Seo, "Analysis on transmission efficiency of wireless energy transmission resonator based on magnetic resonance," in *Microwave Workshop Series on Innovative Wireless Power Transmission: Technologies, Systems, and Applications (IMWS), 2011 IEEE MTT-S International*, 2011, pp. 199-202.
- [50] S. Gabriel, R. W. Lau, and C. Gabriel, "The dielectric properties of biological tissues: III. parametric models for the dielectric spectrum of tissues," *Phys. Med. Biol.* 41(11), pp. 2271, 1996.
- [51] A. Robichaud, M. Boudreault, and D. Deslandes, "Comparison between inductance topologies for resonant wireless power transmission applications," in *Microwave Conference Proceedings (APMC), 2012 Asia-Pacific*, 2012, pp. 397-399.
- [52] H. Hirayama, T. Amano, N. Kikuma, and K. Sakakibara, "An investigation on self-resonant and capacitor-loaded helical antennas for coupled-resonant wireless power transfer," *IEICE Trans. Commun.*, vol. E96.B, no. 10, pp. 2431-2439, 2013.
- [53] N. Inagaki, T. Tabata, and S. Hori, "Wireless resonance connection employing a single resonator between transmitting and receiving electrically small non-resonant antennas," in *Microwave Workshop Series on Innovative Wireless Power Transmission: Technologies, Systems, and Applications (IMWS), 2012 IEEE MTT-S International*, 2012, pp. 75-78.
- [54] H. C. Son, J. W. Kim, D. H. Kim, K. H. Kim, and Y. J. Park, "Self-resonant coil with coaxial-like capacitor for wireless power transfer," in *Microwave Conference Proceedings (APMC), 2011 Asia-Pacific*, 2011, pp. 90-93.
- [55] S. S. Mohan, M. M. Hershenson, S. P. Boyd, and T. H. Lee, "Simple accurate expressions for planar spiral inductances," *Solid-State Circuits, IEEE Journal of*, vol. 34, no. 10, pp. 1419-1424, 1999.
- [56] W. B. Kuhn, and N. M. Ibrahim, "Analysis of current crowding effects in multiturn spiral inductors," *Microwave Theory and Techniques, IEEE Transactions on*, vol. 49, no. 1, pp. 31-38, 2001.

- [57] G. K. Felic, D. Ng, and E. Skafidas, "Investigation of frequency-dependent effects in inductive coils for implantable electronics," *Magnetics, IEEE Transactions on*, vol. 49, no. 4, pp. 1353-1360, 2013.
- [58] S. Raju, R. Wu, M. Chan, and C. P. Yue, "Modeling of mutual coupling between planar inductors in wireless power applications," *Power Electronics, IEEE Transactions on*, vol. 29, no. 1, pp. 481-490, 2014.
- [59] G. Byun, S. Ji, B. Jang, C. Seo, and H. Choo, "Design of a loop resonator with improved power transmission efficiency using a ferrite plate," *Journal of Electromagnetic Analysis and Application*, vol. 5, pp. 196-200, 2013.
- [60] W. Wei, Y. Kawahara, N. Kobayashi, and T. Asami, "Characteristic analysis of double spiral resonator for wireless power transmission," *Antennas and Propagation, IEEE Transactions on*, vol. 62, no. 1, pp. 411-419, 2014.
- [61] N. Ueda, and M. Fujimoto, "Improvement of position error tolerance in wireless power transfer utilizing magnetic resonance," *IEICE Tech. Rep.*, vol. 112, no. 285, pp. 99-102, Nov. 2012.